

ANALYSIS AND DESIGN OF REACTIVELY LOADED DUAL BAND
MICROSTRIP ANTENNA

A THESIS SUBMITTED TO
THE GRADUATE SCHOOL OF NATURAL AND APPLIED SCIENCES
OF
MIDDLE EAST TECHNICAL UNIVERSITY

BY

CANER BAYRAM

IN PARTIAL FULFILLMENT OF THE REQUIREMENTS
FOR
THE DEGREE OF MASTER OF SCIENCE
IN
ELECTRICAL AND ELECTRONICS ENGINEERING

SEPTEMBER 2015

Approval of the thesis:

**ANALYSIS AND DESIGN OF REACTIVELY LOADED DUAL BAND
MICROSTRIP ANTENNA**

submitted by **CANER BAYRAM** in partial fulfillment of the requirements for the degree of **Master of Science in Electrical and Electronics Engineering Department, Middle East Technical University** by,

Prof. Dr. Gülbin Dural Ünver
Dean, Graduate School of **Natural and Applied Sciences** _____

Prof. Dr. Gönül Turhan Sayan
Head of Department, **Electrical and Electronics Eng.** _____

Prof. Dr. S. Sencer Koç
Supervisor, **Electrical and Electronics Eng. Dept.,METU** _____

Examining Committee Members:

Prof. Dr. Gönül Turhan Sayan
Electrical and Electronics Eng. Dept.,METU _____

Prof. Dr. S. Sencer Koç
Electrical and Electronics Eng. Dept.,METU _____

Prof. Dr. Özlem Aydın Çivi
Electrical and Electronics Eng. Dept.,METU _____

Assoc. Prof. Dr. Lale Alatan
Electrical and Electronics Eng. Dept.,METU _____

Assoc. Prof. Dr. Vakur B. Ertürk
Electrical and Electronics Eng. Dept.,Bilkent University _____

Date: **10.09.2015**

I hereby declare that all information in this document has been obtained and presented in accordance with academic rules and ethical conduct. I also declare that, as required by these rules and conduct, I have fully cited and referenced all material and results that are not original to this work.

Name, Last name: Caner BAYRAM

Signature:

ABSTRACT

ANALYSIS AND DESIGN OF REACTIVELY LOADED DUAL BAND MICROSTRIP ANTENNA

Bayram, Caner

M. S., Department of Electrical and Electronics Engineering

Supervisor: Prof. Dr. S. Sencer Koç

September 2015, 90 pages

This thesis includes the design, production and measurement of a reactively loaded microstrip patch antenna. The dual band and circular polarization operation are achieved through the use of narrow slots etched close to the radiating edges on a nearly square patch. During the design process, the effects of antenna parameters on the input impedance and axial ratio characteristics are investigated. A step-by-step procedure is followed during the design process. First, the dual band characteristic is investigated on a slot loaded rectangular patch. Then, an attention is given to improve the circular polarization. Finally, the desired structure is analyzed and information about the design parameters is obtained by means of parametric study. These parametric analyses are done in full wave electromagnetic solver tool HFSS. The designed dual band circularly polarized microstrip patch antenna is manufactured and measured. Acceptable agreement between simulation and measurement results is obtained.

KEYWORDS: Microstrip antenna, dual band operation, reactively loading, circular polarization, slot loaded microstrip antenna

ÖZ

ÇİFT BANTTA ÇALIŞABİLEN REAKTİF YÜKLÜ MİKROŞERİT ANTEN ANALİZ VE TASARIMI

Bayram, Caner

Yüksek Lisans, Elektrik ve Elektronik Mühendisliği Bölümü

Tez Yöneticisi: Prof. Dr. S. Sencer Koç

Eylül 2015, 90 sayfa

Bu tez yarık açılarak reaktif yüklenmiş mikroşerit antenlerin tasarımını, üretimini ve ölçümlerini içerir. Geometrik olarak neredeyse kare ölçülerinde bir parça üzerinde, radyasyon yayan kenarlara yakın yarılmış dar yarıklar sayesinde çift bantta çalışabilme ve dairesel polarizasyon operasyonları başarılmıştır. Tasarım aşamasında anten parametrelerinin, antenin giriş empedansına ve eksenel oranına olan etkileri incelenmiştir. Tasarım kısmı adım adım geliştirilmiştir. İlk olarak, dikdörtgen bir mikroşerit parça üzerinde yarıklar açılarak çift bantta çalışabilme karakteristiği incelenmiştir. Sonra, dairesel polarizasyonu geliştirmek üzerine odaklanılmıştır. Son olarak nihai yapı analiz edilmiştir ve parametrik bir çalışma yapılarak dizayn parametreleri ile ilgili bilgi edinilmiştir. Bu parametrik analizler elektromanyetik çözümleyici yazılımı HFSS kullanılarak yapılmıştır. Tasarlanan çift bantta çalışabilir dairesel polarizasyonlu mikroşerit anten üretilmiş ve ölçülmüştür. Ölçüm sonuçları ile simülasyon sonuçları arasında kabul edilebilir bir uyum olduğu görülmüştür.

ANAHTAR KELİMELER: Mikroşerit anten, çift banda çalışabilme, dairesel polarizasyon, yarıklı mikroşerit anten

to my family

ACKNOWLEDGEMENTS

I would like to express my sincere gratitude to my advisor, Prof. Dr. S. Sencer Koç, for his guidance.

I would like to express my sincere appreciation for Erdiñ Erçil, Egemen Yıldırım and Akın Dalkılıç for their valuable friendship, motivation and help.

I would also like to thank to ASELSAN Inc. and METU Electrical and Electronics Engineering Department for the help on the production and measurement stage of the antenna.

For their understanding my spending lots of time on this work, I sincerely thank to my family.

TABLE OF CONTENTS

ABSTRACT	v
ÖZ.....	vi
ACKNOWLEDGEMENTS	viii
TABLE OF CONTENTS	ix
LIST OF TABLES	xi
LIST OF FIGURES.....	xii
CHAPTERS	
1. INTRODUCTION.....	1
2. MULTI FREQUENCY MICROSTRIP ANTENNAS.....	13
3. ANALYSIS AND DESIGN OF REACTIVELY LOADED DUAL BAND MICROSTRIP PATCH ANTENNA	23
3.1 Dual Band Linear Polarization Design with Rectangular Patch Antenna	23
3.2 Dual Band Circular Polarization Design with Nearly Square Patch Antenna	31
4. PARAMETRIC ANALYSIS OF DUAL BAND CIRCULARLY POLARIZED MICROSTRIP ANTENNA.....	41
4.1 Post-Processing for Return Loss in the Change of Capacitance Value....	43
4.2 Effect of Changing Length	47
4.3 Effect of Changing Capacitor	50
4.4 Effect of Changing Feed Position.....	52
4.5 Effect of Changing Slot Width	58

4.6	Effect of Changing Substrate Thickness.....	61
4.7	Effect of Changing Distance of Slots to Edges	63
4.8	Effect of Changing $Ls1$ and $Ls2$	66
4.9	Conclusions	70
5.	MANUFACTURING DUAL BAND CIRCULARLY POLARIZED MICROSTRIP ANTENNA AND MEASUREMENT RESULTS	73
6.	CONCLUSIONS	83
	REFERENCES.....	85

LIST OF TABLES

TABLES

Table 1.1 Feeding types of microstrip antennas.....	6
Table 4.1 Design parameters of nearly square slot loaded microstrip antenna.....	41
Table 4.2 Parameters and their values in effect of length analysis	48
Table 4.3 Feed positions on diagonal axis used in parametric analysis.....	52
Table 4.4 Feed positions on X axis used in parametric analysis.....	54
Table 4.5 Feed positions on Y axis used in parametric analysis.....	54
Table 4.6 Parameters and their values in effect of slot length analysis	66
Table 4.7 Parameters and their values in effect of length analysis	68
Table 4.8 Parameters and their effects on antenna performance.....	71

LIST OF FIGURES

FIGURES

Figure 1.1 Fringe fields of microstrip antenna [3]	3
Figure 1.2 Linear polarization [6]	8
Figure 1.3 Horizontal/Vertical linear polarization	8
Figure 1.4 Elliptical polarization [6]	9
Figure 1.5 Circular polarization [6].....	9
Figure 1.6 Axial ratio; electric field created by two components E_x and E_y	10
Figure 2.1 Dual frequency patch antennas using orthogonal modes with a single feed point.....	14
Figure 2.2 Dual frequency patch antennas using orthogonal modes with dual feed points	14
Figure 2.3 Multilayer stacked patch antenna (Side view)	15
Figure 2.4 Co-planar multi frequency patch dipoles.....	15
Figure 2.5 Cross sub-array multi frequency patch antenna different	16
Figure 2.6 Notch loaded multi frequency patch antennas	17
Figure 2.7 Multi frequency patch antenna with 6 shorting vias	17
Figure 2.8 Dual band slot loaded patch antenna	18
Figure 2.9 Combination of slot loading and inserting pins on a patch antenna	18
Figure 2.10 ‘T’ or ‘Y’ shaped slot loaded dual band patch antennas.....	19
Figure 2.11 Dual band patch antenna CP achieved with a center cross slot	19
Figure 3.1 Probe feed slot-loaded patch antenna	24
Figure 3.2 Current line distributions on slot-loaded rectangular patch (a) unperturbed TM_{100} (b) perturbed TM_{100} (c) unperturbed TM_{300} (d) perturbed TM_{300}	25
Figure 3.3 E-Plane far field pattern for different slot lengths on slot-loaded patch	26
Figure 3.4 Equivalent model for second resonant frequency	27

Figure 3.5 Rectangular microstrip antenna with dual-slot and chip capacitors loading for dual-band operation	29
Figure 3.6 Return loss for rectangular patch with various capacitance	30
Figure 3.7 Square microstrip antenna with circular polarization	31
Figure 3.8 Return loss for square patch ($\epsilon_r = 4.4$, $h = 1.6\text{mm}$, $W = L = 54\text{mm}$, $L_{s1} = 42.5\text{mm}$, $L_{s2} = 41\text{mm}$, $w = 1\text{mm}$, $d = 1\text{mm}$, capacitance = 0.9pF)	33
Figure 3.9 Axial ratio for upper resonance band of square patch	33
Figure 3.10 Axial ratio for square patch - lower band = (1.22GHz to 1.25GHz) upper band = (1.57GHz to 1.585GHz)	34
Figure 3.11 The model of square patch antenna with a diagonal slot	35
Figure 3.12 The model of nearly square patch antenna with diagonal feeding	36
Figure 3.13 Return loss for nearly square patch ($\epsilon_r = 4.4$, $h = 1.6\text{mm}$, $W = 55.8\text{mm}$, $L = 54\text{mm}$, $L_{s1} = 41.6\text{mm}$, $L_{s2} = 41\text{mm}$, $w = 1\text{mm}$, $d = 1\text{mm}$, capacitance = 0.9pF)	36
Figure 3.14 Axial ratio for lower resonance band of nearly square patch	37
Figure 3.15 Axial ratio for upper resonance band of nearly square patch	37
Figure 3.16 RHCP-Directivity (dB) for lower (1224MHz) and upper (1577MHz) resonance band of nearly square patch respectively	38
Figure 3.17 The model of left hand circularly polarized nearly square patch antenna with diagonal feeding	39
Figure 3.18 LHCP-Directivity (dB) for lower (1224MHz) and upper (1577MHz) resonance band of nearly square patch respectively	39
Figure 4.1 Geometry of nearly square slot loaded microstrip antenna	42
Figure 4.2 Use of lumped ports instead of the chip capacitors	43
Figure 4.3 Microwave network representation of the antenna	44
Figure 4.4 Comparison of two methods to get return loss	46
Figure 4.5 Return losses for different values of length	48
Figure 4.6 Axial ratio values for the lower resonance band for different values of length	49

Figure 4.7 Axial ratio values for the upper resonance band for different values of length	49
Figure 4.8 Return losses for different values of capacitance	50
Figure 4.9 Axial ratio values for the lower resonance band for different values of capacitance	51
Figure 4.10 Axial ratio values for the upper resonance band for different values of capacitance	51
Figure 4.11 Return losses for cases given in Table 4.3	53
Figure 4.12 Axial ratio for the lower resonance band for cases given in Table 4.3	53
Figure 4.13 Axial ratio for the upper resonance band for cases given in Table 4.3.	54
Figure 4.14 Return losses for cases given in Table 4.4	55
Figure 4.15 Axial ratio for the lower resonance band for cases given in Table 4.4	56
Figure 4.16 Axial ratio for the upper resonance band for cases given in Table 4.4	56
Figure 4.17 Return losses for cases given in Table 4.5	57
Figure 4.18 Axial ratio for the lower resonance band for cases given in Table 4.5	57
Figure 4.19 Axial ratio for the upper resonance band for cases given in Table 4.5	58
Figure 4.20 Return losses for different values of slot width	59
Figure 4.21 Axial ratio values for the lower resonance band for different values of slot width	60
Figure 4.22 Axial ratio values for the upper resonance band for different values of slot width	60
Figure 4.23 Return losses for different values of substrate thickness	61
Figure 4.24 Axial ratio values for the lower resonance band for different values of substrate thickness	62
Figure 4.25 Axial ratio values for the upper resonance band for different values of substrate thickness	63
Figure 4.26 Return losses for different values of distance of slots to edges	64
Figure 4.27 Axial ratio values for the lower resonance band for different values of distance of slots to edges	65

Figure 4.28 Axial ratio values for the upper resonance band for different values of distance of slots to edges	65
Figure 4.29 Return losses for different values of slot lengths with same difference	66
Figure 4.30 Axial ratio for the lower resonance bands for the cases given in Table 4.6.....	67
Figure 4.31 Axial ratio for the upper resonance band for the cases given in Table 4.6.....	68
Figure 4.32 Return losses for different values of slot lengths given in Table 4.7...	69
Figure 4.33 Axial ratio for the lower resonance band for the cases given in Table 4.7.....	69
Figure 4.34 Axial ratio for the upper resonance band for the cases given in Table 4.7.....	70
Figure 5.1 Fabrication of the antenna.....	74
Figure 5.2 Return loss measurements of the antennas with different capacitance values.....	75
Figure 5.3 Return loss measurement of the antenna with 6002 duoid laminate substrate.....	75
Figure 5.4 Gain comparison between the materials 6002duroid laminate and FR4	76
Figure 5.5 Fabricated dual band circularly polarized nearly square patch antenna	77
Figure 5.6 Return loss comparison between fabricated and simulated antenna.....	78
Figure 5.7 Near field measurement system.....	78
Figure 5.8 Placement of the antenna on the measurement system.....	79
Figure 5.9 Axial ratio comparison between fabricated and simulated antenna for resonance lower band	79
Figure 5.10 Axial ratio comparison between fabricated and simulated antenna for resonance upper band	80
Figure 5.11 Comparison of RHCP and LHCP patterns between simulation and measurement.....	81

CHAPTER 1

INTRODUCTION

Many modern communication systems such as Global Positioning System (GPS) and Global System for Mobile Communications (GSM) require dual or multi-frequency operations. The aim of this thesis is to build an antenna for dual band operation with adjustable frequency ratio (FR) between the two operating frequencies. Specifically, an antenna for GPS application that covers L1 (1575.42 MHz) and L2 frequencies (1227.60 MHz) is considered. At these given center frequencies, GPS has bandwidths from 2.046 MHz to 20.46 MHz depending on the coding type, code rate, and modulation type [1]. Another point of focus on the desired antenna is its polarization. Circular polarization (CP) has been used for microwave radar, tracking and communication applications for its advantages as compared to the linear polarization. CP eliminates polarization mismatch losses caused by multipath interference, reflection, absorption and other weather conditions. Because of that CP delivers better connectivity with both fixed and mobile services. GPS also uses circular polarization. Because of this specification, desired antenna should have a circularly polarized radiation pattern.

A unique radiating structure would be suitable to carry out these operations. This structure should hold a similar performance in all operating frequency bands in terms of radiating properties and impedance matching. These features can be obtained by using wide band antennas or multi-frequency antennas.

Microstrip antennas have the well-known advantages of low cost, low profile and easy fabrication. Also, their usage in double frequency applications appears very attractive as compared to the troubles in achieving wide bandwidths. One layer of

FR-4 substrate is used in many applications which give them a low profile. Since the patch antennas only consist of two metal surfaces and a substrate layer, the patch antennas can be made at a low cost depending on the choice of substrate and feeding technique. FR-4 is relatively low cost substrate material. In many designs, patch antennas are easy to manufacture. The structure of a patch antenna makes it possible to integrate the antenna with RLC components. Also, there are many feeding techniques to choose between. Considering these facts, microstrip antenna type is selected to go on since it can carry out the desired antenna specifications. A microstrip antenna consists of a dielectric substrate, a radiating patch on one side of this dielectric and a ground plane on the other side. Regular shapes (rectangular, circular, square) are generally chosen for simplicity to clearly analyze the performance of the antenna. The fringe fields between the two sides of the dielectric (patch and ground plane) generates the radiation. The radiation caused by the fringe field can be increased or decreased by varying the parameters like the dielectric constant and the substrate thickness [2].

Due to finite dimensions of the patch, the fields undergo fringing as shown in Figure 1.1. The electric field does not end abruptly at the edges and therefore create the fringing fields. The fringing fields occur at the ends of the patch. The fringing fields depends on the substrate thickness, permittivity and patch width. *“Because of the fringing fields, the effective length of the patch appears greater than its physical size”* [3]. Fringing fields show its effect by adding an extra distance ΔL on each side of the patch as shown in Figure 1.1.

Fringing fields need to be taken into account to calculate the effective length of the patch antenna. These fields can be represented as two radiation slots which mean that the patch looks electrically larger than the physical size. Because of that the calculated length need to be extended by the term ΔL so the antenna design is for patch with $L = \lambda/2$ and no fringing [2].

The most popular approximation for the extension ΔL is given in [3] as;

$$\frac{\Delta L}{h} = 0.412 \frac{(\epsilon_{\text{eff}} + 0.3) \left(\frac{W}{h} + 0.264\right)}{(\epsilon_{\text{eff}} - 0.258) \left(\frac{W}{h} + 0.8\right)} \quad (1.1)$$

The effective length of the patch becomes

$$L_{\text{eff}} = L + 2\Delta L \quad (1.2)$$

The effective dielectric constant ϵ_{eff} is given in [3] as;

$$\epsilon_{\text{eff}} = \frac{\epsilon_r + 1}{2} + \frac{\epsilon_r - 1}{2} \left[1 + 12 \frac{h}{W}\right]^{-1/2}, \quad W/h > 1 \quad (1.3)$$

The resonant frequency of the antenna is expressed as

$$f_r = \frac{c}{2(L + 2\Delta L)\sqrt{\epsilon_{\text{eff}}}} \quad (1.4)$$

where c is the speed of light. The width of the patch is given by the formula [3];

$$W = \frac{c}{2f_r} \sqrt{\frac{2}{\epsilon_r + 1}} \quad (1.5)$$

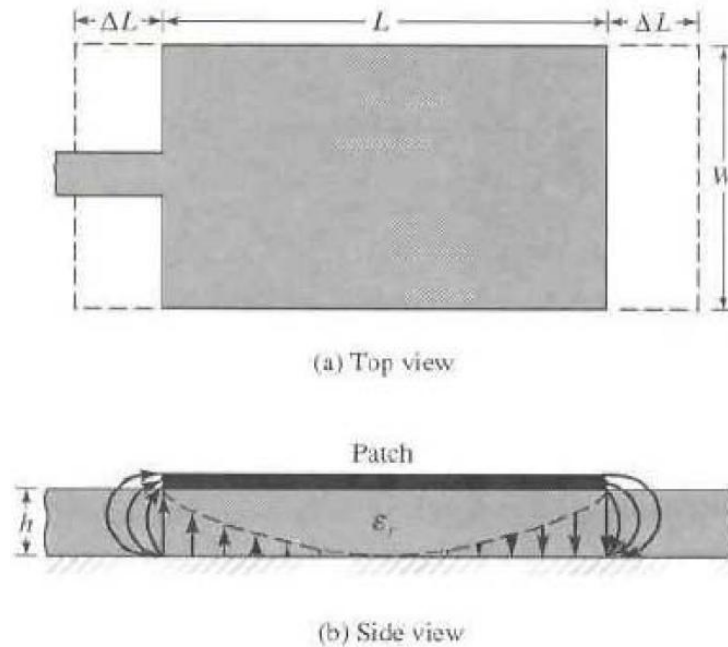


Figure 1.1 Fringe fields of microstrip antenna [3]

Substrate materials play an essential role in the patch antenna design. Substrate properties like dielectric constant, thickness uniformity of the substrate, loss tangent, their variation with temperature and frequency, homogeneity, temperature range and thermal coefficient, humidity and aging are taken into account of an antenna design. Permittivity is very important as can be seen from the given formulas (ϵ_r). The permittivity is associated with how much electrical charge a material can store in a given volume. The permittivity (ϵ) is complex and has a real part (ϵ') and an imaginary part (ϵ'')

$$\epsilon = \epsilon' - j \epsilon'' \quad (1.6)$$

The imaginary part (ϵ'') is associated with the dissipation of energy into the medium. The loss tangent $\tan(\delta)$ measures the amount of electrical energy converted to heat in the dielectric and accounts for the power losses in passive devices like a transmission line or a patch antenna and defined as the ratio between the real part and imaginary part of the complex permittivity [4]

$$\tan(\delta) = \epsilon' / \epsilon'' \quad (1.7)$$

The relative permittivity or dielectric constant ϵ_r is the ratio between the real part of the complex permittivity and the permittivity of vacuum ($\epsilon_0 = 8.854 \cdot 10^{-12}$ F/m)

$$\epsilon_r = \epsilon' / \epsilon_0 \quad (1.8)$$

The speed of propagation in a medium is given as

$$c = \frac{1}{\sqrt{\epsilon\mu}} = \frac{1}{\sqrt{\epsilon_0\epsilon_r\mu_0\mu_r}} = \frac{c_0}{\sqrt{\epsilon_r\mu_r}} \quad (1.9)$$

The dielectric constant affects the speed and therefore the wavelength at a given frequency. If all other parameters are fixed, the size of the circuit is proportional to $1/\sqrt{\epsilon_r}$.

There are many methods to feed a patch antenna and all have their advantages and disadvantages. Feeding methods can be separated into two groups, contacting and non-touching. For the contacting methods, the source is connected directly to the patch via a conducting material, while for the non-conducting method

electromagnetic field coupling is used to transfer the power to the patch. Different types of feeding techniques and geometries that are most commonly used to excite microstrip antennas are listed in Table 1.1.

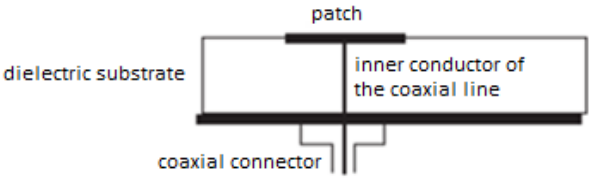
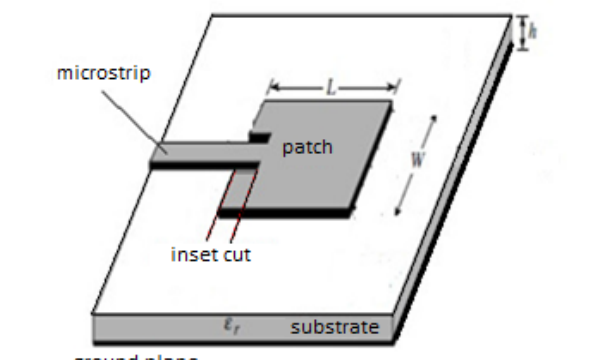
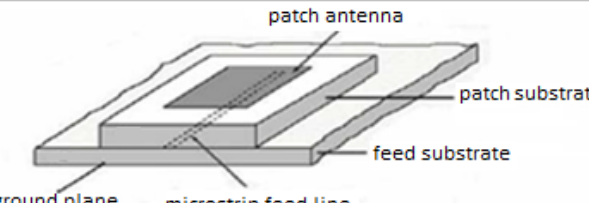
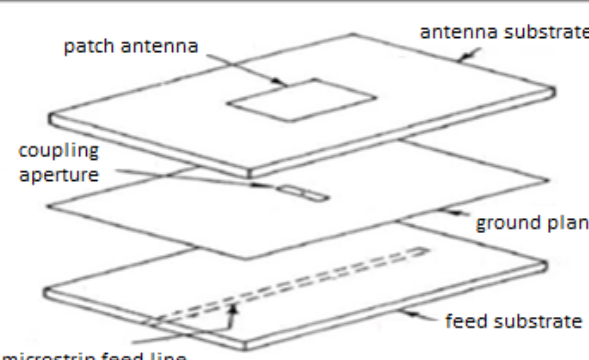
The coaxial feed method is one of the most common feed techniques. Coaxial feeds transmit power through a coaxial line to the patch by using a probe. The inner conductor of the coaxial goes through the substrate from the ground to the patch and the outer conductor is connected to the ground plane [3] as shown in Table 1.1. The most important parameter in the design of a coaxial feed is the selection of the location of the probe because impedance matching is determined by this parameter. It is easy to receive a good impedance matching because the feed can be placed anywhere in the patch. Coaxial feed is easy to implement. However, narrow bandwidth is a trouble. For thick substrates, matching problems can occur due to the inductive loading on the input impedance which is caused by the increased probe length.

Another feeding method is the microstrip line feed. If the various feed configurations are compared in terms of manufacturing difficulty, it can be said that the microstrip line feed configuration is the simplest one, since the feed and the patch are produced on the same substrate. The microstrip line consists of a conducting strip connected to the patch. The microstrip line often has the same conductor thickness as the patch, but the width is smaller. To obtain a good impedance matching, an inset cut can be made, as shown in Table 1.1. This feeding technique has the disadvantage of making the patch larger. Also unintentional radiation from the feed affects the antenna pattern. Narrow bandwidth is another problem with this feeding method.

Proximity (electromagnetically) coupled feeds require two layers of dielectric substrates. Radiating patch stays on the top dielectric layer whereas the microstrip feed line lies between the two substrates. The ground plane lies under the bottom dielectric layer [5] as shown in Table 1.1. Power couples from the feed line to the patch by passing through the upper substrate. Therefore, another name of this feed configuration is “electromagnetically coupled feed”. The primary advantage of this

feed configuration with respect to the others is that, wide bandwidth operations can be obtained with this configuration, since the dielectric constant and the substrate thickness of the feed line and the patch antenna can be controlled independently. Moreover, these parameters can be selected properly to increase the bandwidth of the antenna.

Table 1.1 Feeding types of microstrip antennas

Feeding Technique	Image
Probe (Coaxial) feed	
Microstrip line feed	
Proximity (Electromagnetically) coupled feed	
Aperture-Coupled feed	

Aperture coupled microstrip feed consist of two layers of substrate. The substrate layers are separated with a ground plane. A microstrip line is positioned beneath the lower substrate layer. The energy is coupled to the patch from the microstrip line by a slot in the ground plane [4] as seen in Table 1.1. Aperture coupled microstrip feeds are utilized in applications that need larger bandwidth. Bandwidth is enhanced by slot lengths and dielectric substrate properties. Height of substrate, width, length and position of the slot are the parameters that can be controlled to match the antenna to the feed line. These parameters can be optimized to obtain bandwidths much larger than that can be achieved by using other feeding methods. Better cross-polarization isolation can be obtained since, the feed is isolated from the ground plane which is between the substrates. The disadvantage is difficulty to fabricate this type of feed.

One important criterion about antennas is the polarization that has been mentioned before and will be discussed here. *“The polarization of an antenna in a given direction is defined as the polarization of the wave transmitted (radiated) by the antenna. A time-harmonic wave is linearly polarized at a given point in space if the electric-field (or magnetic-field) vector at that point is always oriented along the same straight line at every instant of time”* [3]. Figure 1.2 shows that the electric field oscillates in one plane and the magnetic field oscillates in the plane orthogonal to that. Figure 1.3 shows that the electric field of a linearly polarized wave can be decomposed into two orthogonal components. These two components oscillate in two orthogonal planes. An antenna is vertically polarized when its electric field is perpendicular to the Earth’s surface. An example of a vertical antenna is the whip antenna on an automobile. The antenna is horizontally polarized when its electric field is parallel to the Earth’s surface. *“A time-harmonic wave is elliptically polarized if the tip of the field vector (electric or magnetic) traces an elliptical locus in space. At various instants of time the field vector changes continuously with time at such a manner as to describe an elliptical locus. It is right-hand (clockwise) elliptically polarized if the field vector rotates clockwise, and it is left-hand (counterclockwise) elliptically polarized if the field*

vector of the ellipse rotates counterclockwise” [3]. Clockwise and counterclockwise directions are defined when looking behind the wave whereas left-hand and right-hand definitions are defined by the thumb point of direction of propagation.

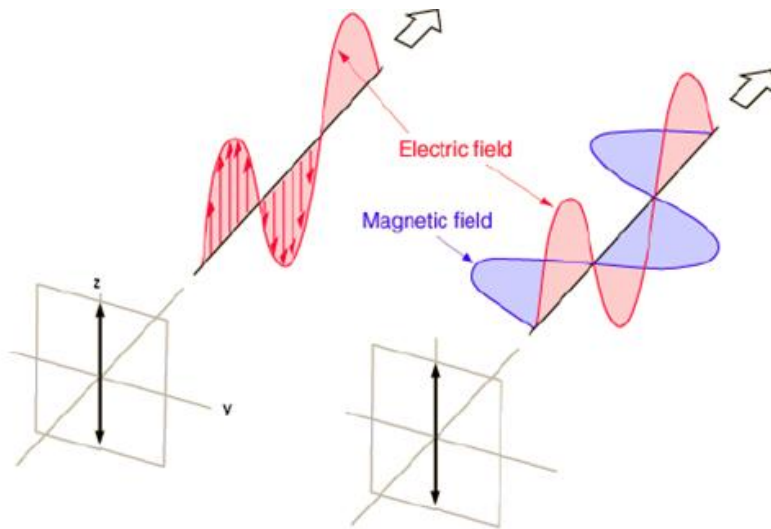


Figure 1.2 Linear polarization [6]

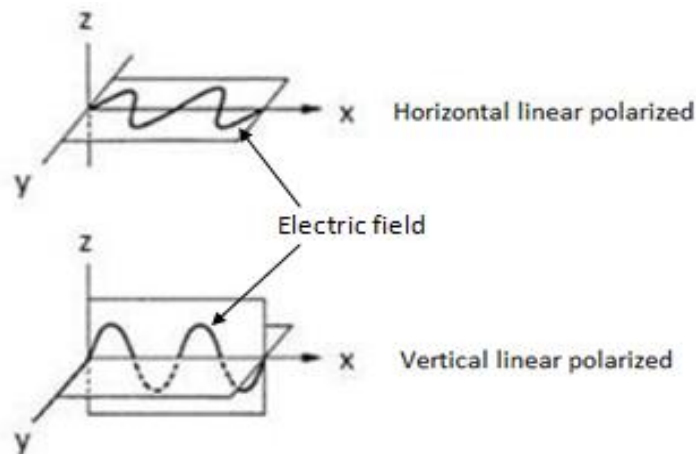


Figure 1.3 Horizontal/Vertical linear polarization

Figure 1.4 shows how the elliptically polarized wave propagates. The electric field oscillates in two orthogonal planes at the same time with different phase and amplitude. The tip of the electric field vector of an elliptically polarized wave traverses an ellipse in the plane orthogonal to its propagation.

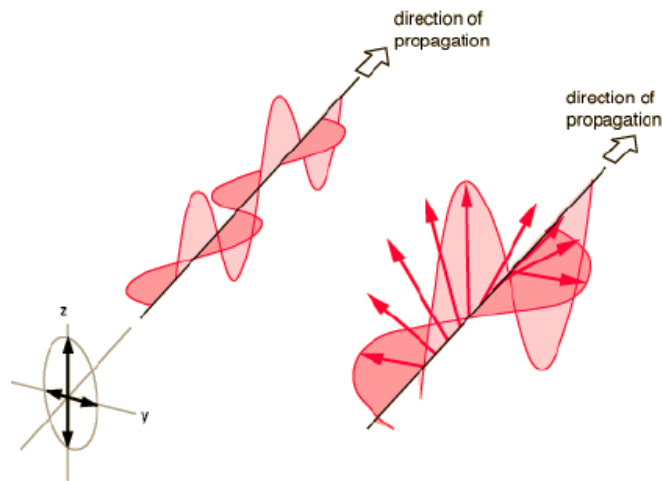


Figure 1.4 Elliptical polarization [6]

“A time-harmonic wave is circularly polarized at a given point in space if the electric (or magnetic) field vector at that point traces a circle as a function of time” [3]. There are two types of circular polarization. If the field rotation is clockwise, then it is right-hand circularly polarized (RHCP) or if the field rotation is counterclockwise, then it is left-hand circularly polarized (LHCP) [3]. The sense of rotation is defined same as before. Figure 1.5 shows how the circularly polarized wave propagates. The electric field oscillates in two planes at the same time with equal amplitude.

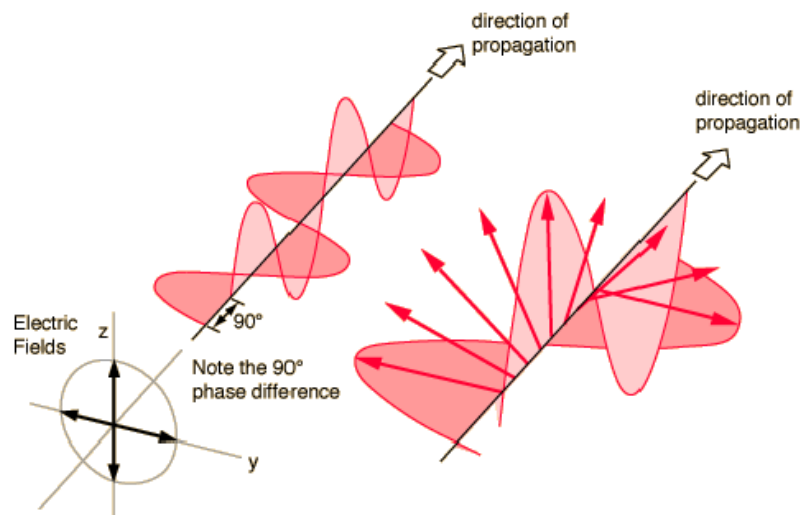


Figure 1.5 Circular polarization [6]

Polarization of the waves is also specified by their axial ratio. The axial ratio ($AR=OA/OB$) is the ratio between the length of the major axis (OA) and the minor axis (OB) of the ellipse where the tip of the electric field vector moves on, ($OA \geq OB$). The E-field consists of an x, y component (E_x, E_y) [3].

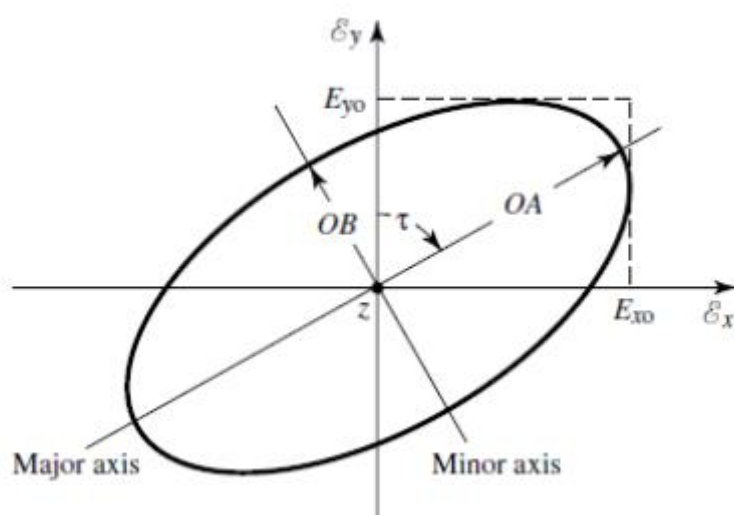


Figure 1.6 Axial ratio; electric field created by two components E_x and E_y

For a linearly polarized wave the $AR = \infty$ ($\text{dB} \gg 0$) since the electric field has one component and then $OB = 0$. For a circularly polarized wave the major and minor axes are equal ($OA = OB$) which gives $AR = 1$ (0 dB). For an elliptically polarized wave the major and minor axes have different length, which gives $1 < AR < \infty$ [3].

Axial ratio is an important control parameter for the design. Desired antenna should provide this value less than 3 dB at operating frequencies. There are many methods to get circular polarization for the patch antennas that will be investigated later in Chapter 2.

The objective of this thesis is to investigate a particular kind of slot-loaded patch antenna to achieve a circularly polarized, dual-band operation on a single-feed, single layer structure. Initially, slot-loaded rectangular patch antenna with two narrow parallel slots given in [7] is investigated for dual band characteristic. The effects of various parameters on the dual band performance of the antenna are studied. After that, proposed dual-band circular polarization design on a square microstrip antenna with four narrow slots is investigated [8]. It is seen that, the simulation and manufactured square patch antenna's measurement results are not efficient enough for circular polarization performance. Then, it is focused on circular polarization techniques on patch antennas, and a solution with a nearly square patch antenna with four narrow slots etched close and parallel to the radiating edges is found. *“When these slots are etched close to the radiating edges, they do not change significantly the first resonant frequency and the radiation pattern of the patch. Furthermore, they introduce another resonance with a radiation pattern similar to the former. This latter resonance is strongly dominated by the slot lengths”* [31].

In this work the use of slot loaded patches is extended to circular polarization. This is obtained by properly changing the antenna parameters and by using chip capacitors. The loading of chip capacitors can further extend the capacitive loading [8]. The outcomes indicate that the frequency ratio meets with GPS requirements. All the analyses are done on HFSS.

Chapter 2 gives some information about multi frequency microstrip antennas in the literature. In addition, some techniques on microstrip patch antennas to improve circular polarization performance are given.

In Chapter 3, the design of a right-hand circularly polarized dual-band microstrip patch antenna is suggested and investigated for GPS applications. The antenna operates at both L1 (1575.42 MHz) and L2 (1227.60 MHz) frequencies with frequency ratio 1.283. The suggested antenna can be implemented by loading chip capacitors across two pairs of unequal-length slots on a nearly square patch.

Procedure for the suggested antenna design is traced, and experimental results for the circular polarization are presented with details.

In Chapter 4, parametric study of the specified slot-loaded patch antenna is performed using the HFSS simulation tool. Design parameters of the antenna are investigated.

Chapter 5 focuses on the fabricated antenna structure. It is measured and observed if the simulation results match the experimental results.

Chapter 6 presents the conclusion and future work which can be performed on the field of the thesis.

CHAPTER 2

MULTI FREQUENCY MICROSTRIP ANTENNAS

Microstrip patch antennas are popular for their well-known features such as a light weight, low profile, and compatibility. Their main disadvantages are their narrow bandwidth limitation and low gain, which are due to the resonant nature of the patch structure. In spite of these disadvantages, communication systems, wireless local networks, satellite applications often require compact and low-cost antennas which makes microstrip patch antennas unavoidable. An alternative to overcome the narrow bandwidth limitation is given by multi-frequency patch antennas. Microstrip antennas make dual and triple band applications possible as well as linear and circular polarization. Multi frequency patch antennas give an alternative to large-bandwidth antennas, in applications where large bandwidth is needed for operating at two separate sub-bands. In this chapter, various structures in the literature for double-frequency operation is given.

The simplest way to operate at dual frequencies is to use the first resonance of the two orthogonal dimensions (length and width) of the rectangular patch; the TM_{100} and the TM_{010} modes. Some antennas of this type are fed by a probe [9] whereas some others are fed by slot coupling in which there should be an angle between slot and microstrip feed line [10]. Simple figures are given in Figure 2.1.

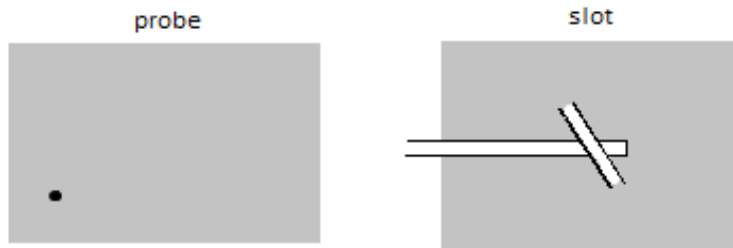


Figure 2.1 Dual frequency patch antennas using orthogonal modes with a single feed point

Orthogonal modes may be excited by microstrip lines positioned on the two orthogonal axes which are dual feed models [11] [12] like in Figure 2.2

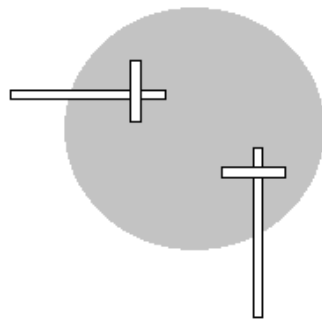


Figure 2.2 Dual frequency patch antennas using orthogonal modes with dual feed points

In the case of using orthogonal modes for dual band, the frequency ratio between two operating frequencies is approximately equal to the ratio between the two orthogonal sides of the patch. Simultaneous matching of the input impedance at the two frequencies with a single feed structure is the advantageous capability of these antennas. This approach results with a fact that the two different frequencies excite two orthogonal polarizations and this is not suitable for most of the dual band applications. Nevertheless, if polarization requirements are not pressing, this method is really profitable.

“Generally the multi frequency patch antennas are subdivided into two categories which are named as multi-resonator antennas and reactively loaded antennas. In the first kind of structure, multi frequency behavior is obtained by means of multiple radiating elements, each supporting strong currents and radiation at

resonance” [42]. This category includes multilayer stacked-patch antennas fabricated by using circular [13], annular [14] and rectangular [15] patches which are shown in Figure 2.3.

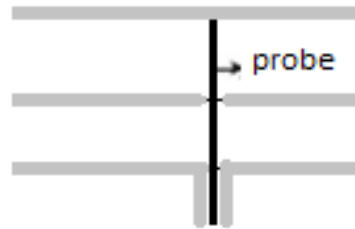


Figure 2.3 Multilayer stacked patch antenna (Side view)

These antennas can operate with the same polarization at the two frequencies which is an important feature. The same multilayer structures can also be used to provide a wide bandwidth antenna, when the interested frequencies are forced to be closely spaced. Multi-frequency antennas can also be obtained by printing more resonators on the same substrate. Parallel rectangular dipoles which are shown in Figure 2.4 is that kind of structure coupled by a slot. Radiation patterns have been shown to be consistent at all operating frequencies, and the antenna is attractive for its simplicity [16].



Figure 2.4 Co-planar multi frequency patch dipoles

“Multi-resonator antennas generally allow only a limited value of the frequency ratio. Some applications may require a large separation between the frequencies, so that the multi-resonator structure must involve patches of very different sizes” [42]. A multi-resonator example of this concept is the antenna given in Figure 2.5 that consists of a cross-shaped patch for the lower frequency, and a subarray of four patches for the upper frequency [17].

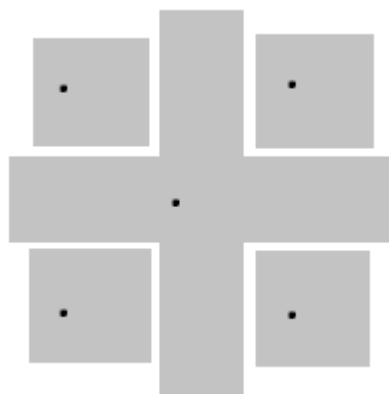


Figure 2.5 Cross sub-array multi frequency patch antenna different

Another example of a multi patch dual band operation is achieved for a GSM application in [18]. The multi resonator structure is seen in a single layer geometry of a small patch inside a larger one. Coupling and separation are provided by a U slot. A similar approach is seen in [19] with double ‘U’ slots again for GSM. Single layer structures are more functional for dual frequency applications and many designs are proposed in this type.

The other most popular technique for obtaining a dual-frequency behavior is to introduce a reactive loading to a single patch. Notches, pins, capacitors and slots can be used for reactive loading. The reactive-loaded patch antenna consists of a single radiating element in which the double resonant behavior can be obtained. The simplest way is to connect a stub to one radiating edge, in such a way to introduce a further resonant length that is responsible for the second operating frequency. The reactive-loading approach was first used in [20] where an adjustable coaxial stub was employed. This structure may provide both tuning and design of the frequency ratio in a simple manner. Loading the radiating edge with an inset (“notch loading”) [21] as seen in Figure 2.6 or a spur-line [22] is an alternative way to introduce a dual frequency behavior that creates the same effect as the reactive loading effect, with the advantage of reduced size.



Figure 2.6 Notch loaded multi frequency patch antennas

Spur-line reactive loading technique given in [23] and [22] has a large circular polarization bandwidth whereas return loss is not as good.

To obtain higher values of the frequency ratio, different approaches have been proposed. In some antennas the double-frequency behavior is obtained by means of shorting vias which are symmetrically located with respect to the patch axes as seen in Figure 2.7. In particular, one can modify the resonant frequency of the TM_{100} and/or the TM_{300} mode, by using shorting vias or lumped capacitors between the patch and the ground plane. As shown in [24] “*by locating the shorting pin where the current distribution of the TM_{300} mode exhibits a minimum, a strong perturbation of its resonant frequency is obtained, while the TM_{100} mode remains almost unperturbed. This permits a frequency ratio of from 2 to 3, by increasing the number of vias*” [42].



Figure 2.7 Multi frequency patch antenna with 6 shorting vias

The disadvantage is that the radiation pattern of the perturbed TM_{300} mode is affected by spurious lobes. An exhaustive investigation of the use of shorting pins for changing the resonant frequency and the polarization is carried out in [25]. There, the use of pin diodes at appropriate positions within the antenna boundary is proposed for changing the loading configuration, thus allowing frequency agility. The use of pin diodes is seen in a GSM application in [26]. “*Very high values of the frequency ratio (4-5) can be obtained by means of two lumped capacitors, connected from the patch to the ground plane*” [27] [42]. Another kind of reactive loading can be introduced by etching slots on the patch as seen in Figure 2.8.



Figure 2.8 Dual band slot loaded patch antenna

The slot loading allows modifying the resonant mode of a patch, particularly when the slots cut the current lines of the unperturbed mode. In particular, as shown in [28] and Figure 2.9, the simultaneous use of slots and short-circuit vias allows a frequency ratio from 1.3 to 3, depending on the number of vias.



Figure 2.9 Combination of slot loading and inserting pins on a patch antenna

Other kinds of slot-loaded patches, especially have been studied in this thesis are independently introduced in [29] and [30], and consist of a rectangular patch with two narrow slots etched close to and parallel to the radiating edge. The same configuration has been investigated in [7] and extended to dual polarization with dual feed in [31]. This type of dual band operation is particularly explained in Chapter 3. Another presented design with two feeds provide reconfiguration on the operating frequencies by changing the feed for excitation. It has a square ring shaped slots and two feed points in this ring [32]. A comparison has been done between multi-resonator patches, stacked patches and reactively loaded patches in [33].

Some of these dual band designs focused on the circular polarization. Several circularly polarized microstrip antenna configurations have been searched. CP can be achieved by using two diagonally symmetric feeds on a slot loaded square patch antenna [31] which has a disadvantage of using multiple feed. Also, too much

attention has been given on the single feed dual band circularly polarized microstrip antennas. Some designs achieve CP by using a slot in the center of a slit loaded square patch. In this kind of design ‘T’ or ‘Y’ shaped slits are used instead of etched slots close to the radiating edges [34] [35] as seen in Figure 2.10.

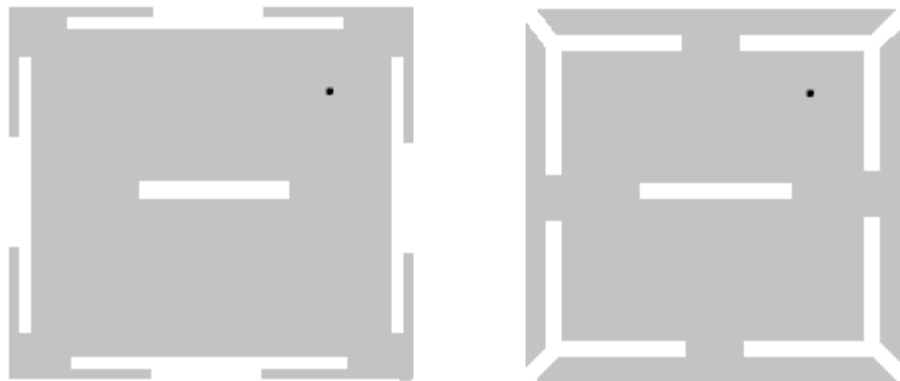


Figure 2.10 ‘T’ or ‘Y’ shaped slot loaded dual band patch antennas

A design has been seen in a satellite application that it provides dual frequency feature with thick slots close to the edges and circular polarization feature with a center cross slot on a square patch as seen in Figure 2.11 [36].

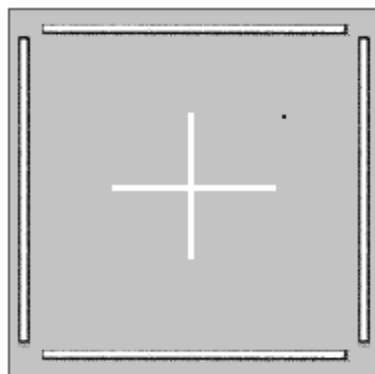


Figure 2.11 Dual band patch antenna CP achieved with a center cross slot

A GPS antenna is suggested in [37] which has four slots etched near edges of the patch for dual frequency operation and a center cross slot for generating circular polarization. Additional four short circuit microstrip stubs are loaded to reduce the frequency ratio.

These given designs for CP are on a square or a rectangular patch. Some designs are printed on a circular patch. The circular patch antenna which has a large (20MHz) circular polarization bandwidth for two frequency band with a 1.5 frequency ratio proposed in [38] is implemented by embedding two pairs of arc-shaped slots, with one of the arc-shaped slots having a narrow radial protruding slot, close to the boundary of the circular patch. Another circular patch design is formed by two concentric annular-ring patches that are placed on opposite sides of a substrate [39] which has a complex feeding mechanism. Wide circular polarization bandwidths (larger than 2%) determined by 3 dB axial ratio, are achieved at both bands for GPS. As mentioned in [40], the circular polarization is achieved with an embedded cross slot again, this time a circular patch is used instead of a rectangular patch.

Several circularly polarized microstrip antenna configurations have been reported. Also, some other methods are searched and studied for circular polarization too; diagonal feed on a nearly square patch, square patch with truncated corners, and a square patch with a diagonal slot. *“In the nearly square diagonal fed antenna configuration circular polarization is obtained because the two modes of resonance (corresponding to the adjacent sides of the rectangle) are spatially orthogonal. The antenna is excited at a frequency in between the resonant frequencies of these two modes in order to obtain the phase quadrature relationship between the voltages (and therefore magnetic currents) of two modes. Corner or diagonal feeding is required to allow both the modes to be excited with a single feed. In the truncated corners square patch antenna, the two orthogonal modes of resonance are diagonal modes which would individually yield linear polarization along the directions of the two diagonals. Chopping of the two corners makes the resonant frequency of the mode along this diagonal to be higher than that for the mode along the unchopped diagonal. The frequency of operation and the feed point are chosen such that the two modes are excited in phase quadrature. In square patch antenna with a diagonal slot, the two orthogonal modes are*

diagonal modes. The difference in the resonant frequencies is caused by the rectangular slot which disturbs one mode more than the other” [41].

CHAPTER 3

ANALYSIS AND DESIGN OF REACTIVELY LOADED DUAL BAND MICROSTRIP PATCH ANTENNA

3.1 Dual Band Linear Polarization Design with Rectangular Patch Antenna

In this chapter, a slot-loaded rectangular patch antenna with two narrow parallel slots is investigated to understand how to get the dual band characteristic. Its structure has been independently introduced in [7] and [29]. It consists of a rectangular patch with two narrow slots etched close and parallel to the radiating edge. The basic configuration is shown in Figure 3.1. Two narrow slots with dimensions $(W - 2l)$ and w are etched on the rectangular patch. The location of the slots with respect to the patch is defined by the dimensions d and l . In the basic structure, they are very small as compared to the dimensions L and W of the patch [7]. In this analysis, the probe feed is used to reduce the complexity.

“The resonant behavior of the slot-loaded patch antenna may be explained by starting from the cavity model description of an unslotted rectangular patch. The first three modes in a cavity are denoted by TM_{100} , TM_{200} and TM_{300} . These modes correspond to longitudinal currents distributed on the patch which have nulls at the radiating edges. The TM_{100} is the most used in practical applications since the TM_{200} mode has a broadside-null radiation pattern and the TM_{300} produces grating lobes. When the two narrow slots are etched close to the radiating edges (small values of l and d), minor perturbations of TM_{100} are expected because the slots are located close to the current minima” [7]. In this case, the patch current distribution is as shown in Figure 3.2.b.

“The radiative mechanism associated with this first mode is essentially the same as that of a patch without slots. As a consequence, its resonant frequency is only slightly different from that of a standard patch” [7].

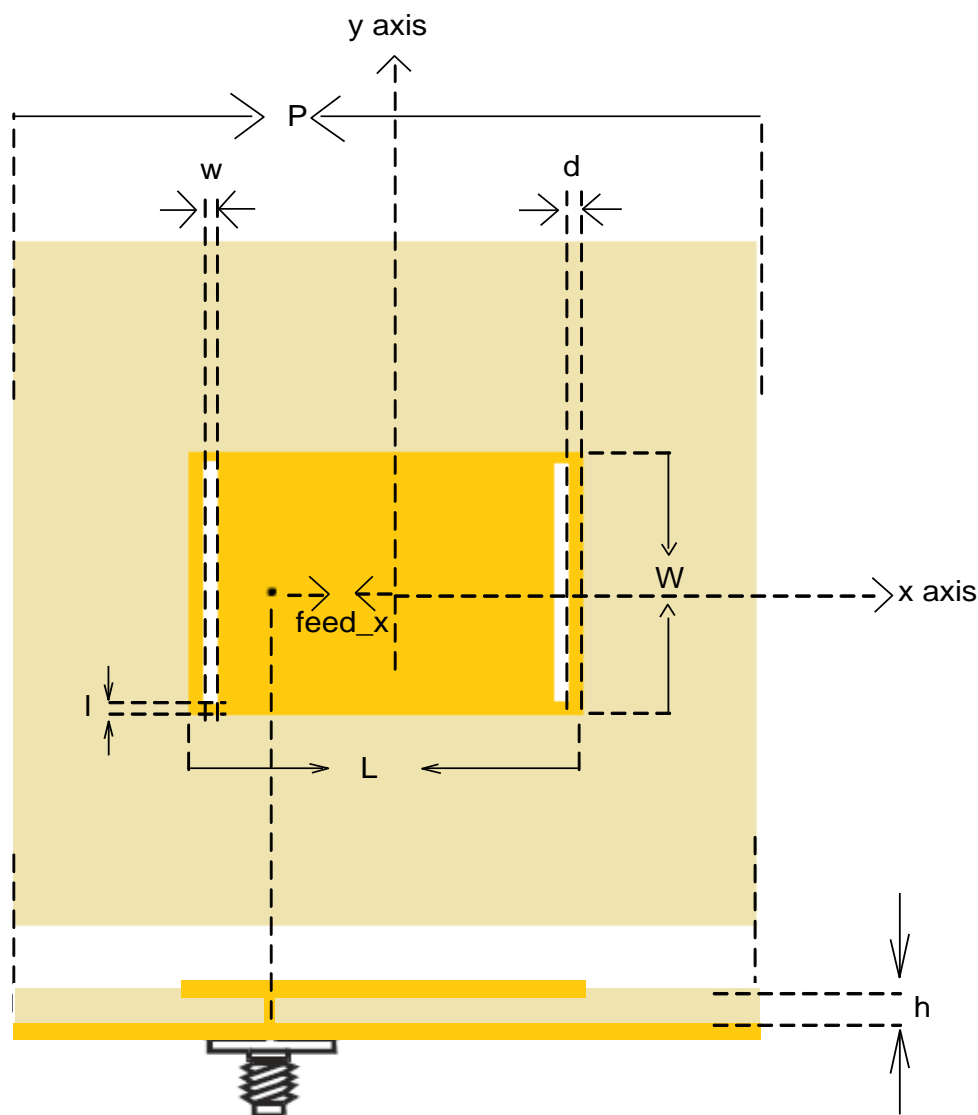


Figure 3.1 Probe feed slot-loaded patch antenna

“On the other hand, the slots are located where the current of the unperturbed TM_{300} are significant, so that this current is strongly modified” [7] and assumes the distribution depicted in Figure 3.2.d. “The currents circulate around the slot and find a resonant condition with nulls close to the two edges of each slot. This condition forces the central portion of the current distribution to be broader than

that associated with an unperturbed TM_{300} and becomes similar to that of the TM_{100} mode” [42]. Although Figure 3.2.d suggests that this mode is similar to TM_{100} mode for the region between slots, we will call this mode as the perturbed TM_{300} mode in the following. In fact the modes are not pure in this case and our naming is rather arbitrary. The perturbed TM_{300} mode has two properties; the resonant frequency is considerably decreased and, as shown subsequently, the radiation pattern loses the typical three-lobe shape of the unperturbed TM_{300} mode and becomes similar to that of the TM_{100} mode. So the radiation patterns of the antenna at the two frequencies are almost the same as that of an unslotted patch [7].

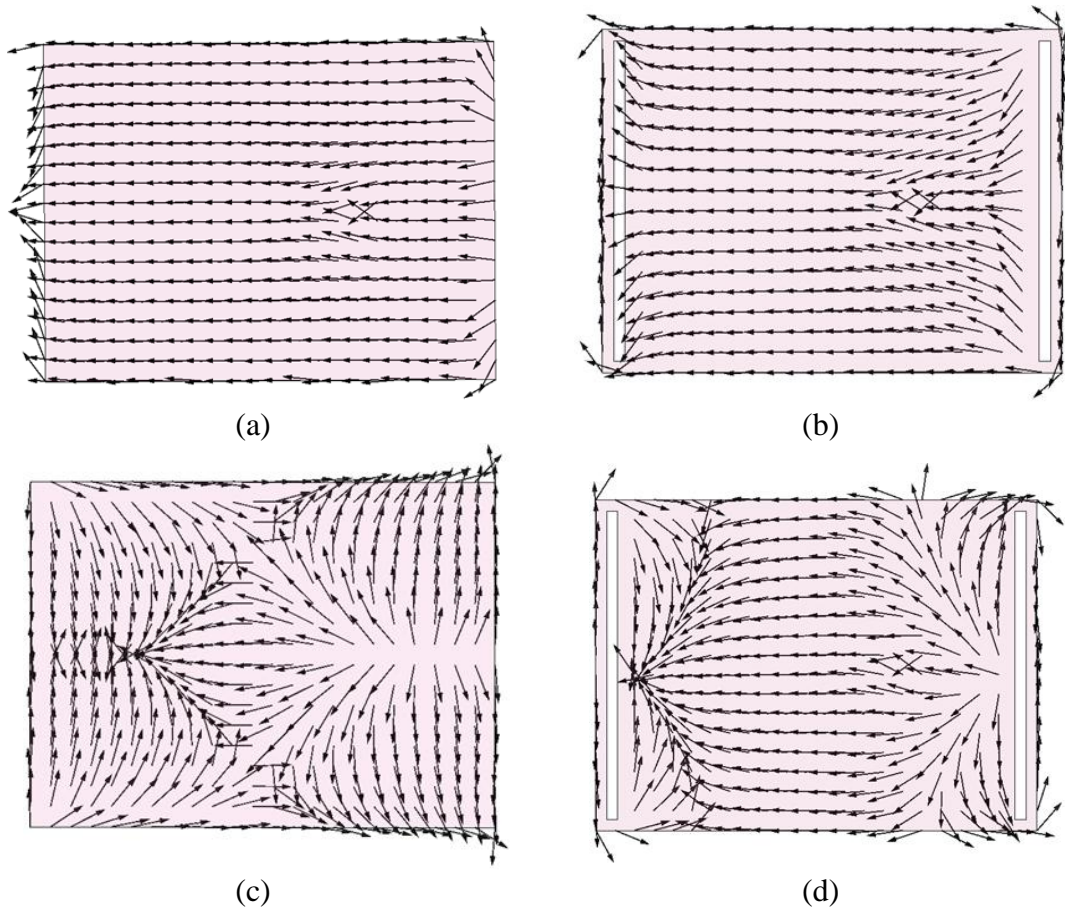


Figure 3.2 Current line distributions on slot-loaded rectangular patch (a) unperturbed TM_{100} (b) perturbed TM_{100} (c) unperturbed TM_{300} (d) perturbed TM_{300}

The perturbation of the TM_{300} mode current distribution also depends on the slot length that can lead to a significant deformation in the radiation pattern. Figure 3.3

shows the effect of a reduction of the slot length on the TM_{300} radiation pattern.

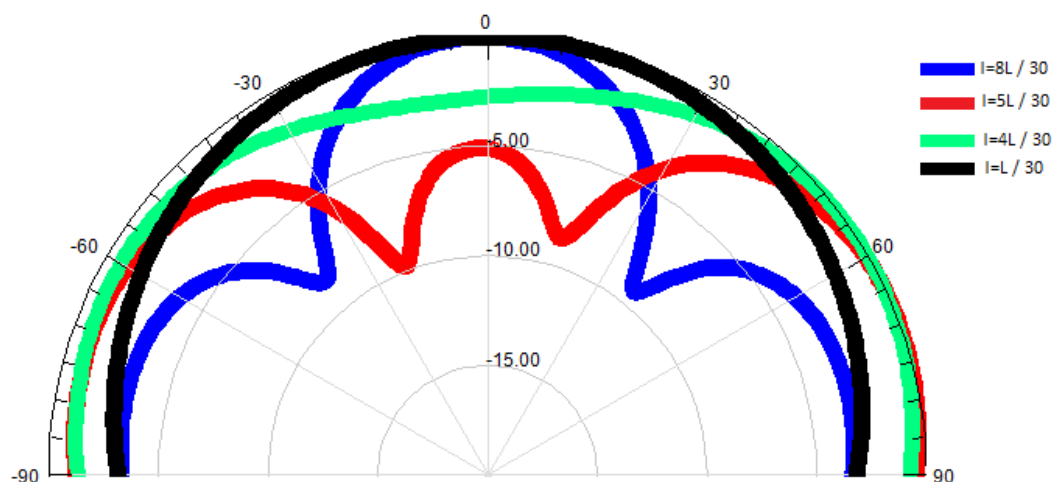


Figure 3.3 E-Plane far field pattern for different slot lengths on slot-loaded patch

For short slots, the radiation pattern has three lobes, such as that of an unperturbed TM_{300} mode. When the slot length increases, the central lobe reduces and disappears, as shown in Figure 3.3, when the far-field contribution of the current circulating around the slots completely cancels out the contribution of the currents in the central portion. This last mentioned contribution becomes gradually stronger when the slot length further increases, due to a larger extension of the central currents. The radiation pattern becomes increasingly similar to that of a standard patch in the TM_{100} configuration.

“The best antenna performance in terms of both radiative properties and simultaneous impedance matching at the two operating frequencies is obtained when the width w of the two slots is comparable with the thickness h of the substrate” [7].

Simple semi-empirical formulas for predicting the resonant frequencies are given in which the physical behavior of the slot-loaded patch antenna is easily readable [7] [42]. These formulas have been found very useful for antenna design. Denote by f_{100} and f_{300} the resonant frequencies associated with the modified TM_{100} and TM_{300} modes, respectively. As mentioned previously, the first resonance is not much affected by slot loading, so that its frequency can be predicted by slightly

modifying the well-established formula given in (1.4) for rectangular standard patches;

$$f_{100} = \frac{c}{2(L + \Delta L)\sqrt{\epsilon_e(W/h, \epsilon_r)}} G \quad (3.1)$$

where c is the free-space speed of light, ϵ_e is a function;

$$\epsilon_e(x, y) = \frac{y + 1}{2} + \frac{y - 1}{2} \left[1 + \frac{10}{x} \right]^{-1/2} \quad (3.2)$$

where ΔL is a function;

$$\Delta L = \frac{h W/h + 0.336}{\pi W/h + 0.556} + \left\{ 0.28 + \frac{\epsilon_r + 1}{\epsilon_r} \left[0.274 + \ln \left(\frac{W}{h} + 2.518 \right) \right] \right\} \quad (3.3)$$

and

$$G = \left[1 + \frac{\left(1.5 \frac{d}{L} - 0.4 \frac{1}{W} \right)}{1 + \frac{\Delta L}{L}} \right]^{-1} \quad (3.4)$$

where G is a correction factor that accounts for the slot-loading effect. The upper resonant frequency can be predicted according to a simple transmission line model, which can be derived from a direct inspection of the current distribution at the modified TM_{300} mode (Figure 3.2.d). “*The currents around the slots satisfy a resonant condition by circulating around the slots. The narrow portion of the conductor that encircles the slot behaves like two half wavelength open-circuit stubs*” [7], as schematized in Figure 3.4.



Figure 3.4 Equivalent model for second resonant frequency

“The effective dielectric constant of these equivalent stubs can be determined by assuming the microstrip line model with width d to describe the current distribution around the slot. This allows predicting the second resonant frequency according to” [42]

$$f_{300} = \frac{c}{2(W - 2l + w)\sqrt{\epsilon_e(d/h, \epsilon_r)}} \quad (3.5)$$

“It is worth noting that the distance between the two slots does not appear in this formula. In other words, the resonance condition of the TM_{300} mode is assumed independent of the central portion of the current distribution” [7]. On the other hand, the distance between the slots plays an important role on the radiation pattern. As mentioned before, TM_{100} resonant frequency is slightly different from a standard unslotted patch. The resonant frequency of TM_{300} mode depends on the reactive loading effect of slots. This confirms the capability of adjusting only the TM_{300} mode resonant frequency by changing the slot length.

In this study, it is found that relative differences between resonant frequencies evaluated from these semi-empirical formulas and the simulation results are in agreement within %2 error tolerances for the frequencies of interest.

By using this model, frequency ratio (FR) can be varied in a range from 1.6 to 2. Although this range can cover several cases of practical applications, lower values of FR is sometimes required. A simple arrangement that allows extension of the lower limit of the FR is proposed in [8]. This structure incorporates chip capacitors that are located across the slots that further increase the reactive loading. It is observed by simulations that using chip capacitors, frequency ratio can be reduced down to 1.25. The placement of chip capacitors is seen in Figure 3.5. Chip capacitors are placed at the center of the slots for simplicity.

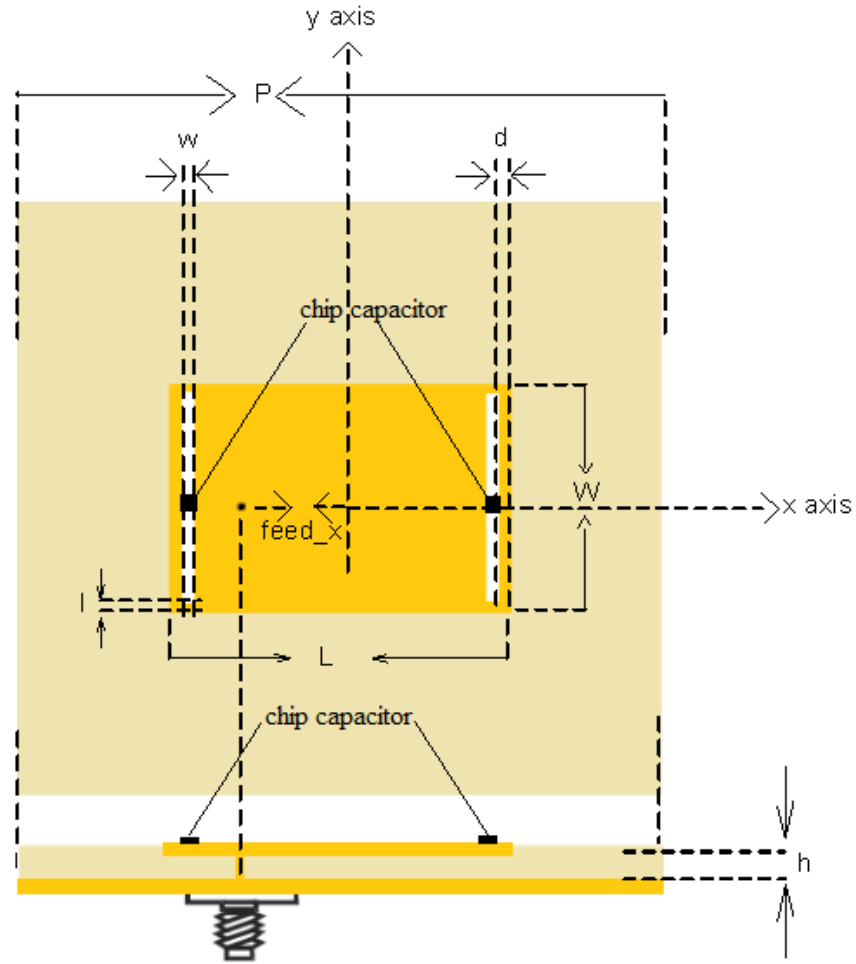


Figure 3.5 Rectangular microstrip antenna with dual-slot and chip capacitors loading for dual-band operation

For this structure, the given formulas for resonant frequencies of TM_{100} and TM_{300} modes are updated as;

$$f_{100} = \frac{c}{2(L + \Delta L)\sqrt{\epsilon_e(W/h, \epsilon_r) + k1 * p}} \quad (3.6)$$

$$f_{300} = \frac{c}{2(W - 2l + w)\sqrt{\epsilon_e\left(\frac{d}{h}, \epsilon_r\right) + k2 * p}} \quad (3.7)$$

where correction factors are $k1=0.008$ and $k2=0.045$ and p is the capacitance in pF [8].

The return loss for the different values of capacitance from 0 to 1pF with 0.2pF steps is shown Figure 3.6. FR4 substrate ($\epsilon_r = 4.4$) with thickness 1.6mm is used. The rectangular patch has dimensions 40mmx30mm, and a pair of slots of size 28mmx1mm are etched near the radiating edges of the rectangular patch at a distance of 1mm. The size of the ground plane is chosen to be 75mmx75mm.

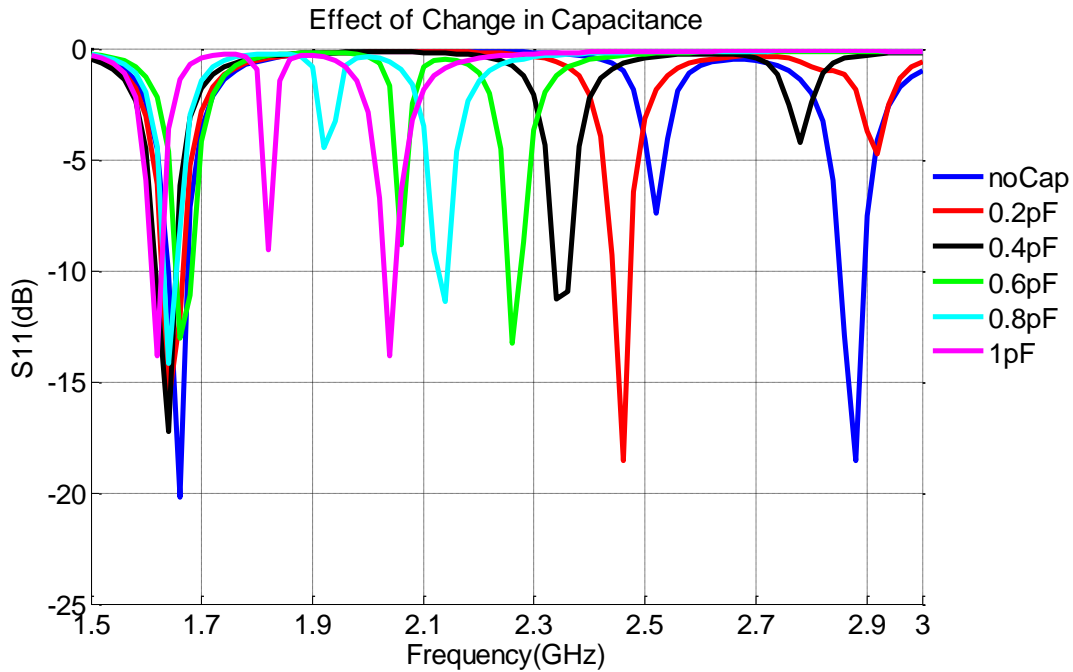


Figure 3.6 Return loss for rectangular patch with various capacitance ($\epsilon_r = 4.4$, $h = 1.6\text{mm}$, $L = 40\text{mm}$, $W = 30\text{mm}$, $l = 1\text{mm}$, $w = 1\text{mm}$, $d = 1\text{mm}$)

“It is found that the resonance of the first (lower) operating mode (the perturbed TM_{100} mode) was slightly affected by the variation in the capacitance. However, the resonant frequency of the second (higher) operating mode (the perturbed TM_{300} mode) is significantly decreased with increasing capacitance” [8].

Dual band characteristic of reactively loaded microstrip patch antenna and chip capacitor effect on frequency ratio is investigated on a rectangular patch. Proposed semi-empirical formulas are used and compared with the simulation results.

The lower frequency can be predicted according to equation (3.6), in which the factor G assumes the different expression;

$$G = 1.13 - 0.19 \frac{L_s}{W} - 0.73 \frac{d}{W} \quad (3.8)$$

where $L_s = (L_{s1} + L_{s2})/2$ is taken into calculation. Regarding the upper frequency, the same model as reported for the slotted rectangular-patch antenna can be applied, thus leading to equation (3.7). *“However, in this case, the accuracy is worse than that for the slotted rectangular-patch antenna, due to the fact that the model does not account for the coupling between the parallel slots. This deficiency, which is not significant for the slotted rectangular patch antenna, assumes here more importance, due to the square geometry. Furthermore, the slotted square-patch antenna exhibits a smaller range of frequency ratio than the slotted rectangular-patch antenna”* [42].

“Both the resonant frequency f_{100} and f_{300} of the square microstrip patch can be split into two near-degenerate resonant modes with equal amplitudes and 90° phase difference, respectively. With such an arrangement of different slot lengths, the frequency of the resonant mode in a direction perpendicular to the long slot will be slightly lower than that of the resonant mode in a direction perpendicular to the shorter slot” [8]. When $L_{s1} > L_{s2}$, right-hand circular polarization operation can be obtained. Alternatively, when $L_{s1} < L_{s2}$, left-hand circular polarization operation can be achieved. In the situation of the equivalence of the slot lengths, circular polarization operation cannot be obtained.

The simulation results for a square patch which has dimensions of 54mmx54mm and two pairs of slots of size $L_{s1}=42.5\text{mm}$ and $L_{s2}=41\text{mm}$ with 1mm width on FR4 substrate with thickness 1.6 mm are given in Figure 3.8, Figure 3.9 and Figure 3.10.

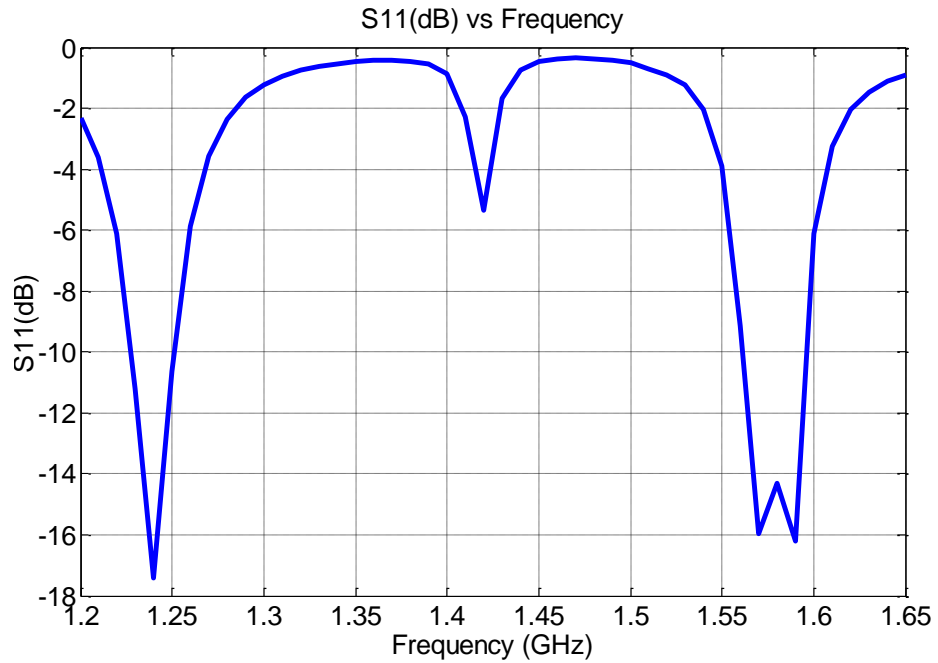


Figure 3.8 Return loss for square patch ($\epsilon_r = 4.4$, $h = 1.6\text{mm}$, $W = L = 54\text{mm}$, $L_{s1} = 42.5\text{mm}$, $L_{s2} = 41\text{mm}$, $w = 1\text{mm}$, $d = 1\text{mm}$, capacitance = 0.9pF)

As seen from Figure 3.8, the square patch antenna can operate at both L1 (1575MHz) and L2 (1227MHz) operating frequencies for GPS application.

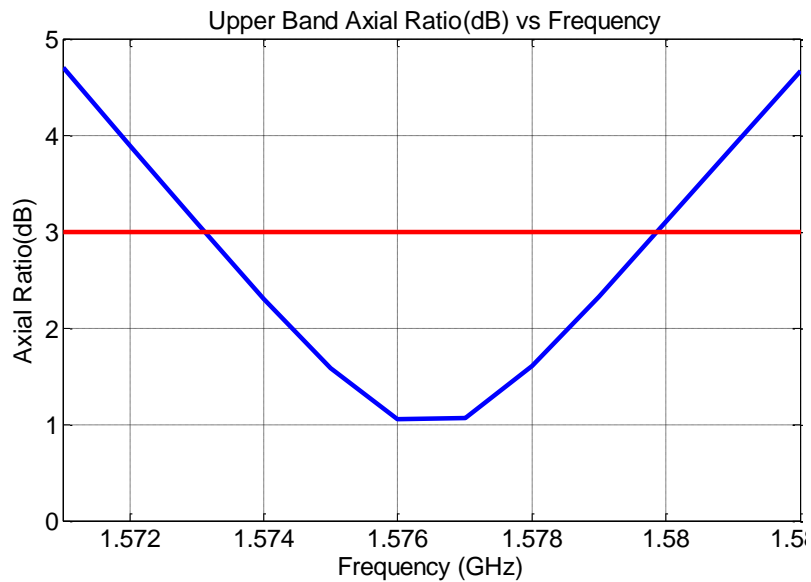


Figure 3.9 Axial ratio for upper resonance band of square patch

The upper resonance band shows a good circular polarization performance for 8MHz CP bandwidth as seen from Figure 3.9. However, as seen from Figure 3.10 circular polarization criterion is not satisfied with this design.

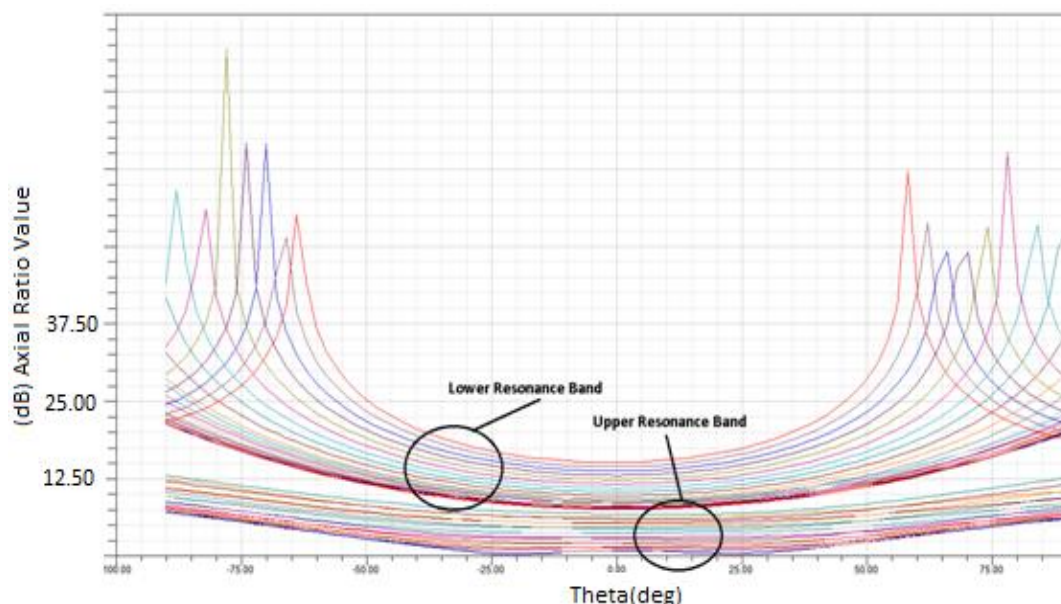


Figure 3.10 Axial ratio for square patch - lower band = (1.22GHz to 1.25GHz)
upper band = (1.57GHz to 1.585GHz)

The values of axial ratio are too high over the lower resonance band as seen in Figure 3.10. Therefore, we focused on improving the circular polarization over the lower band. Techniques explained in Chapter 2 for circular polarization are considered. Cutting of the corners of the square patch is tried. Feed is positioned on the y axis for this study. However, this technique is not useful. To explain this result, we can consider the antenna as composed of two parts: the narrow portion outside the slots that behaves like open circuit stubs of one wavelength and the portion inside the slots. The latter part shapes the TM_{100} mode (lower frequency) while the former affects the TM_{300} mode (higher frequency). Trimming of the corners is not useful since the corners are isolated from the inner part by the slots. HFSS simulation results show that cutting of the corners has little effect on both lower and upper bands. The second structure considered to contain a diagonal slot at the center of the patch. The upper band is not affected, but if the feed is kept on the diagonal, the lower band disappears. Therefore, the feed position is changed seen in Figure 3.11 as described in [3].

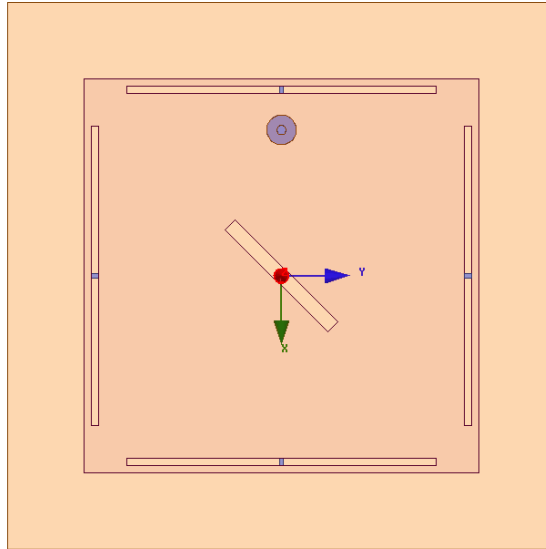


Figure 3.11 The model of square patch antenna with a diagonal slot

The feed is positioned at the right part of the diagonal slot to have the same polarization direction with upper band. However, the change of feed position from the diagonal axis with the existence of a diagonal slot changes the current distribution on the patch that forms TM_{300} mode, which is now different from TM_{100} and causes to worsen the upper band return loss and circular polarization performance.

Finally, the nearly square patch antenna with diagonal feeding is considered. Length of the side which is perpendicular to shorter slots L_{s2} is increased a little. The feed is arranged to be on the diagonal of the patch. Slot lengths L_{s1} and L_{s2} are changed in order to obtain a good impedance matching with respect to the parametric analysis, which is discussed in the next chapter.

A nearly square patch antenna as seen in Figure 3.12 with dimensions $L=54\text{mm}$ and $W=55.8\text{mm}$ which has two pairs of slots, with lengths $L_{s1}=41.6\text{mm}$ and $L_{s2}=41\text{mm}$ and width of $w=1\text{mm}$ close to the radiating edges at a distance of $d=1\text{mm}$, supported by 0.9 pF capacitance values on $h=1.6\text{mm}$ FR4 substrate ($\epsilon_r=4.4$) is designed. From the simulation results good impedance matching is obtained for both bands as shown in Figure 3.13. The lower band is from 1205 MHz to 1251 MHz and the upper band is from 1563 MHz to 1594 MHz .

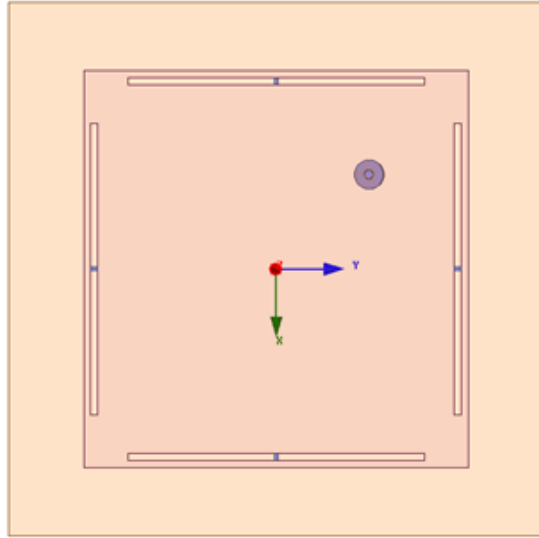


Figure 3.12 The model of nearly square patch antenna with diagonal feeding

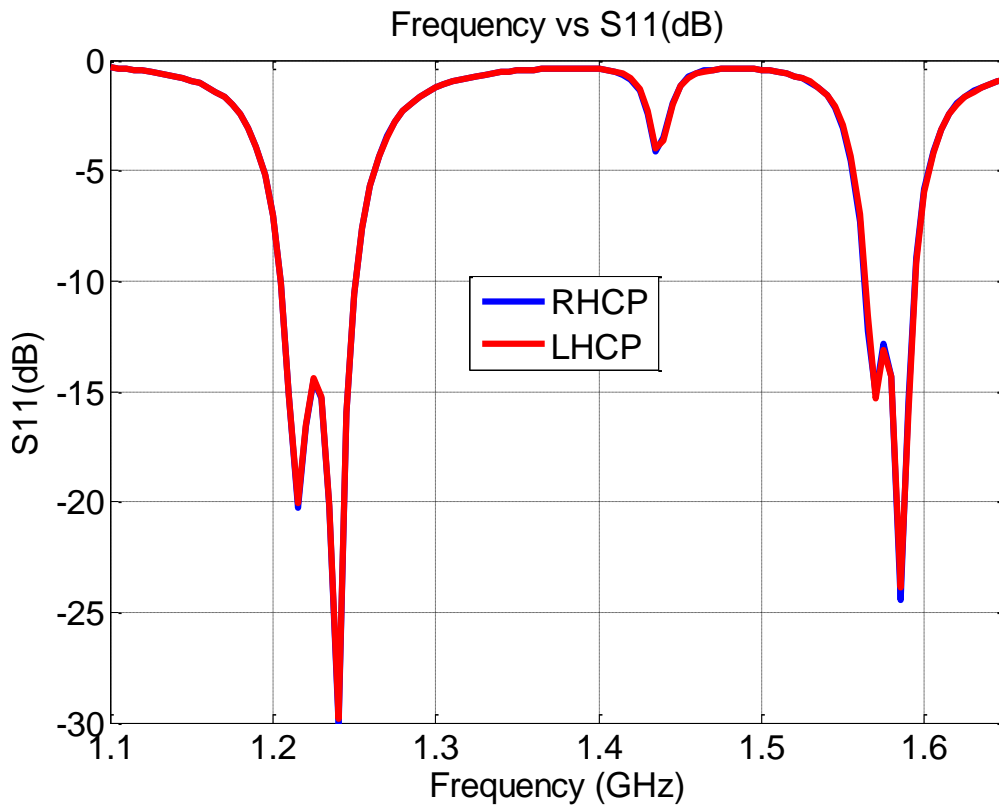


Figure 3.13 Return loss for nearly square patch ($\epsilon_r = 4.4$, $h = 1.6\text{mm}$, $W = 55.8\text{mm}$, $L = 54\text{mm}$, $L_{s1} = 41.6\text{mm}$, $L_{s2} = 41\text{mm}$, $w = 1\text{mm}$, $d = 1\text{mm}$, capacitance = 0.9pF)

Both operating bands have 8 MHz circular polarization bandwidth in which the frequencies that has an axial ratio under 3 dB are included as shown in Figure 3.14 and Figure 3.15.

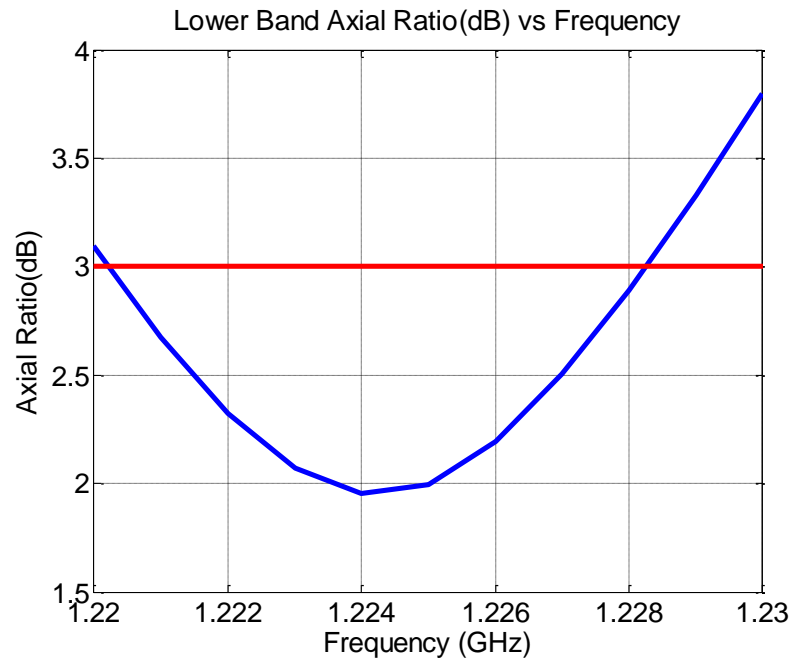


Figure 3.14 Axial ratio for the lower resonance band of nearly square patch

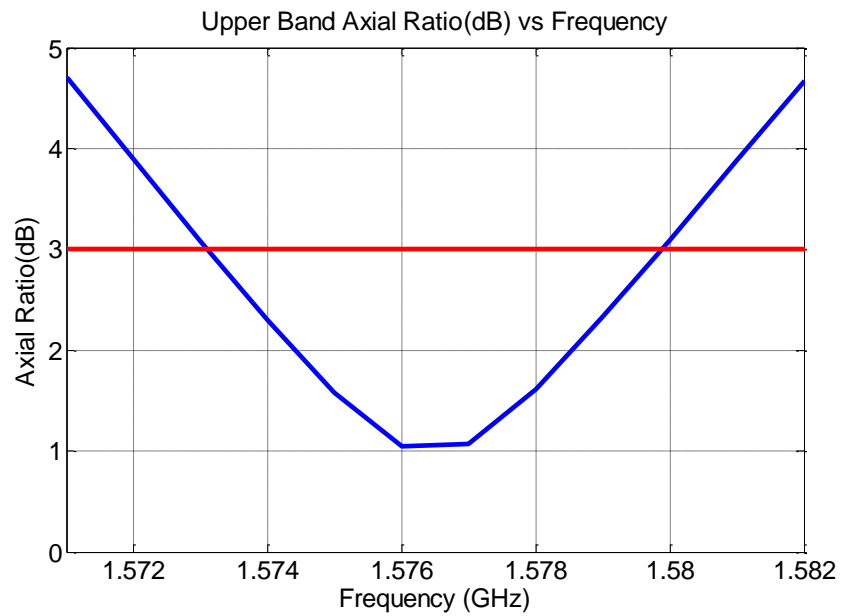


Figure 3.15 Axial ratio for the upper resonance band of nearly square patch

Directivities for right hand circular polarized components of the far field pattern of the two resonant frequencies at the best axial ratio are shown in Figure 3.16. The antenna directivities at both frequencies in the broadside direction ($\theta=0^\circ$) are 6.69 dBi and 7.26 dBi, respectively.

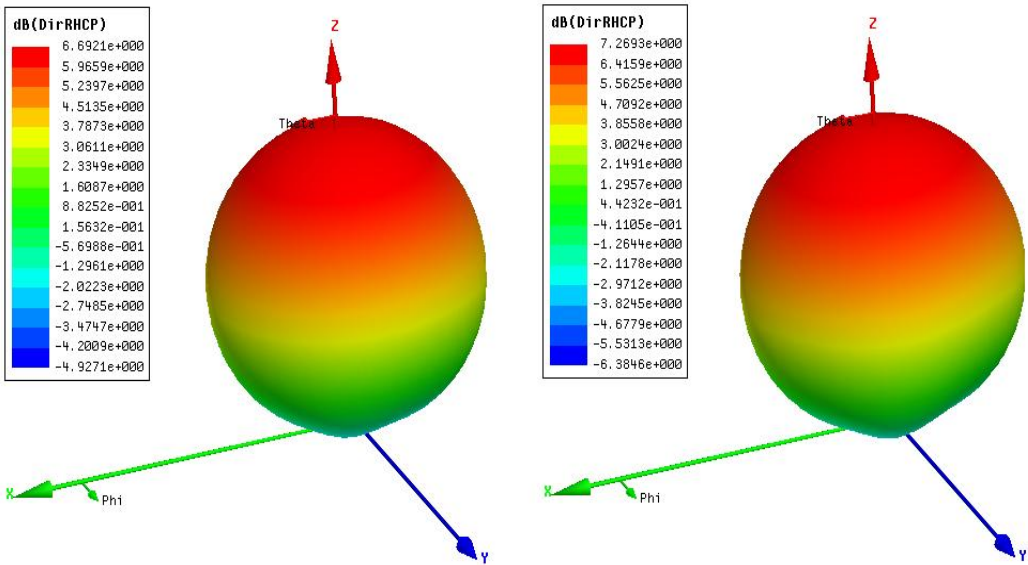


Figure 3.16 RHCP-Directivity (dB) for lower (1224MHz) and upper (1577MHz) resonance band of nearly square patch respectively

If feed is positioned in the next quadrant as shown in Figure 3.17, referring the feed position if $L_{s1} < L_{s2}$, left hand circular polarization can be achieved. LHCP configuration has the same frequencies which have the axial ratio values less than 3 dB, which are plotted in Figure 3.14 and Figure 3.15. Directivity for left hand circular polarized components of the far field pattern of the two resonant frequencies with the best axial ratio is shown in Figure 3.18.

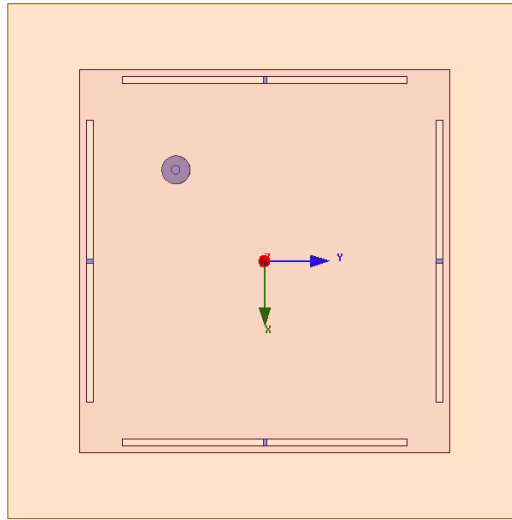


Figure 3.17 The model of left hand circularly polarized nearly square patch antenna with diagonal feeding

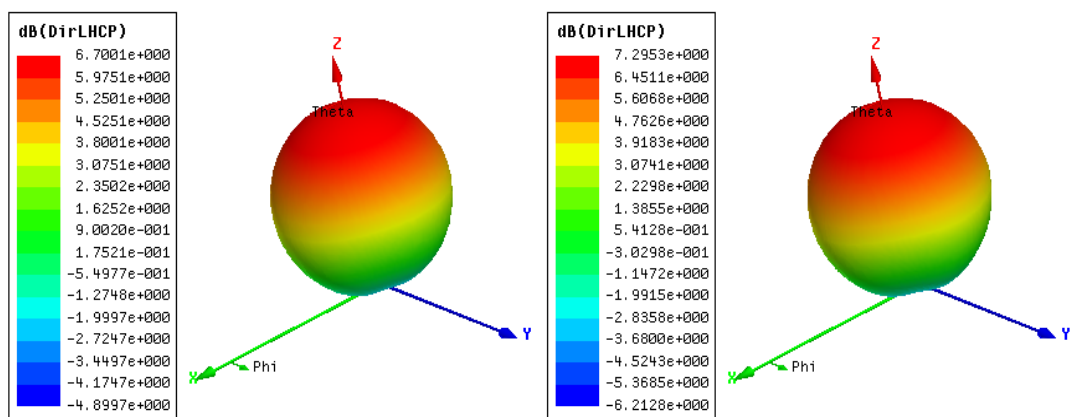


Figure 3.18 LHCP-Directivity (dB) for lower (1224MHz) and upper (1577MHz) resonance band of nearly square patch respectively

The antenna can work well for GPS applications as it operates on both L1 = 1575.42 MHz and L2 = 1227.60 MHz frequencies in terms of its return loss, circular polarization and directivity characteristics.

CHAPTER 4

PARAMETRIC ANALYSIS OF DUAL BAND CIRCULARLY POLARIZED MICROSTRIP ANTENNA

A parametric analysis of dual band slot loaded circularly polarized microstrip antenna is performed and the results are given in this chapter. All the analyses are done in HFSS. Effects of parameters on a nearly square slot loaded patch antenna are observed. Return loss and axial ratio value are investigated for each configuration. FR4 ($\epsilon_r = 4.4$, $h = 1.6\text{mm}$) dielectric substrate is selected for the design. It is selected in accordance with availability and there are many examples in the literature that use a single layer FR4 substrate. Other antenna design parameters are given in Figure 4.1 and Table 4.1

Table 4.1 Design parameters of nearly square slot loaded microstrip antenna

Name of The Parameter	Definition	Nominal Value
L	Patch Length	54mm
ΔL	Difference Between Length and Width	1.8mm
d	Distance of Slots to Edges	1mm
W_s	Slot Width	1mm
L_{s1}	Length of Slot in x Direction	41.6mm
L_{s2}	Length of Slot in y Direction	41mm
Capacitance	Value of Chip Capacitors	0.9pF
h	Substrate Thickness	1.6mm
feed_x	Distance from Center of the Patch to the Feed in x Axis	13.5mm

Table 4.1 (continued)

feed_y	Distance from Center of the Patch to the Feed in y Axis	13.95mm
P	Length of Ground Plane	75mm

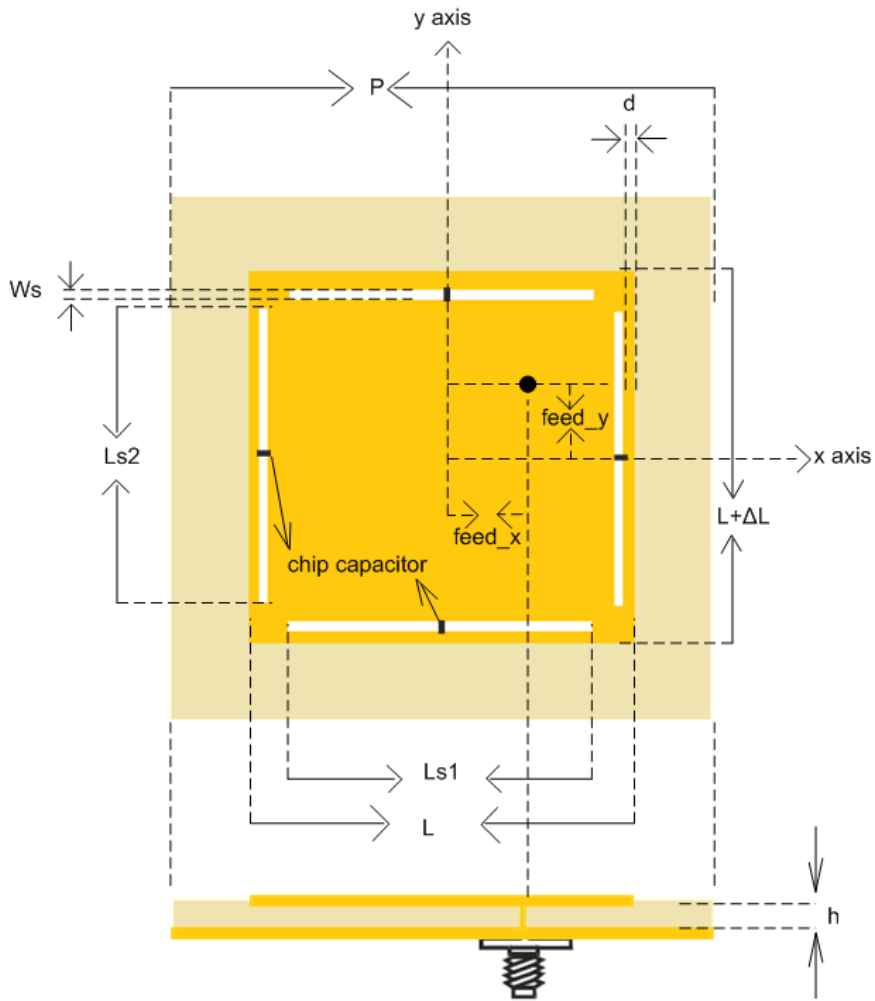


Figure 4.1 Geometry of nearly square slot loaded microstrip antenna

Observing the effect of the change in capacitance values is a time consuming analysis when it has been done for each different value individually in HFSS. Because of that a post-processing to calculate the return loss of the feed port for all capacitance values at one time is described in the following subsection. After that the effect of changing design parameters in Table 4.1 is observed. In each

parametric study, one variable is changed while keeping the others constant except for the patch length. In the parametric analysis of the patch length, the slot length of L_{s1} and L_{s2} are divided by the ratio of change in the patch length to see the effect of changing L more accurate.

4.1 Post-Processing for Return Loss in the Change of Capacitance Value

As mentioned before analyzing all capacitance values individually in HFSS is a time consuming way to get return losses of these designs. Instead of that an approach is suggested in which lumped RLC elements (chip capacitors) in HFSS design are changed to lumped RLC excitation ports terminated with 50ohm. Four rectangular sheets with dimensions of 1mm and 0.5mm have been chosen as an excitation port for the design in the place of the chip capacitors as shown in Figure 4.2.

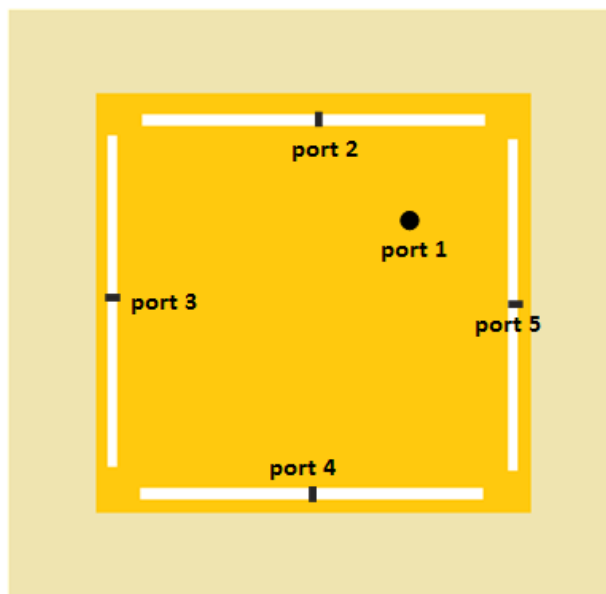


Figure 4.2 Use of lumped ports instead of the chip capacitors

The antenna is realized as a five port microwave network with the existence of lumped RLC excitation ports, as shown in Figure 4.3.

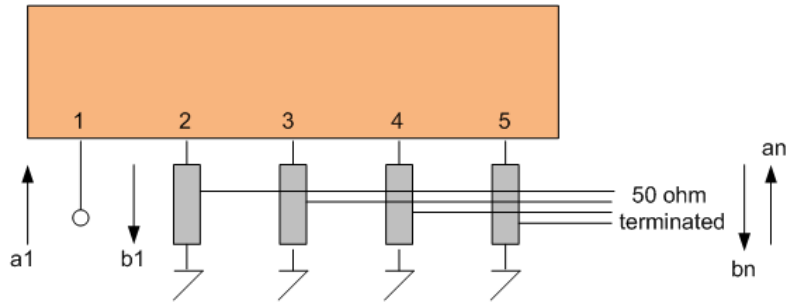


Figure 4.3 Microwave network representation of the antenna

Reflection coefficients for the ports from 2 to 5 are given by;

$$\Gamma_n = \frac{Z_n - Z_0}{Z_n + Z_0} \quad (4.1)$$

where Z_0 is 50 ohm and Z_n is the arbitrary load that is determined by the capacitance value by the equation;

$$Z_n = \frac{1}{j2\pi fC} \quad (4.2)$$

where f is the frequency in Hz and C is the capacitance value in Farad. A matrix form relation between incident and reflected waves of the these lumped ports can be set by using these reflection coefficients;

$$\begin{bmatrix} a_2 \\ a_3 \\ a_4 \\ a_5 \end{bmatrix} = \begin{bmatrix} \Gamma_2 & 0 & 0 & 0 \\ 0 & \Gamma_3 & 0 & 0 \\ 0 & 0 & \Gamma_4 & 0 \\ 0 & 0 & 0 & \Gamma_5 \end{bmatrix} \begin{bmatrix} b_2 \\ b_3 \\ b_4 \\ b_5 \end{bmatrix} \quad (4.3)$$

This 4 by 4 matrix is symbolized by G.

The relation between scattering matrix and complex power waves for the overall five port network is known as;

$$\begin{bmatrix} b_1 \\ b_2 \\ b_3 \\ b_4 \\ b_5 \end{bmatrix} = \begin{bmatrix} S_{11} & S_{12} & S_{13} & S_{14} & S_{15} \\ S_{21} & S_{22} & S_{23} & S_{24} & S_{25} \\ S_{31} & S_{32} & S_{33} & S_{34} & S_{35} \\ S_{41} & S_{42} & S_{43} & S_{44} & S_{45} \\ S_{51} & S_{52} & S_{53} & S_{54} & S_{55} \end{bmatrix} \begin{bmatrix} a_1 \\ a_2 \\ a_3 \\ a_4 \\ a_5 \end{bmatrix} \quad (4.4)$$

Divide the complex power waves and scattering matrix for lumped ports to separate matrices;

$$\alpha = \begin{bmatrix} a_2 \\ a_3 \\ a_4 \\ a_5 \end{bmatrix} \quad \delta = \begin{bmatrix} b_2 \\ b_3 \\ b_4 \\ b_5 \end{bmatrix}$$

$$A = [S_{12} \quad S_{13} \quad S_{14} \quad S_{15}] \quad B = \begin{bmatrix} S_{21} \\ S_{31} \\ S_{41} \\ S_{51} \end{bmatrix} \quad C = \begin{bmatrix} S_{22} & S_{23} & S_{24} & S_{25} \\ S_{32} & S_{33} & S_{34} & S_{35} \\ S_{42} & S_{43} & S_{44} & S_{45} \\ S_{52} & S_{53} & S_{54} & S_{55} \end{bmatrix}$$

Using this partitioning, the scattering matrix becomes;

$$\mathbf{b} \begin{Bmatrix} \begin{bmatrix} b_1 \\ b_2 \\ b_3 \\ b_4 \\ b_5 \end{bmatrix} \\ \end{Bmatrix} = \begin{bmatrix} S_{11} \\ \mathbf{B} \end{bmatrix} \begin{bmatrix} a_1 \\ \alpha \end{bmatrix} \quad (4.5)$$

This partitioned expression can be decomposed into the following two matrix equations:

$$b_1 = S_{11}a_1 + A\alpha \quad (4.6)$$

$$\delta = B\alpha + C\alpha \quad (4.7)$$

Rewriting equation (4.3) as

$$\alpha = G\delta \quad (4.8)$$

Using equation (4.8) in equation (4.7)

$$\begin{aligned}
 b_1 &= Ba_1 + CGb_1 \\
 \downarrow \\
 b_1(I - CG) &= Ba_1 \\
 \downarrow \\
 b_1 &= (I - CG)^{-1}Ba_1
 \end{aligned}$$

Using this result in equation (4.7),

$$b_1 = S_{11}a_1 + AG(I - CG)^{-1}Ba_1 \quad (4.9)$$

is found. For any arbitrary load, b_1/a_1 gives the return loss for port 1.

$$S_{11}' = \frac{b_1}{a_1} = S_{11} + AG(I - CG)^{-1}B \quad (4.10)$$

is the formula to easily get the return loss for different capacitance values.

This approach is expected to work because the boundary conditions of the antenna are not changing significantly and all the equations are linear. This process is checked with the results of a simulation with chip capacitors and another simulation with lumped RLC ports on design. The return losses are sketched together in Figure 4.4.

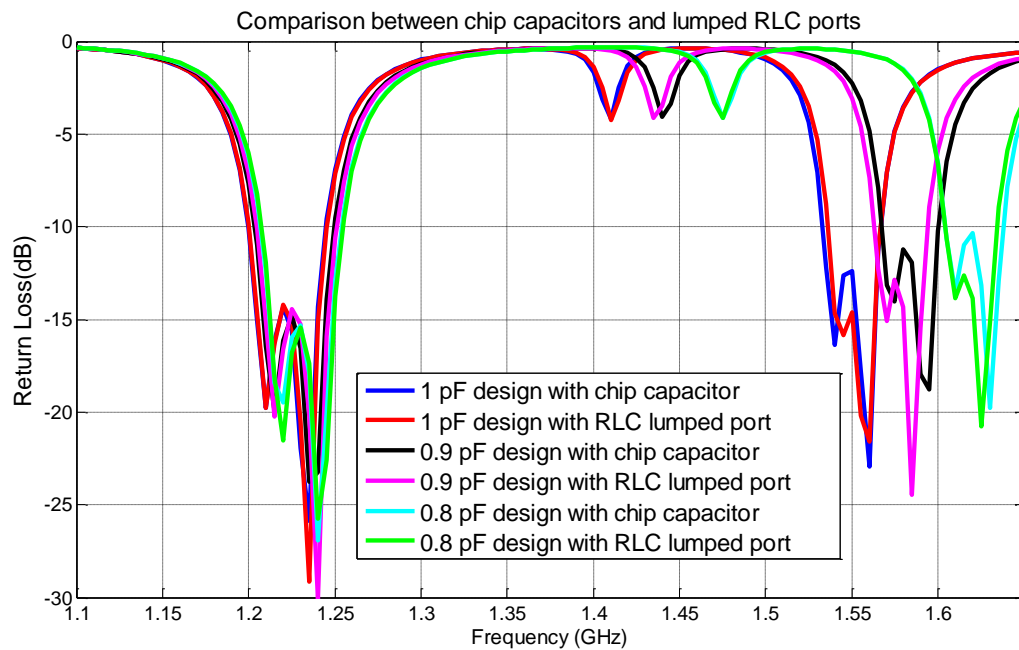


Figure 4.4 Comparison of two methods to get return loss

Some difference is observed because the solution frequency of HFSS which is a HFSS property affects the general solution a little. This difference is seen even when solving the design with chip capacitors in slightly different solution frequencies. In spite of that fact this method is fast and useful to estimate the return loss of the antenna.

4.2 Effect of Changing Length

This parameter has an effect on the resonant frequency of the unslotted microstrip patch antenna whereas same effect is seen in the dual frequency operation. In this dual frequency design initially the length of the microstrip is chosen to resonate at TM_{100} mode. Length is chosen by the formula;

$$L = \frac{c}{2f\sqrt{\epsilon_{\text{eff}}}} - 2\Delta L \quad (4.11)$$

where ϵ_{eff} and ΔL are given in the first chapter. This value is 58.1mm for 1227 MHz. After the slots are etched it is seen that reactive loading decreases the resonance frequency of TM_{100} mode so the same resonant frequency can be obtained with smaller length. In this subsection, the effect of changing the patch length is observed under reactive loading.

The effect of changing length is investigated with the results of input impedance and axial ratio value. The width of the microstrip patch has also an effect on the characteristics of the microstrip antenna. However, the aim of this thesis is to design a circularly polarized antenna. Because of that, in all cases, the width of the patch is chosen to be nearly equal to the length of the patch, so that a nearly square patch is considered. Aspect ratio is kept constant between the patch length and patch width. The differences $(L - L_{s1})$ and $(L + \Delta L - L_{s2})$ Are kept constant too for clearly investigating the effect of changing the length. Other parameters are kept constant at values given in Table 4.1.

Table 4.2 Parameters and their values in effect of length analysis

Case	Length(mm)	Width(mm)	ΔL (mm)	L_{s1} (mm)	L_{s2} (mm)
1	52	53.73	1.73	39.6	38.93
2	53	54.76	1.76	40.6	39.96
3	54	55.8	1.8	41.6	41
4	55	56.83	1.83	42.6	42.03
5	56	57.86	1.86	43.6	43.07

As shown in Figure 4.5, first resonant frequency decreases by increasing the length of the microstrip patch. This scenario is true for an unslotted patch too. As the first resonant frequency decreases, TM_{300} generated second resonant frequency decreases too.

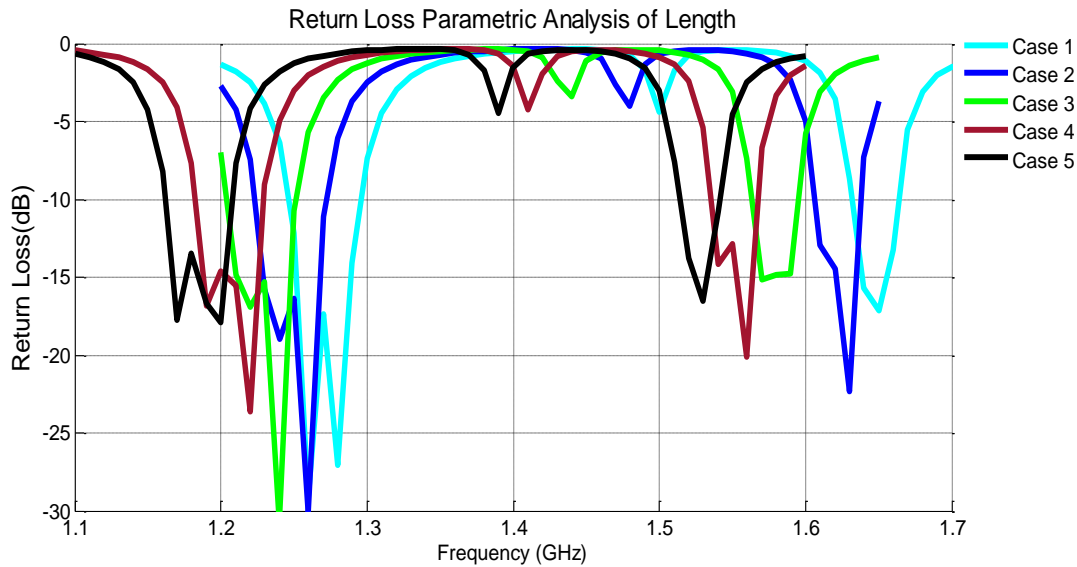


Figure 4.5 Return losses for different values of length

The change in the second resonant frequency is comparable with the first one. It can be seen from Figure 4.6 and Figure 4.7 circularly polarized bandwidths are 7-8 MHz for all cases. The circularly polarized frequency band follows the resonance band as length of the patch changes. Length of the patch shifts the resonance frequencies of both the lower and upper band.

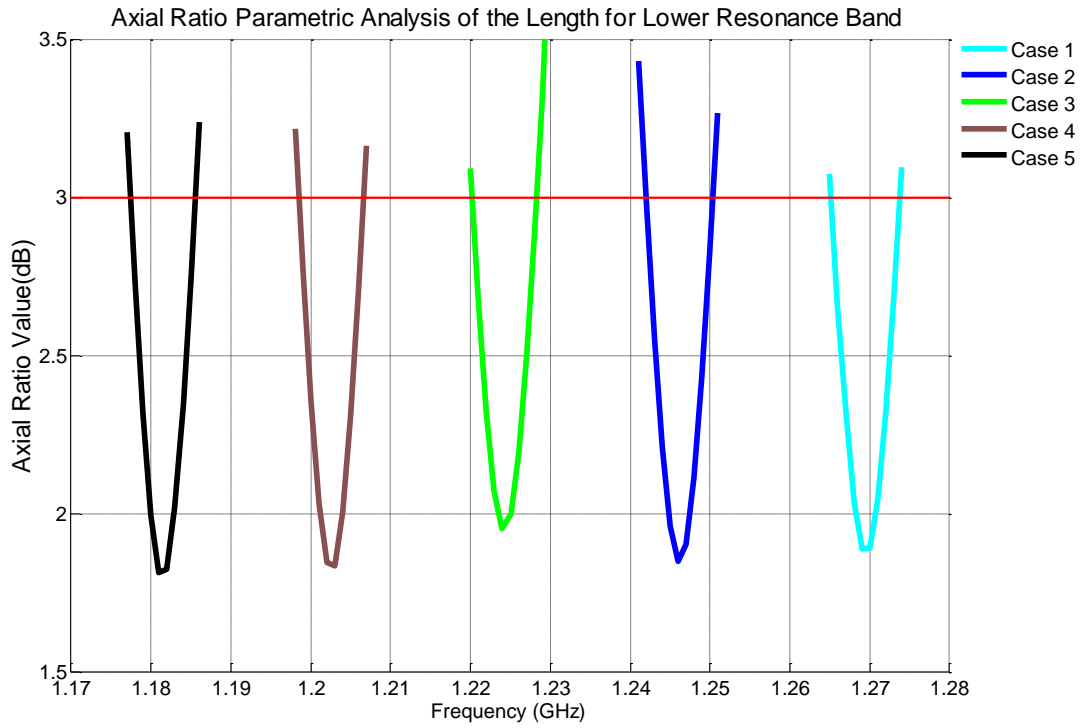


Figure 4.6 Axial ratio values for the lower resonance band for different values of length

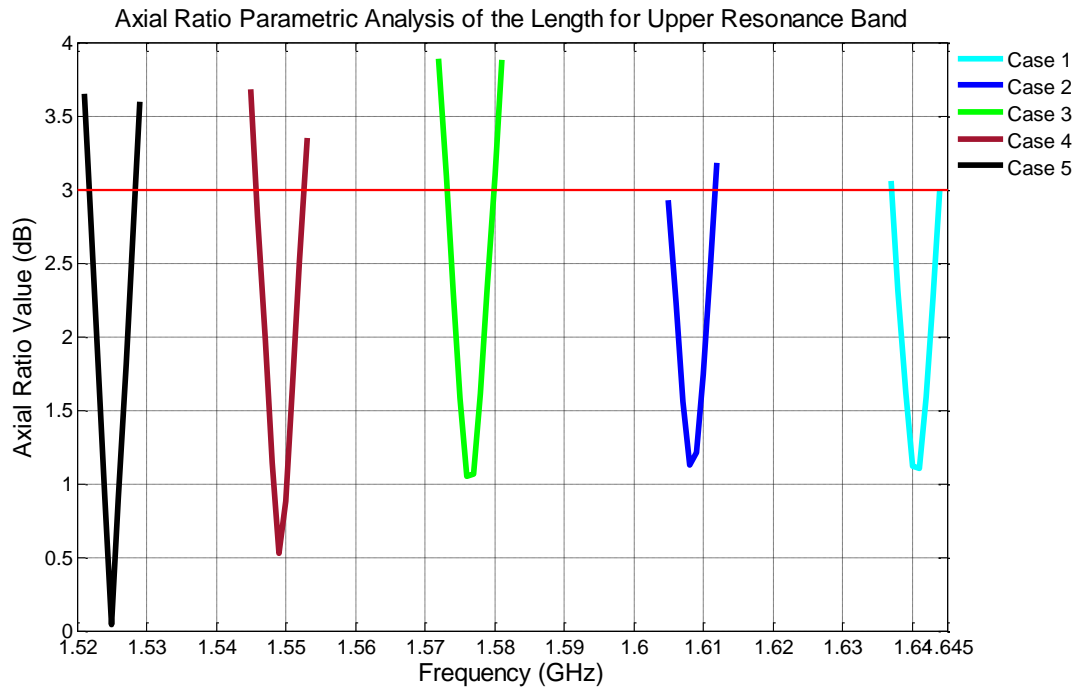


Figure 4.7 Axial ratio values for the upper resonance band for different values of length

4.3 Effect of Changing Capacitor

Effects of capacitance variation on the return loss and axial ratio are given in this subsection. Parametric analysis is done by changing the capacitance values from 1pF to 0.

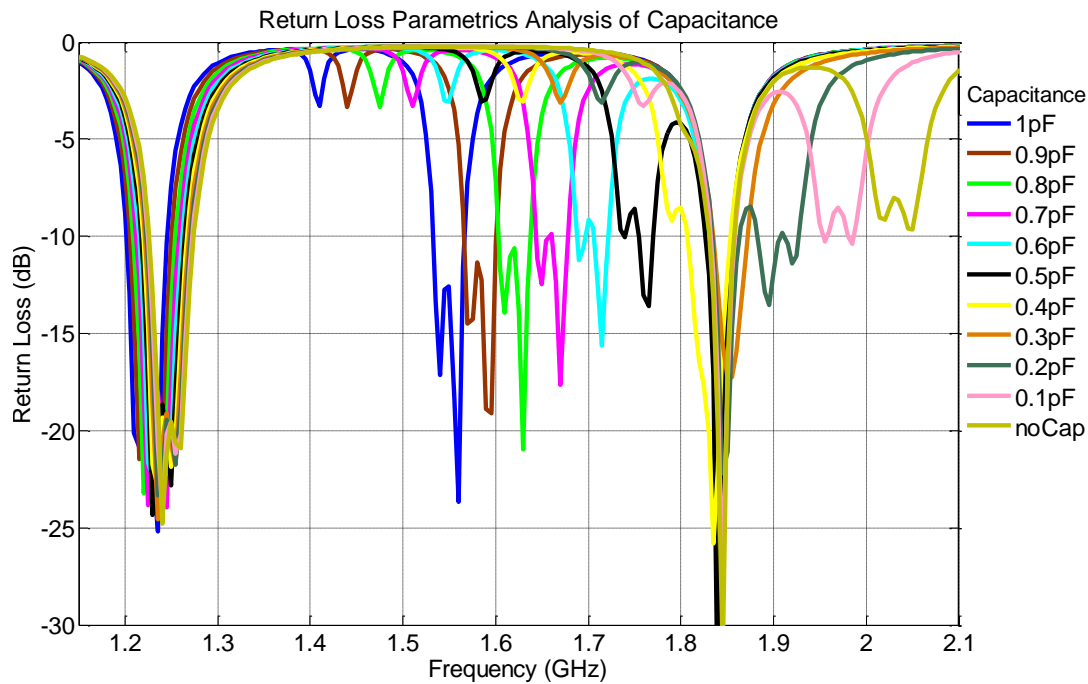


Figure 4.8 Return losses for different values of capacitance

The return loss is shown in Figure 4.8 for the different values of capacitance from 0 to 1 pF. The resonance of the first operating mode is slightly affected by the variation in the capacitance. However, the resonant frequency of the second operating mode significantly increases with the decrease in capacitance. This parameter has the biggest role on the frequency ratio. As seen from Figure 4.9 and Figure 4.10, the axial ratio is not affected by changing capacitance and remains 7-8 MHz circular polarization bandwidth. The circularly polarized frequency band follows the resonance band as capacitance changes.

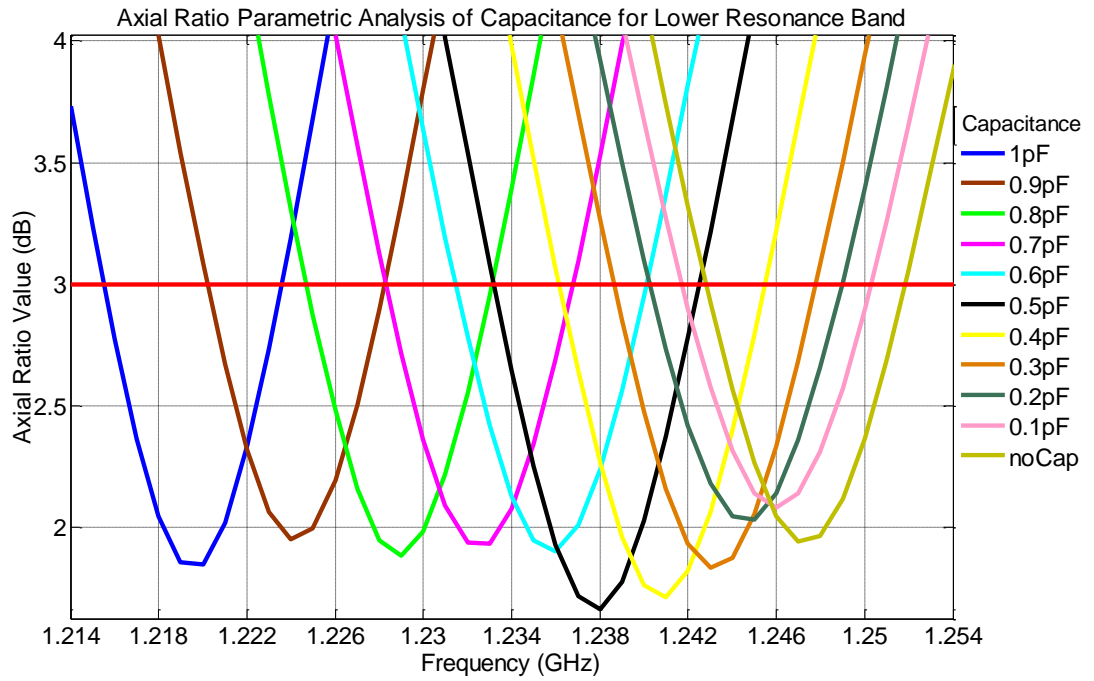


Figure 4.9 Axial ratio values for the lower resonance band for different values of capacitance

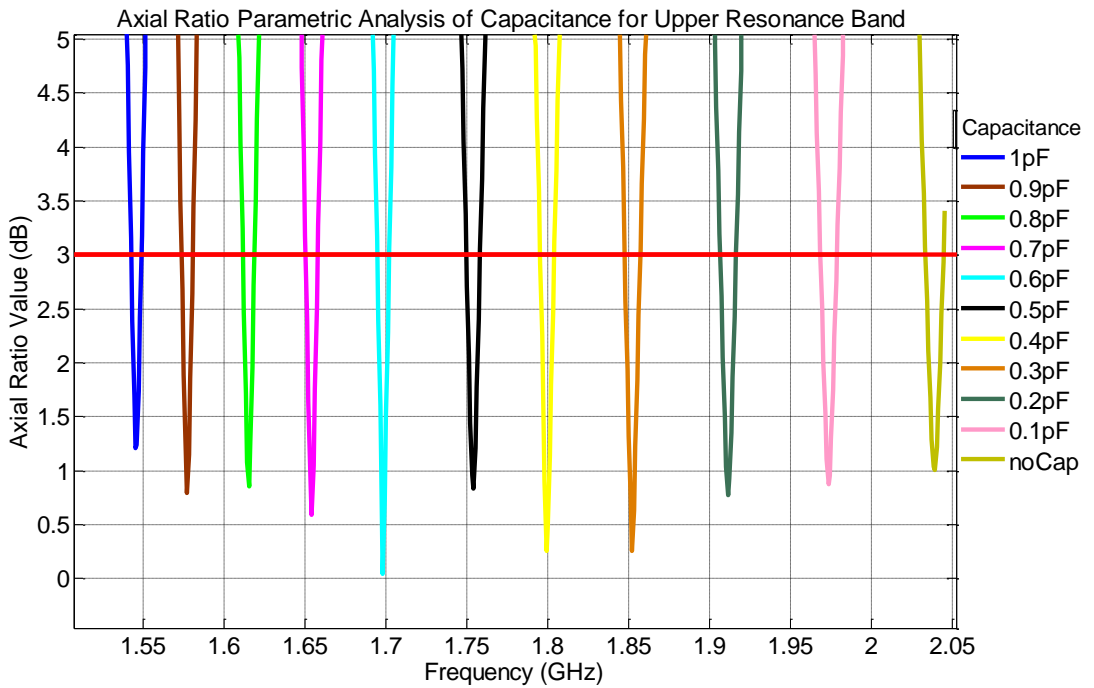


Figure 4.10 Axial ratio values for the upper resonance band for different values of capacitance

4.4 Effect of Changing Feed Position

In this subsection, return loss and axial ratio variations are investigated with respect to feed position. The geometry is given in Figure 4.1 and the feed position is changed on three axes named X, Y and diagonal axis. All other parameters are kept constant as given in Table 4.1. Parametric studies are done for each axis separately. Initially feed is moved on the diagonal axis where the locations are given in Table 4.3.

Table 4.3 Feed positions on diagonal axis used in parametric analysis

Case	feed_x(mm)	feed_y(mm)
1	5	5.16
2	11	11.36
3	13.5	13.95
4	16	16.53
5	22	22.73

The simulation results for return losses are shown in Figure 4.11. As seen from the results return loss of the antenna is not good when the feed is positioned too close to the center or too close to the corner. Best performance is achieved when the feed is positioned near to the middle point of the line between center and corner.

It can be seen from Figure 4.12 and 4.13 that 3 dB axial ratio is not affected much by the movement of the feed on this axis. However, the resonance frequency is slightly shifted.

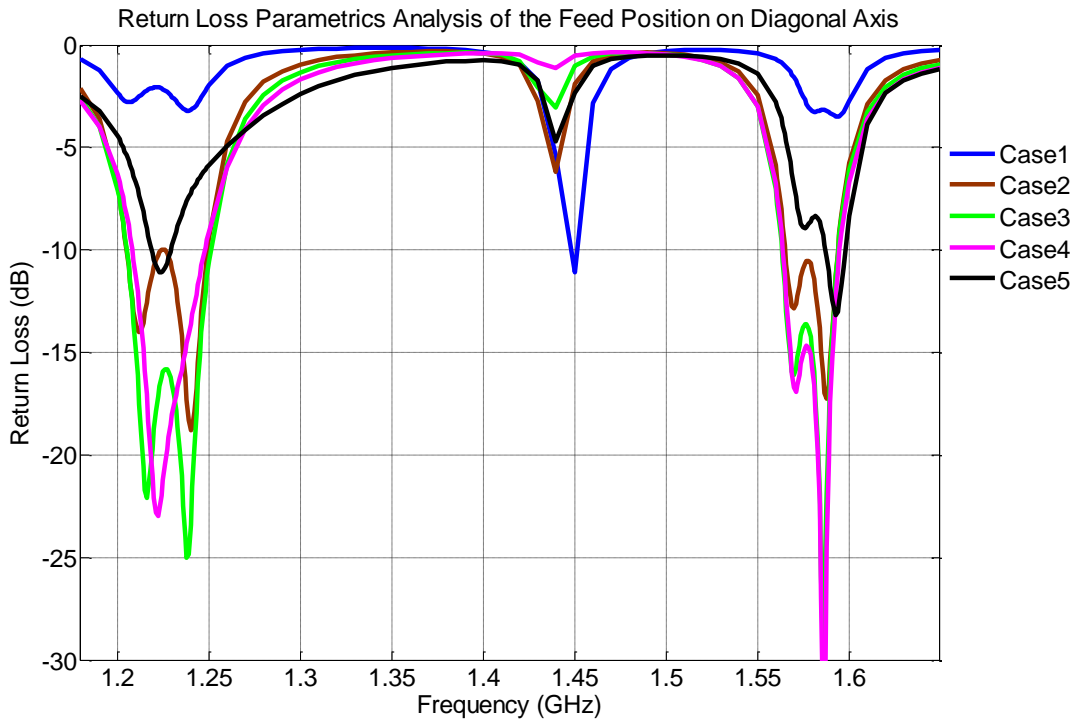


Figure 4.11 Return losses for cases given in Table 4.3

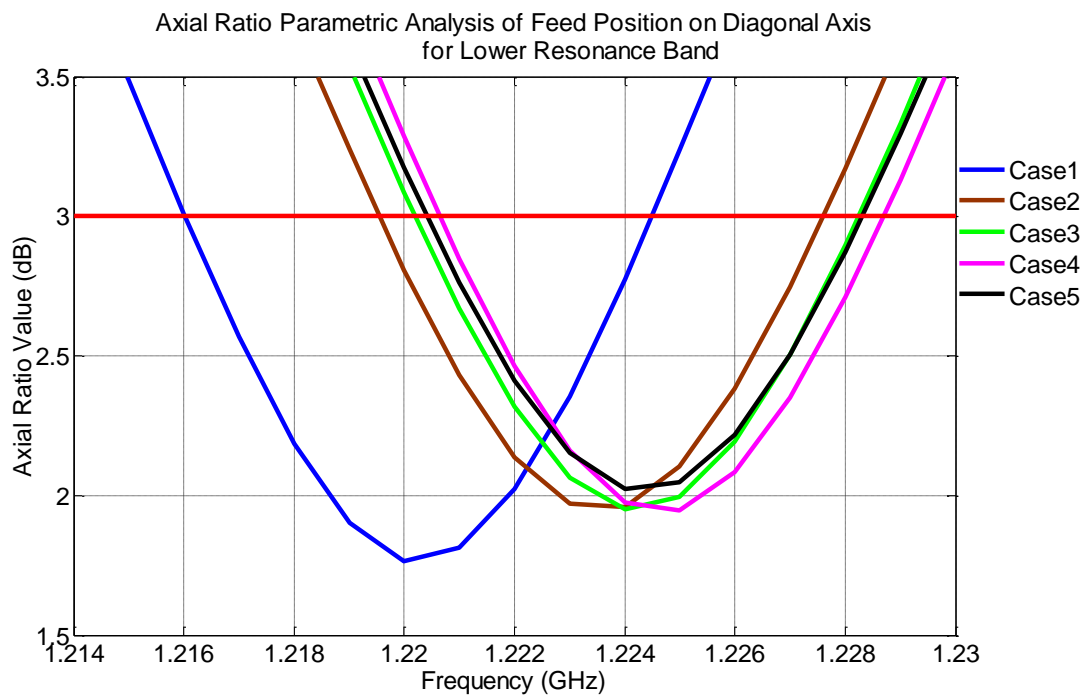


Figure 4.12 Axial ratio for the lower resonance band for cases given in Table 4.3

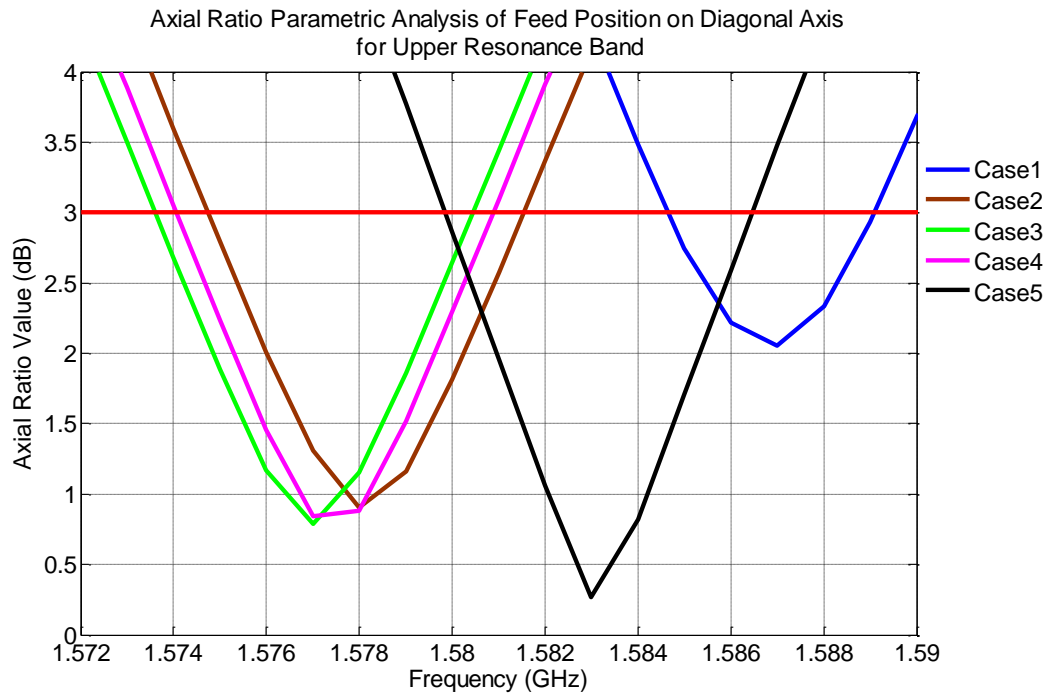


Figure 4.13 Axial ratio for the upper resonance band for cases given in Table 4.3

In the second parametric analysis, feed is moved along X axis where the locations are given in Table 4.4.

Table 4.4 Feed positions on X axis used in parametric analysis

Case	feed_x(mm)	feed_y(mm)
1	5	13.95
2	10	13.95
3	13.5	13.95
4	17	13.95
5	23	13.95

Finally, feed is moved along Y axis where the locations are given in Table 4.5.

Table 4.5 Feed positions on Y axis used in parametric analysis

Case	feed_x(mm)	feed_y(mm)
1	13.5	5.4
2	13.5	11.4
3	13.5	13.95
4	13.5	15.5
5	13.5	22.5

It is observed from Figure 4.14 and 4.17 that the return loss of the antenna is acceptable as long as feed is not too close to the center or the edge. For a good circular polarization characteristic, it is suggested to have the feed on the diagonal for a nearly square antenna [1] [41]. However, this is not the case in this study as can be seen from Figure 4.15, Figure 4.16, Figure 4.18 and Figure 4.19. The 3 dB axial ratio bandwidth remains same for any location on the patch.

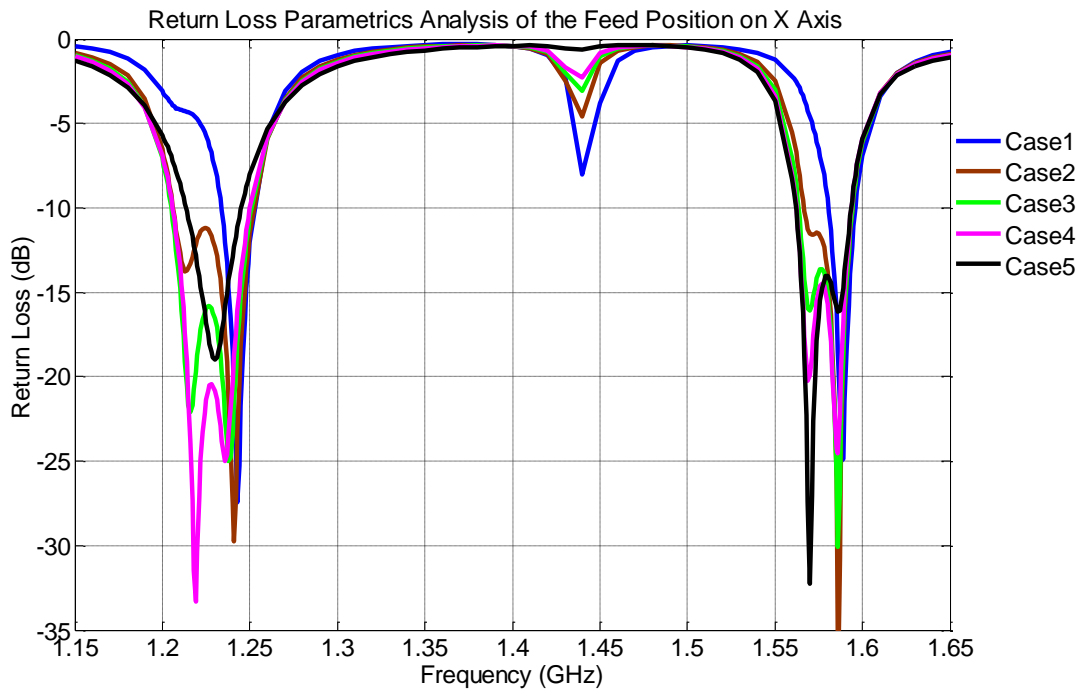


Figure 4.14 Return losses for cases given in Table 4.4

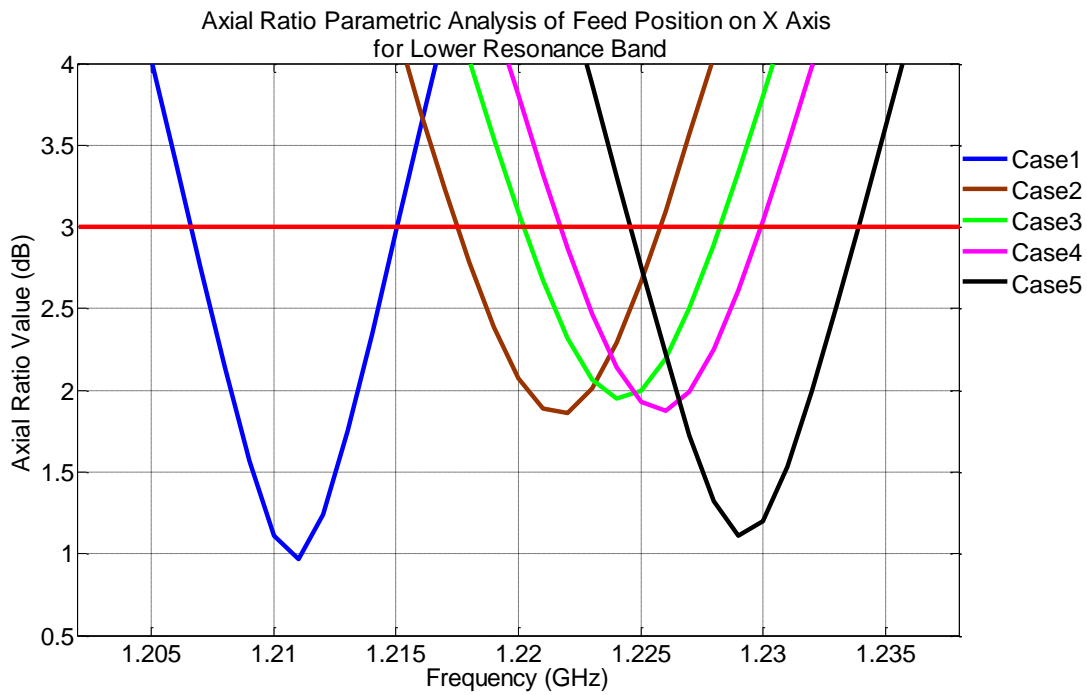


Figure 4.15 Axial ratio for the lower resonance band for cases given in Table 4.4

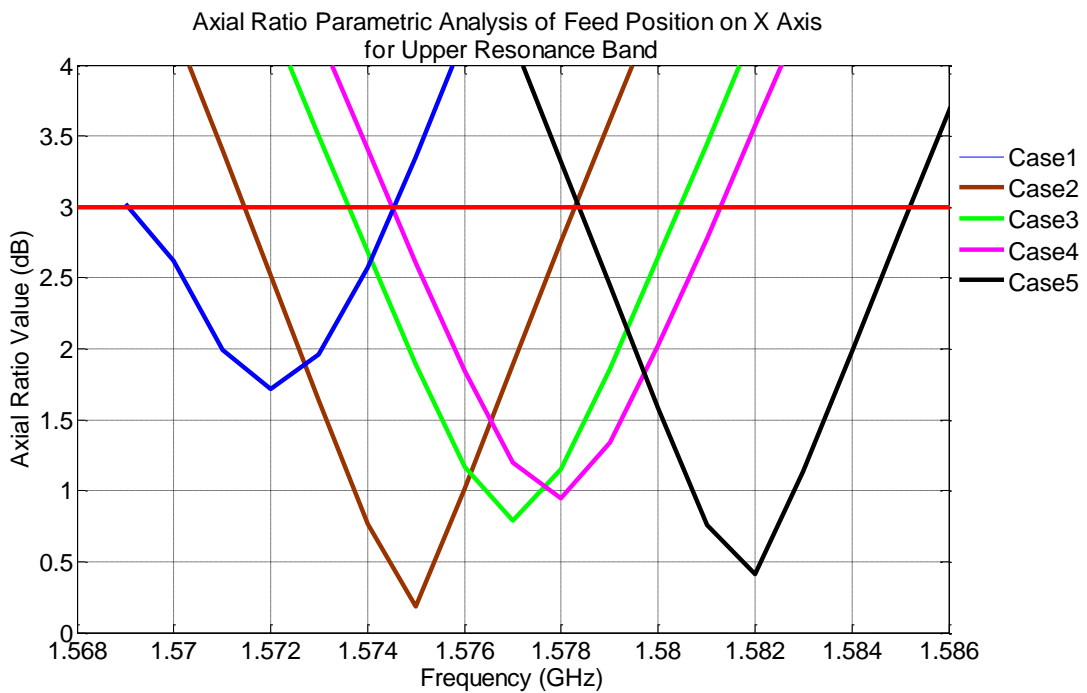


Figure 4.16 Axial ratio for the upper resonance band for cases given in Table 4.4

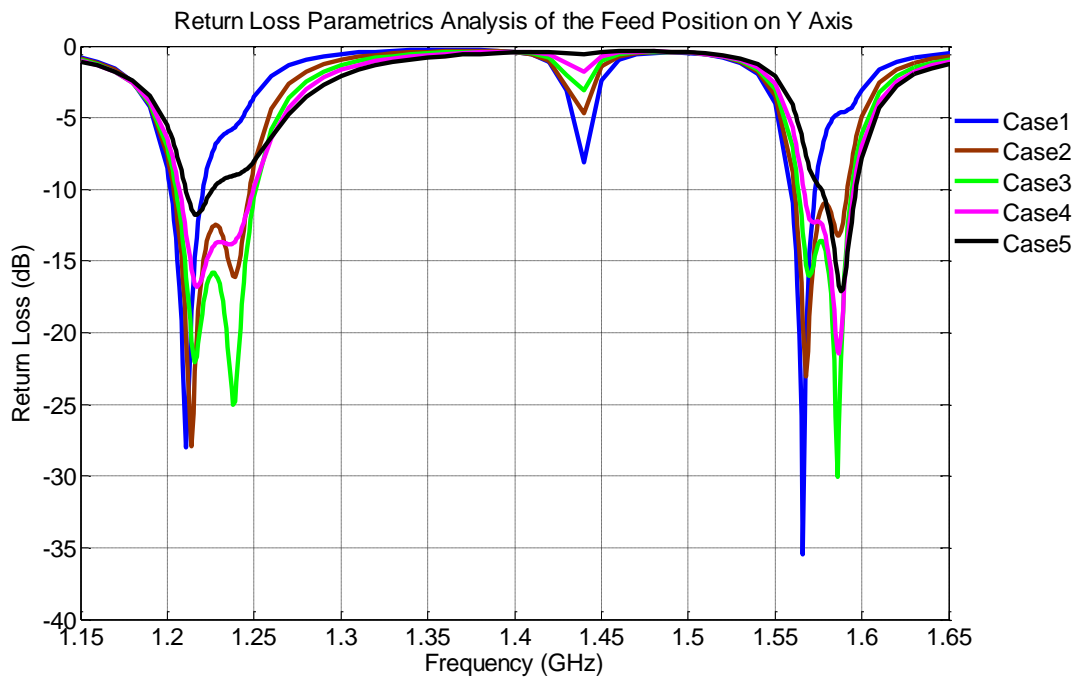


Figure 4.17 Return losses for cases given in Table 4.5

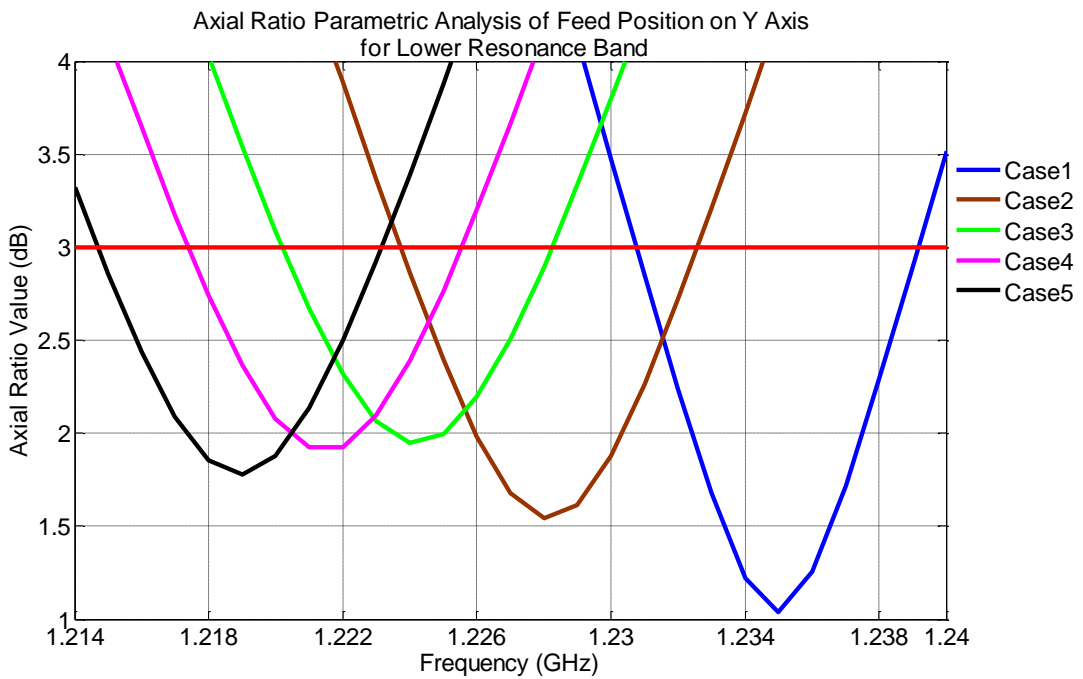


Figure 4.18 Axial ratio for the lower resonance band for cases given in Table 4.5

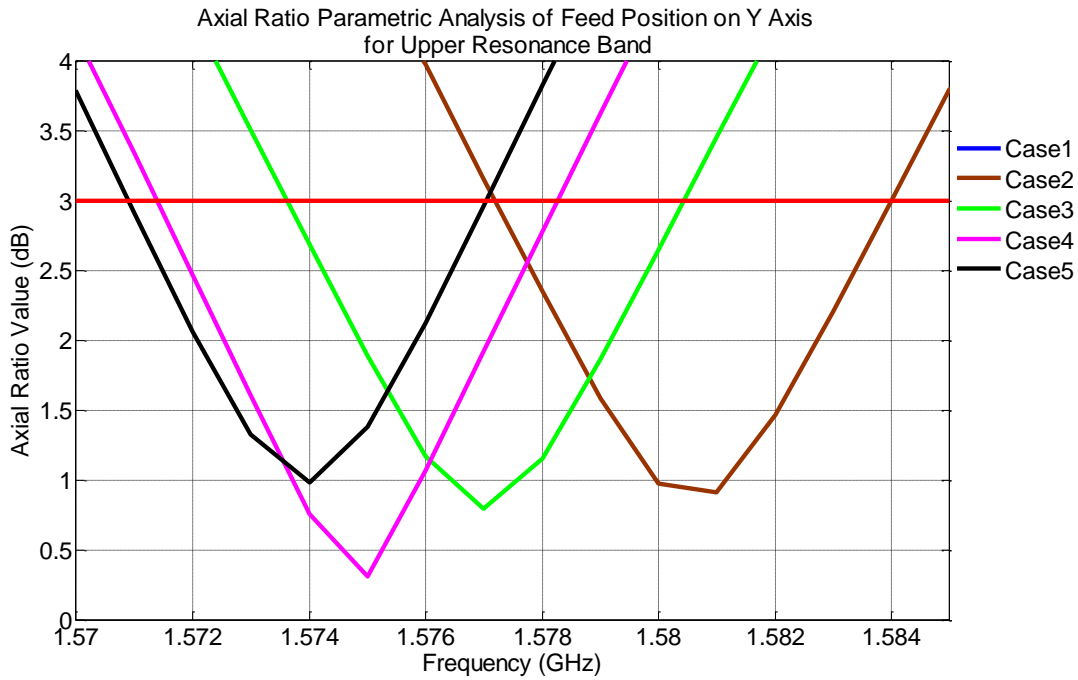


Figure 4.19 Axial ratio for the upper resonance band for cases given in Table 4.5

4.5 Effect of Changing Slot Width

The effects of the width of slot on return loss and axial ratio value characteristics of the antenna are discussed in this subsection. In the basic configuration, this value should be very small as compared to the value of the length of the patch. Parametric analysis is done by changing the slot width values from 0.5mm to 2mm. Return losses for these values are shown in Figure 4.20.

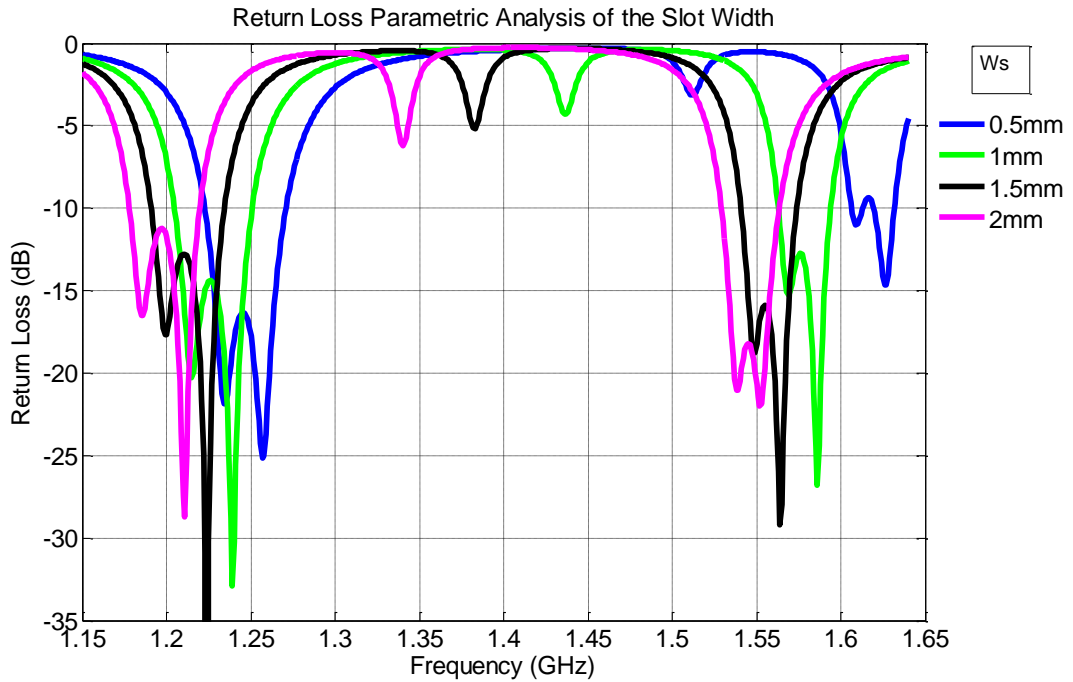


Figure 4.20 Return losses for different values of slot width

For slot width of 0.5mm the return loss is better for the lower resonance frequency than for the upper resonance frequency. As the slot width is increased the situation is gradually reversed. The slot width value should be close to distance from slots to the patch edges. Otherwise for small values of slot width, patch antenna behaves as if there are no slots. When the slot width increases too much as compared to the distance between slots and patch edges, current distribution on the patch antenna is degenerated. Circular polarization bandwidths are 7-8 MHz for all cases as seen from Figure 4.21 and Figure 4.22. The circular polarization band coincides with the resonance band as the slot width changes.

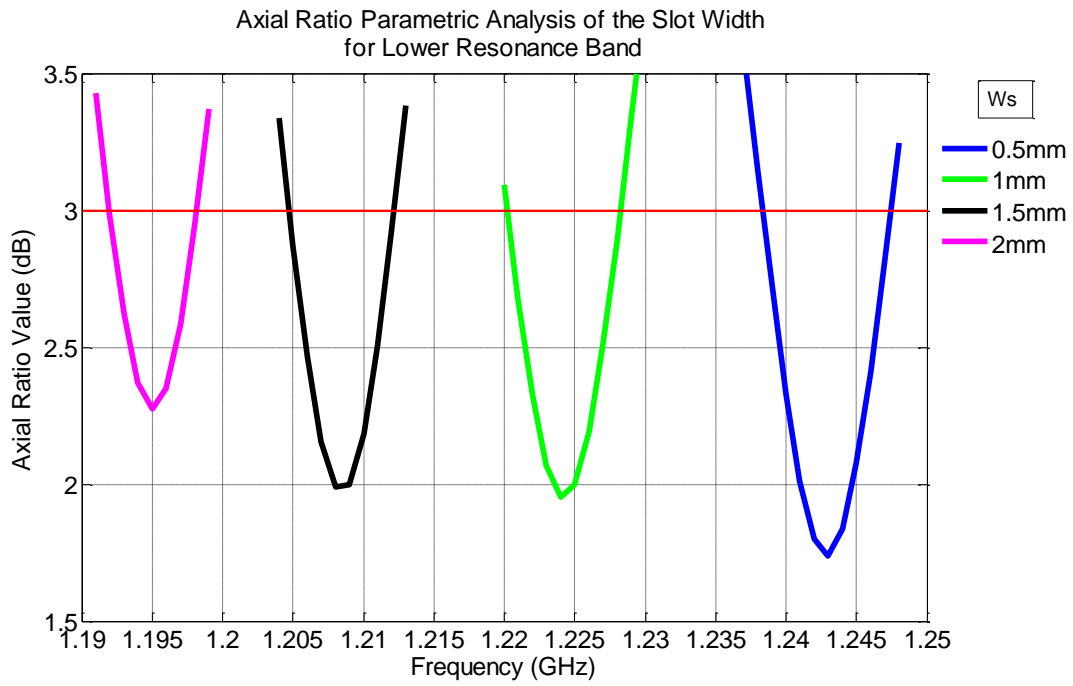


Figure 4.21 Axial ratio values for the lower resonance band for different values of slot width

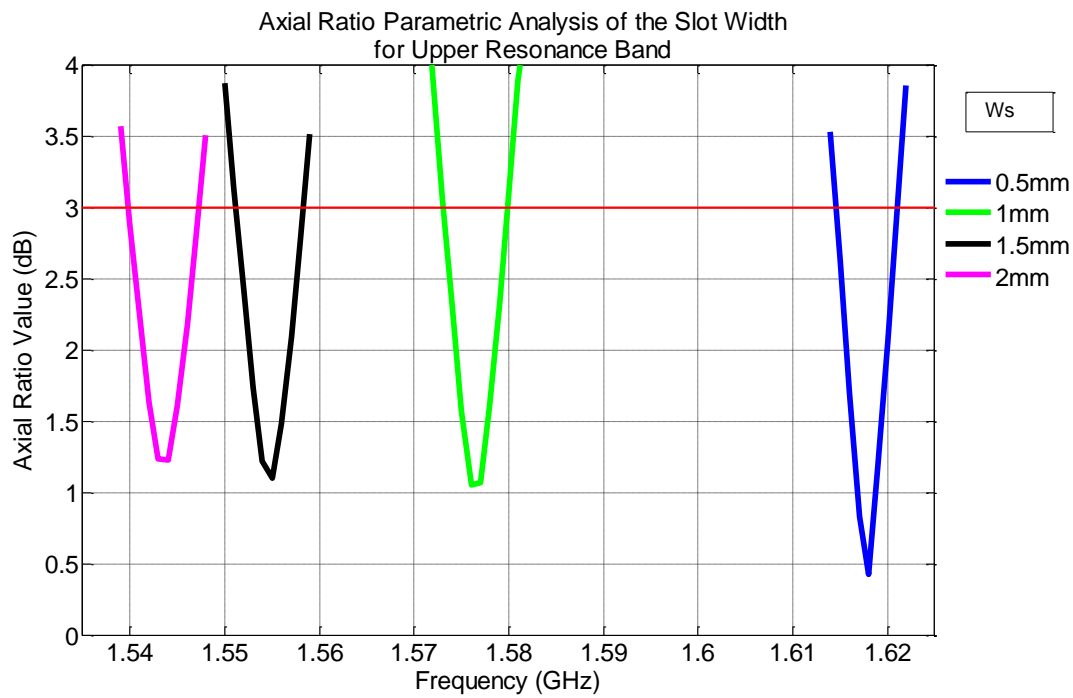


Figure 4.22 Axial ratio values for the upper resonance band for different values of slot width

4.6 Effect of Changing Substrate Thickness

The effects of the thickness of substrate on return loss and axial ratio value characteristics are given in this section. Parametric analysis is done by changing the substrate thickness from 0.4mm to 3.2mm. Return losses for these values are given in Figure 4.23.

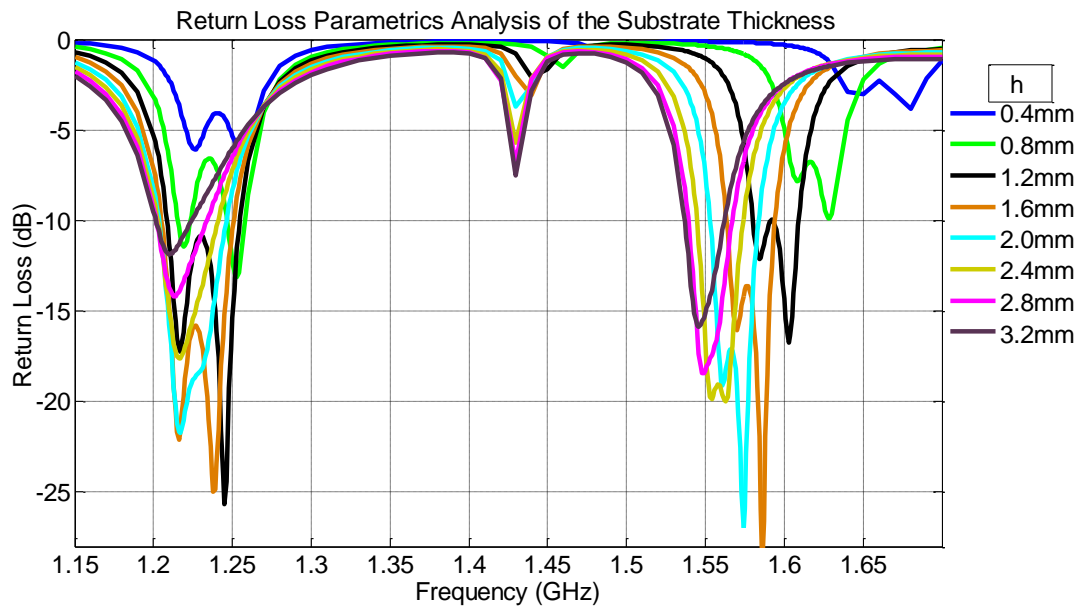


Figure 4.23 Return losses for different values of substrate thickness

The first operating band is almost the same whereas this parameter has an effect on the second resonant frequency. It is observed from Figure 4.23 that the second operating frequency shifts more than the first operating frequency. The return loss is not good for either thin or thick substrates. Best performance is obtained when the substrate thickness is around 1.6mm to 2mm.

This parameter has an effect on the circular polarization characteristic. It is observed from Figure 4.24 that, for the lower resonance band, the 3 dB axial ratio bandwidth starts with 8 MHz and can increase up to 12MHz as the height of the substrate increases. Return loss also increases over -10 dB, however, this result may improve by tuning other parameters. Despite the increase in the first operating

band, the second operating band is not affected by this parameter, as seen from Figure 4.25. The 3 dB axial ratio bandwidth remains about 7-8 MHz for all cases. Actually, other antenna parameters should be tuned after increasing the height of the substrate. This study is planned as future work.

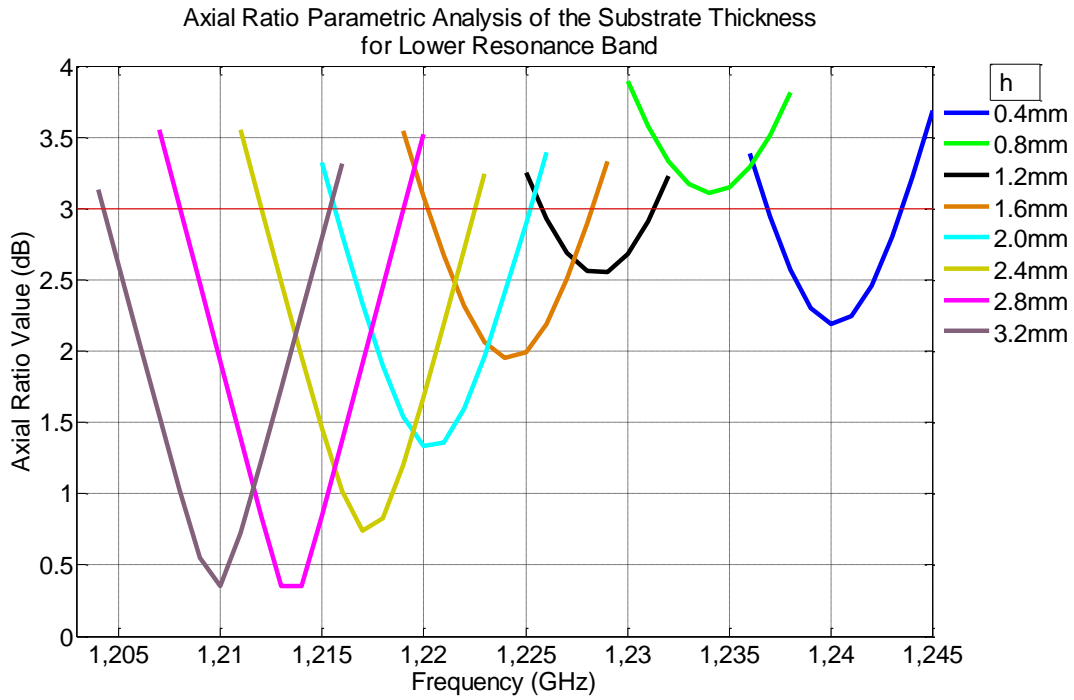


Figure 4.24 Axial ratio values for the lower resonance band for different values of substrate thickness

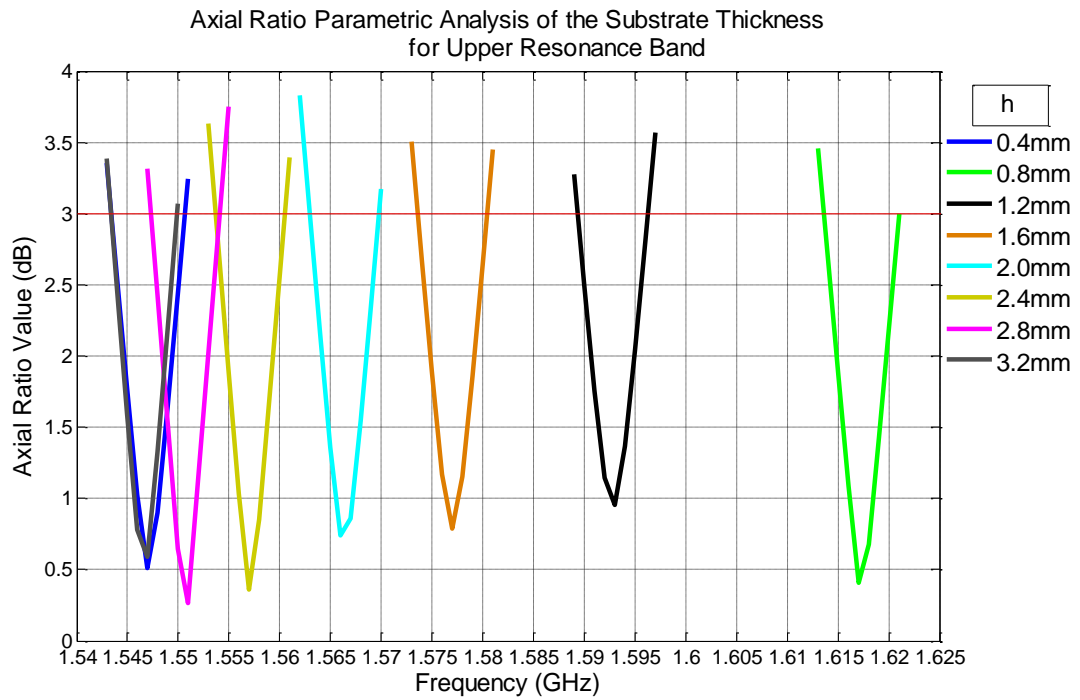


Figure 4.25 Axial ratio values for the upper resonance band for different values of substrate thickness

4.7 Effect of Changing Distance of Slots to Edges

The effects of the distance of slots to edges on the return loss and axial ratio are given in this subsection. This value should be close to the value of slot width and very small as compared to the value of the length of the patch as mentioned before. Parametric analysis is done by changing this value from 0.5mm to 2mm. Return losses for these values are shown in Figure 4.26.

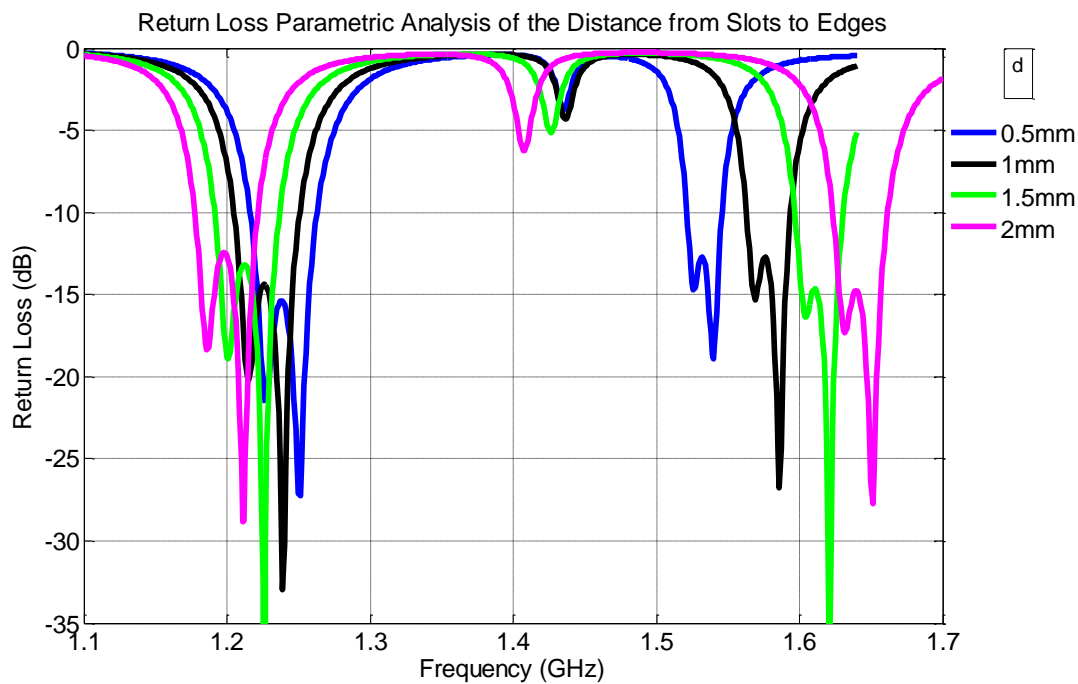


Figure 4.26 Return losses for different values of distance of slots to edges

As the distance of slots to the edges decreases, the lower resonance frequencies increase, but the upper resonance frequencies decrease. As a result, the frequency ratio also decreases. This parameter doesn't affect the magnitude of return loss too much unless it's too different from the length of the slot width. Circular polarization bandwidths remain 7-8 MHz as before as seen from Figure 4.27 and Figure 4.28. This parameter does not affect the axial ratio.

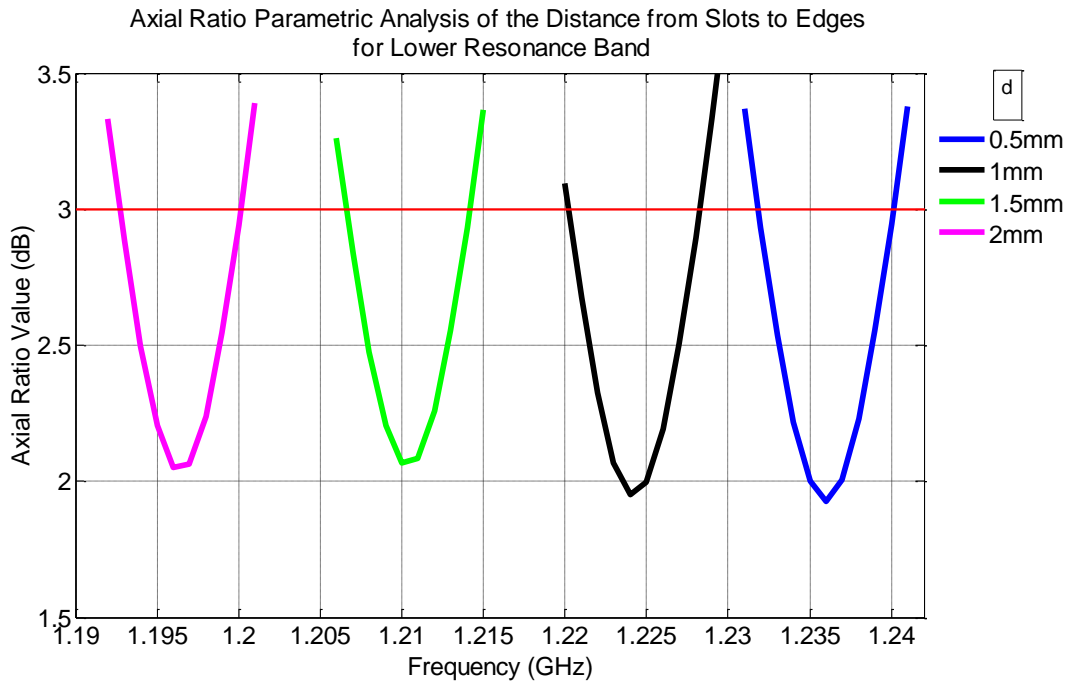


Figure 4.27 Axial ratio values for the lower resonance band for different values of distance of slots to edges

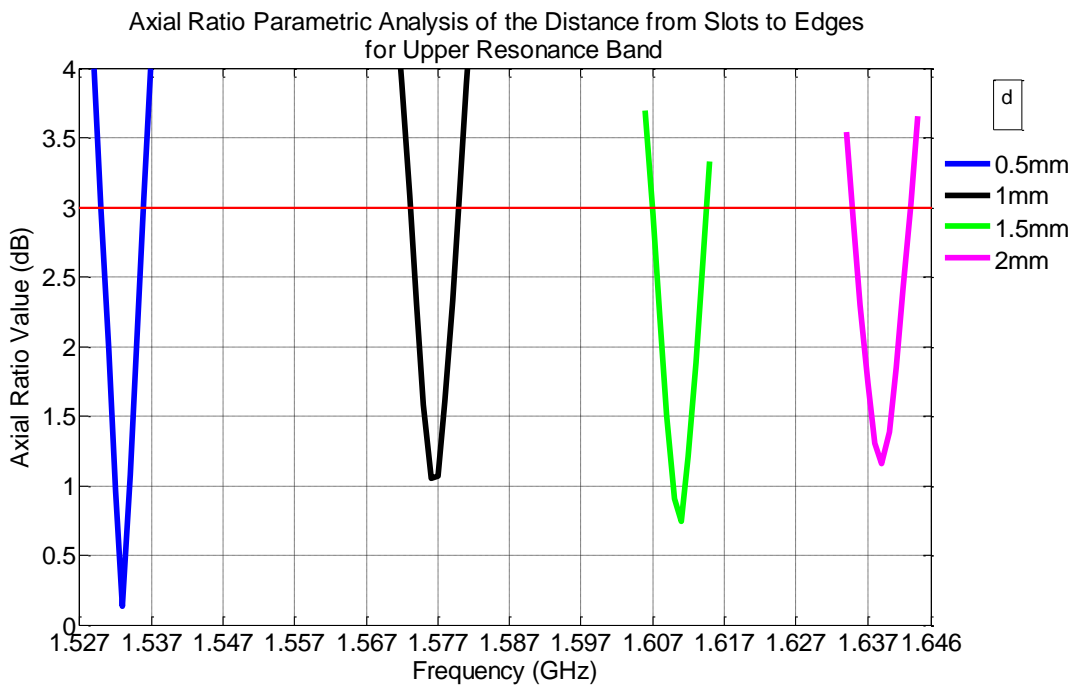


Figure 4.28 Axial ratio values for the upper resonance band for different values of distance of slots to edges

4.8 Effect of Changing L_{s1} and L_{s2}

In this subsection variations of return loss and axial ratio are investigated with changes in slot lengths. Slot lengths are changed using two different methods to understand its effect on return loss and axial ratio. All other parameters are kept constant as in Table 4.1. The first method is kept the difference between two slot lengths constant as given in Table 4.6.

Table 4.6 Parameters and their values in effect of slot length analysis

Case	L_{s1} (mm)	L_{s2} (mm)
1	39.6	39
2	40.6	40
3	41.6	41
4	42.6	42
5	43.6	43

The goal is to change the differences $(L - L_{s1})$ and $(L + \Delta L - L_{s2})$ by the same amount. This difference corresponds to the distance of slot ends to the patch edges. Return losses for this analysis are given in Figure 4.29.

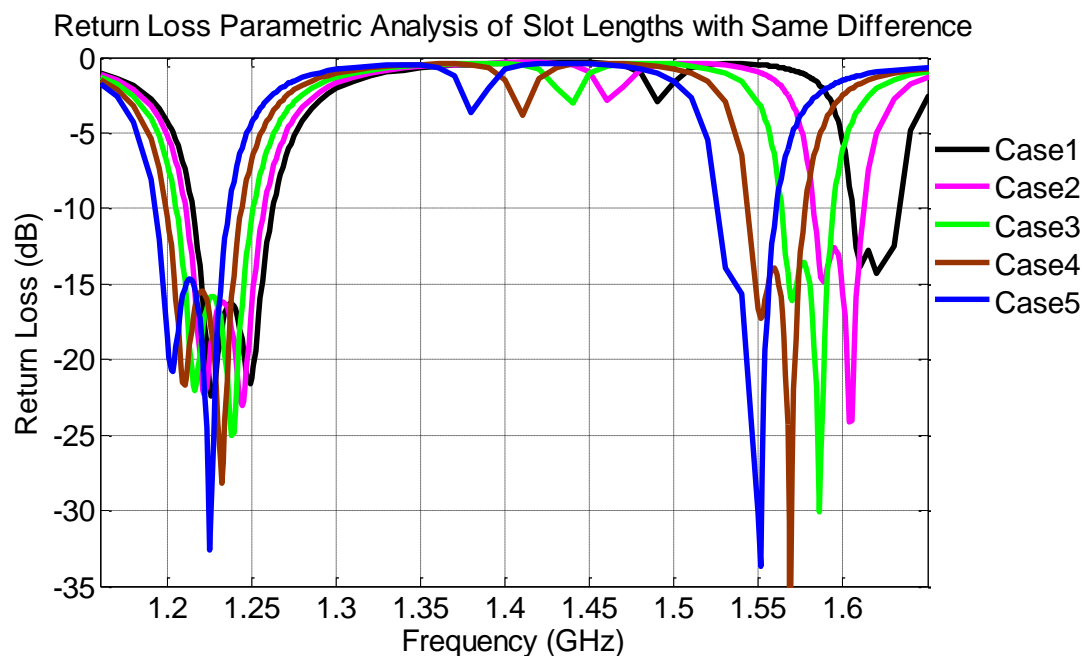


Figure 4.29 Return losses for different values of slot lengths with same difference

As seen from the Figure 4.29, resonance frequencies can be arranged by slot lengths. 1mm change in the slot lengths results in a 15-20 MHz change in resonance frequency for upper band. Very accurate tuning in resonance frequency can be obtained by minor changes in slot lengths. As seen from Figure 4.30 and 4.31 the circular polarization bandwidths are not affected as long as the differences $(L - L_{s1})$ and $(L + \Delta L - L_{s2})$ are changed by the same amount. So this is a very effective way to tune the antenna.

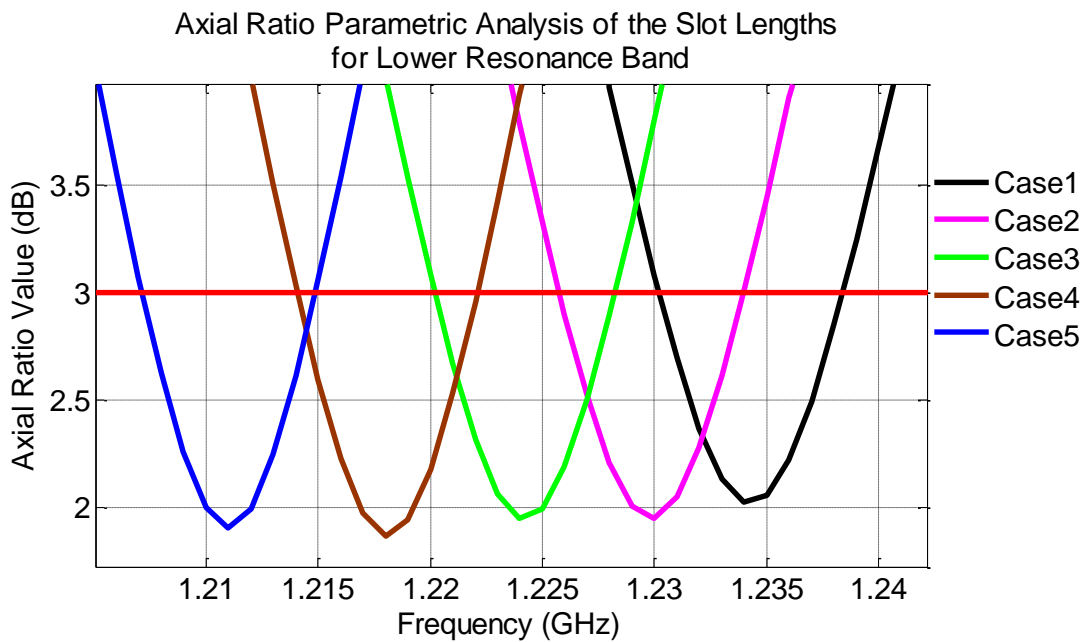


Figure 4.30 Axial ratio for the lower resonance bands for the cases given in Table 4.6

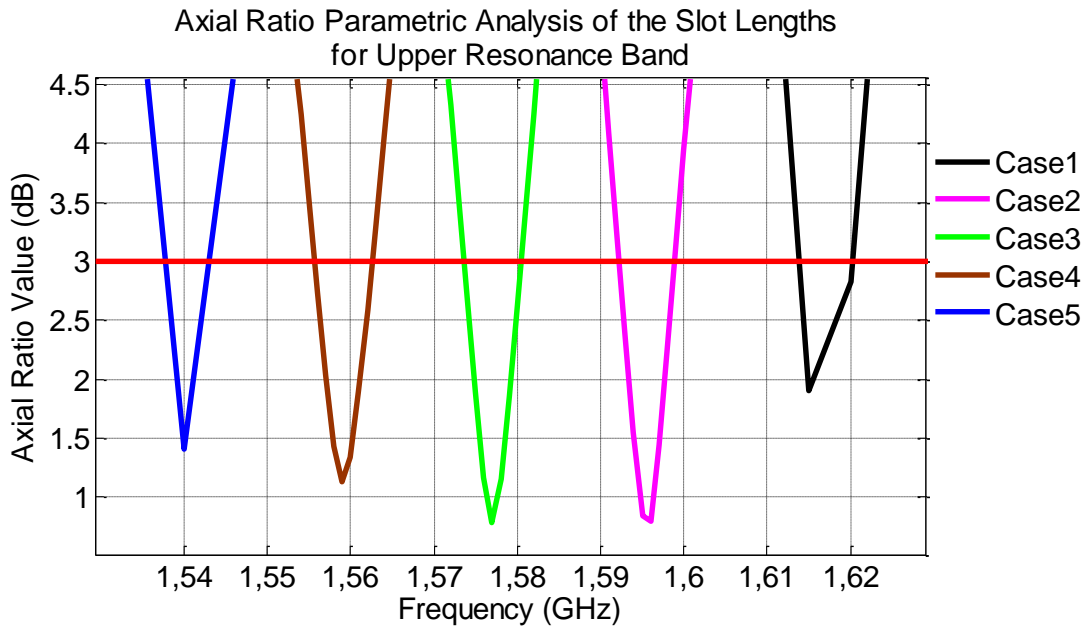


Figure 4.31 Axial ratio for the upper resonance band for the cases given in Table 4.6

In the second method, the slot lengths are changed on a grid, but for brevity only meaningful results listed in Table 4.7 are included.

Table 4.7 Parameters and their values in effect of length analysis

Case	L_{s1} (mm)	L_{s2} (mm)
1	41	41
2	41.4	41.2
3	41.6	41
4	41.8	40.8
5	41.6	41.6

Return losses for this analysis are given in Figure 4.32. The return loss is not affected too much. Axial ratio values for these cases are shown in Figure 4.33 and Figure 4.34

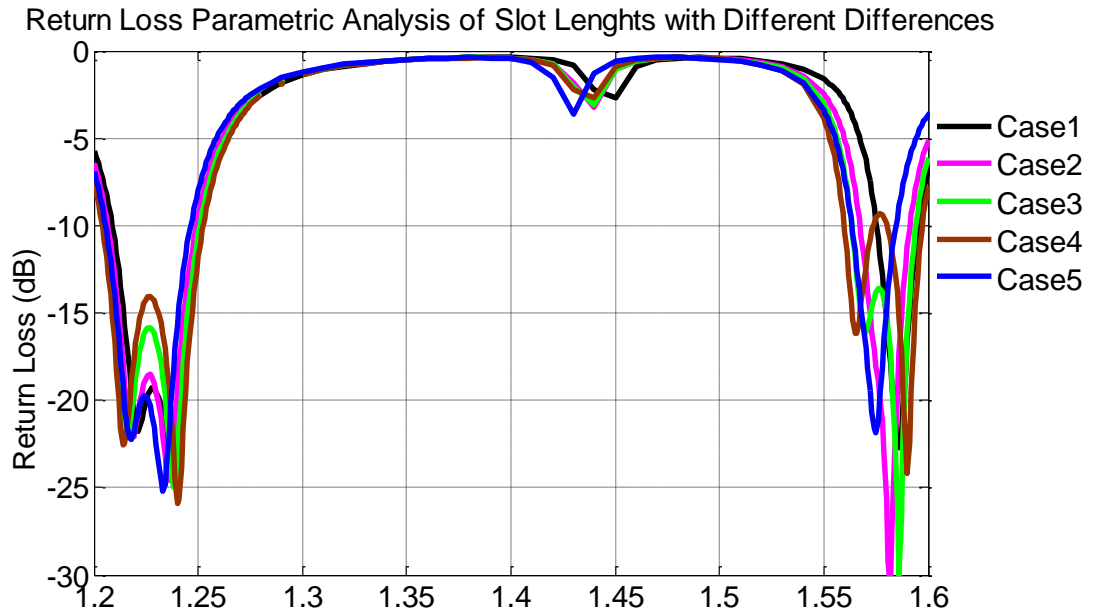


Figure 4.32 Return losses for different values of slot lengths given in Table 4.7

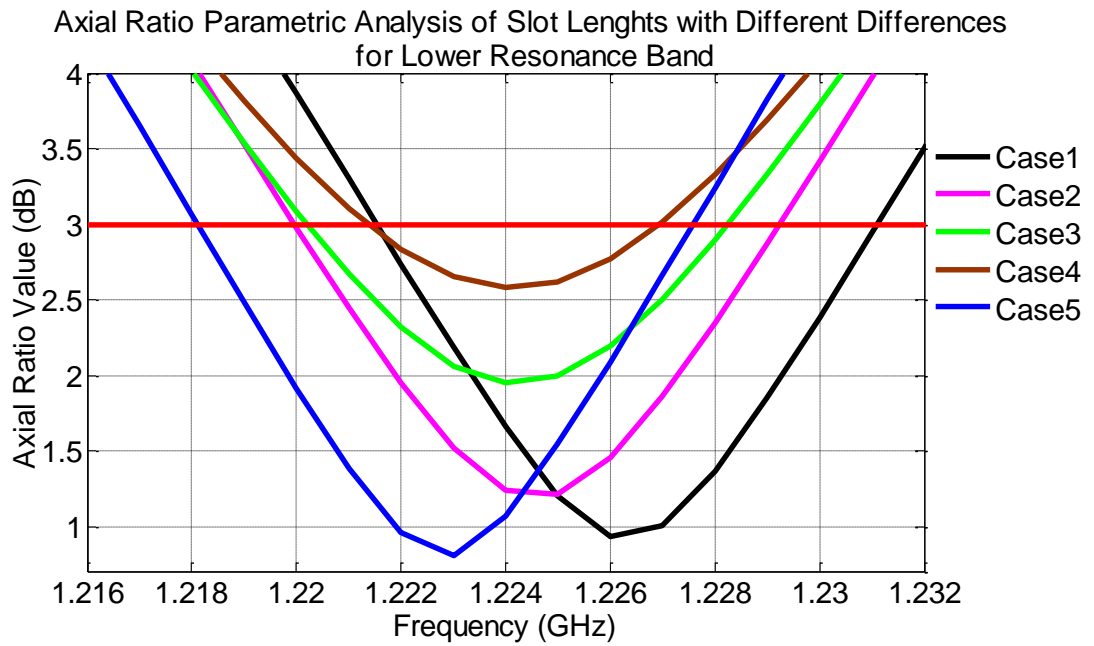


Figure 4.33 Axial ratio for the lower resonance band for the cases given in Table

4.7

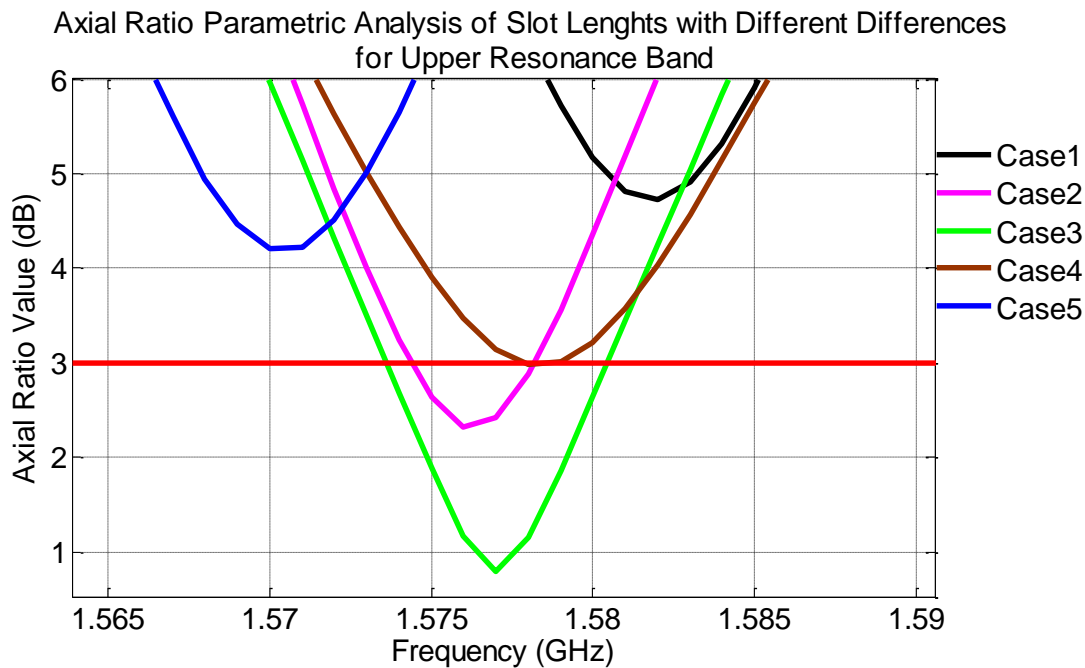


Figure 4.34 Axial ratio for the upper resonance band for the cases given in Table 4.7

Although the return loss is not changed too much, axial ratio changes significantly as seen in Figure 4.33 and Figure 4.34. If cases 2, 3 and 4 are investigated separately it is seen that when the difference between the slot length increases, axial ratio increases above 3 dB and circular polarization bandwidth decreases. Also, if cases 1, 3 and 5 are investigated, the circular polarization band increases to 10-11 MHz for lower band. However, the upper band loses its 3dB axial ratio.

4.9 Conclusions

In this chapter parametric analysis of a dual band circularly polarized microstrip antenna is carried out. The effect of important design parameters given in Table 4.1 is analyzed. Table 4.8 is obtained as a result of this parametric analysis. Circular polarization for lower band is affected by the parameters of substrate height and slot lengths. However, circular polarization for upper band is only affected by the slot lengths and other parameters do not help improving this. Capacitance is the most important parameter in terms of frequency ratio (FR). The FR requirement for GPS cannot be achieved without using capacitors. Distance of slots to the patch

edges also has a slight effect on FR. Slot width and distance of slots to the patch edges should be comparable with each other and much less than the length of the patch to have an acceptable return loss. Feed can be positioned anywhere on the patch for an acceptable return loss, unless it is near the center or edges of the patch. An independent change in one of the parameters of length, capacitance and substrate height can be tuned by other parameters in terms of return loss. Table 4.8 summarizes the design parameters and their effects on the antenna performance

Table 4.8 Parameters and their effects on antenna performance

		Design parameters (increasing values)						
		L	Capacitance	Feed position	Ws	h	d	L_{s1} and L_{s2}
Effect on	Axial ratio for lower band	×	×	×	×	↑	×	✓
	Axial ratio for upper band	×	×	×	×	×	×	✓
	Frequency ratio	×	↑	×	×	×	↑	×
	Return loss	×	×	✓	✓	×	✓	✓
	Resonant Frequency for lower band	↓	↑ slightly	×	↓	×	↓	✓
	Resonant Frequency for upper band	↓	↑	×	↓	↓	↑	✓

✓ :may either decrease or increase ↑ :increasing effect ↓ :decreasing effect × :does not affect

CHAPTER 5

MANUFACTURING DUAL BAND CIRCULARLY POLARIZED MICROSTRIP ANTENNA AND MEASUREMENT RESULTS

To this point some dual band microstrip antenna structures are given in Chapter 3 and one of them is investigated in Chapter 4. Some prototypes are fabricated, including the antenna with the optimized parameter values to further investigate their performances.

At the beginning of the study, the square patch antenna given in the Chapter 3.2 is produced in the facilities of ASELSAN to prove the dual band operation ignoring the circular polarization. Antennas are fabricated by the LPKF Protomat H100PCB milling machine as seen in Figure 5.1. The material used as the dielectric is FR4 substrate. Three pieces of patches are loaded with different capacitor kits of 1pF, 0.9pF and 0.8pF to see the effect of the capacitance. Figure 5.2 shows that; the dual band operation is succeeded and the capacitance effect is observed as studied in Chapter 4.3 for the produced antenna.

Another design is produced with the substrate RT/duroid® 6002 Laminate of Rogers Corporation. This substrate's tangential loss is 0.0012. This value is too much less than the tangential loss of FR4 substrate which is 0.02. This study is done to see the effect of the substrate material on the gain of the antenna. A square patch which has dimensions of 64mmx64mm and two pairs of slots of size $L_{s1}=47\text{mm}$ and $L_{s2}=49\text{mm}$ with 1mm slot width and 2mm distance of slots to edges on 6002 duroid laminate substrate with thickness 2.286 mm ($\epsilon_r = 2.94$, $h = 2.286\text{mm}$, $W = L = 64\text{mm}$, $L_{s1} = 47\text{ mm}$, $L_{s2} = 49\text{ mm}$, $w = 1\text{ mm}$, $d = 2\text{mm}$, capacitance = 1pF) is analyzed. The dual band operation is achieved with

this material too, as seen in Figure 5.3. However, to match the simulation and the measurement results, ground plane of the antenna with 6002 duroid laminate substrate needs to be much larger compared to the antenna with FR4 substrate. Length of the ground plane increases from 75mm to 190mm. Although this is not a compact solution, the gain of the antenna with 6002 duroid laminate substrate is 5-6 dB more than the solution with FR4 substrate as seen in Figure 5.4. This design is not optimized in terms of circular polarization so that the axial ratio value is around 4 dB for the resonant frequencies.

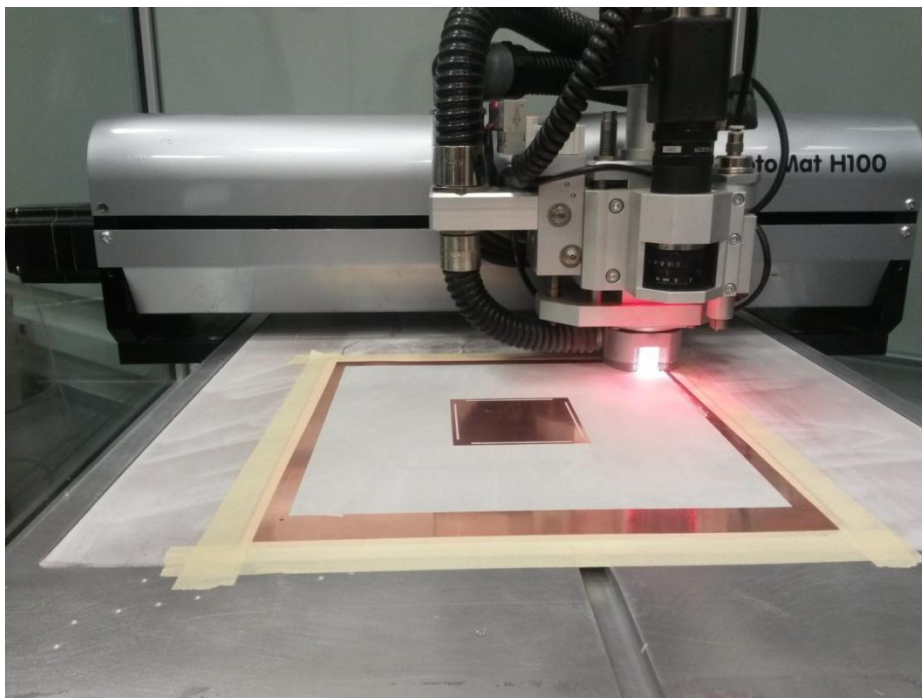


Figure 5.1 Fabrication of the antenna

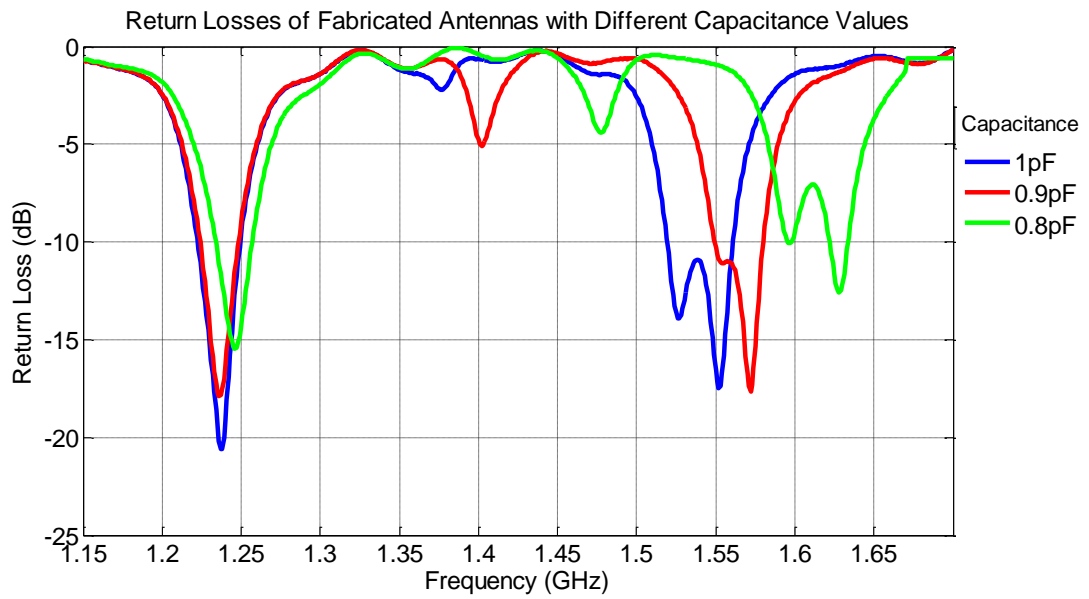


Figure 5.2 Return loss measurements of the antennas with different capacitance values

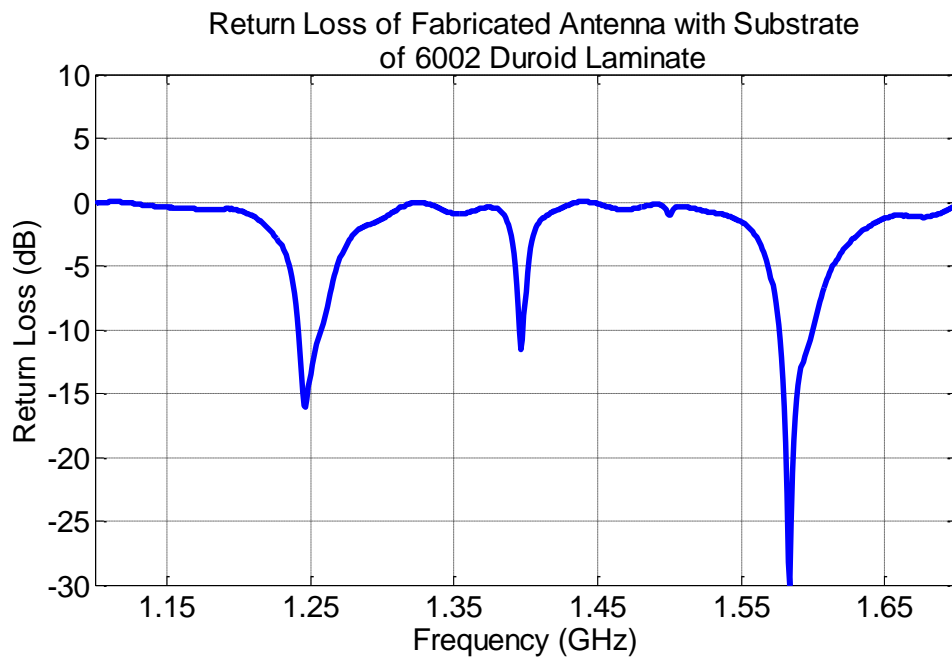


Figure 5.3 Return loss measurement of the antenna with 6002 duoid laminate substrate

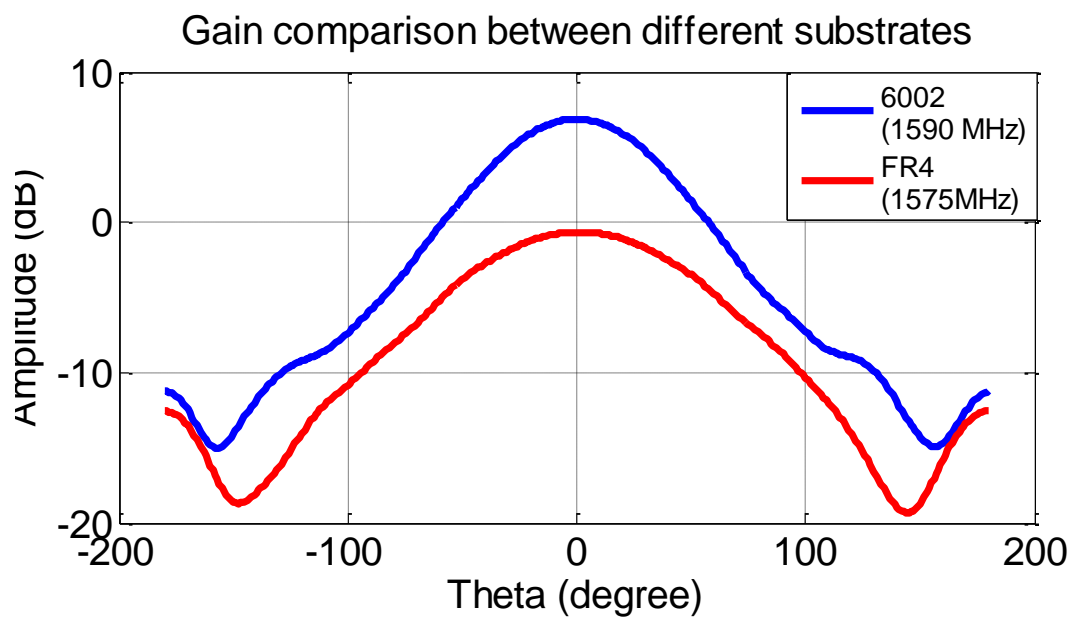


Figure 5.4 Gain comparison between the materials 6002duroid laminate and FR4. After the dual band operation is achieved for the produced antennas, the nearly square patch antenna given in Chapter 3.2 is fabricated in the facilities of METU. This time an extra attention has been given to circular polarization. The produced antenna is shown in Figure 5.5.

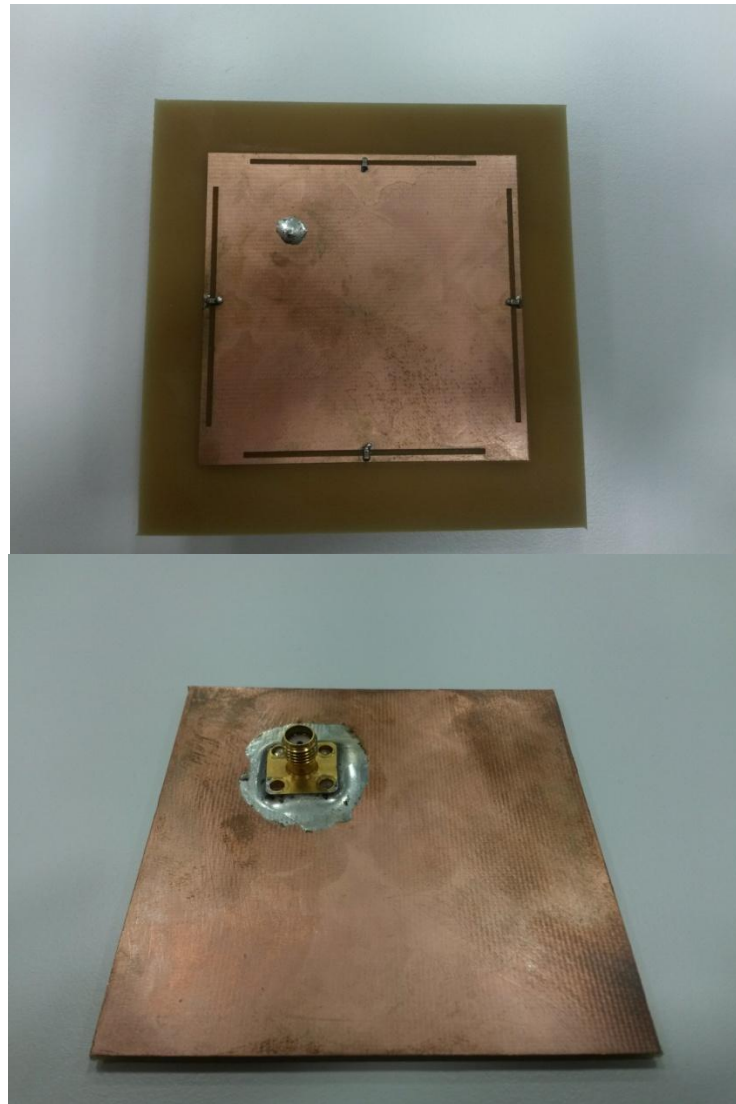


Figure 5.5 Fabricated dual band circularly polarized nearly square patch antenna

After the fabrication of the antenna is completed, return loss is measured by a network analyzer and return loss values are compared with the simulation. Comparison results are shown in Figure 5.6. There exists a little difference in the return loss between simulation and measurement. This might be caused by the tolerance value of the capacitors. Generally 0.1pF to 1pF capacitors are used and their tolerance is 0.1pF. Another reason may be the reactive loading caused by the solder used in connecting the coaxial connector to the patch.

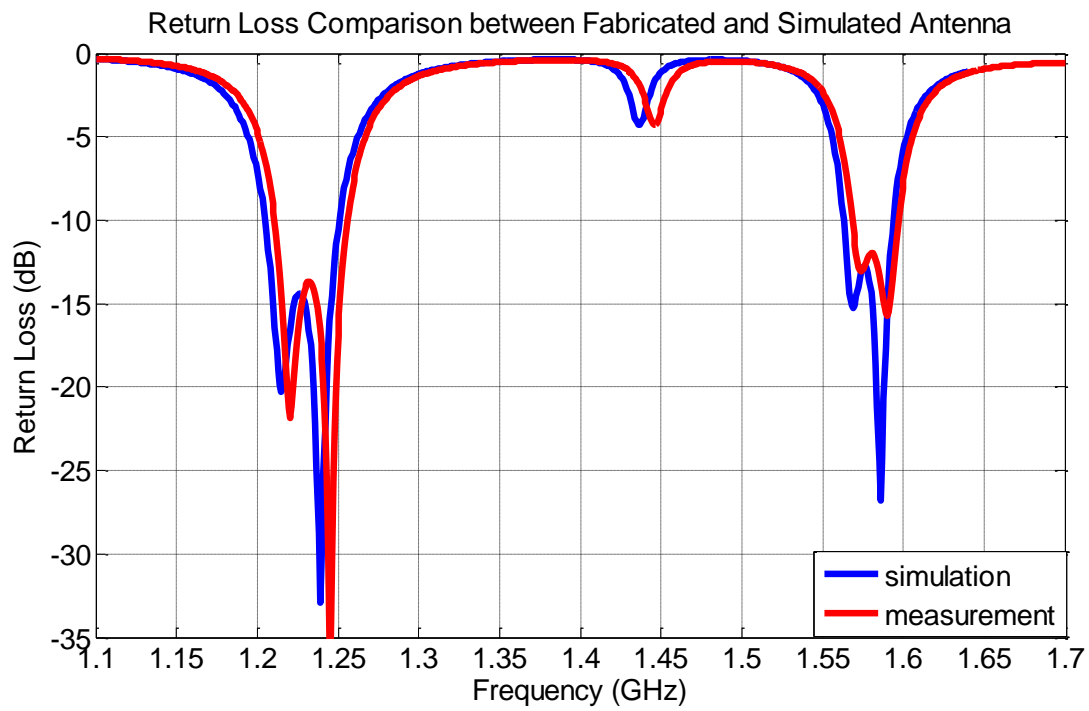


Figure 5.6 Return loss comparison between fabricated and simulated antenna

After the return loss measurement, far field pattern of the antenna is measured. The antenna is measured in SATIMO Starlab Spherical Near Field Measurement System which is shown in Figure 5.7 and Figure 5.8.

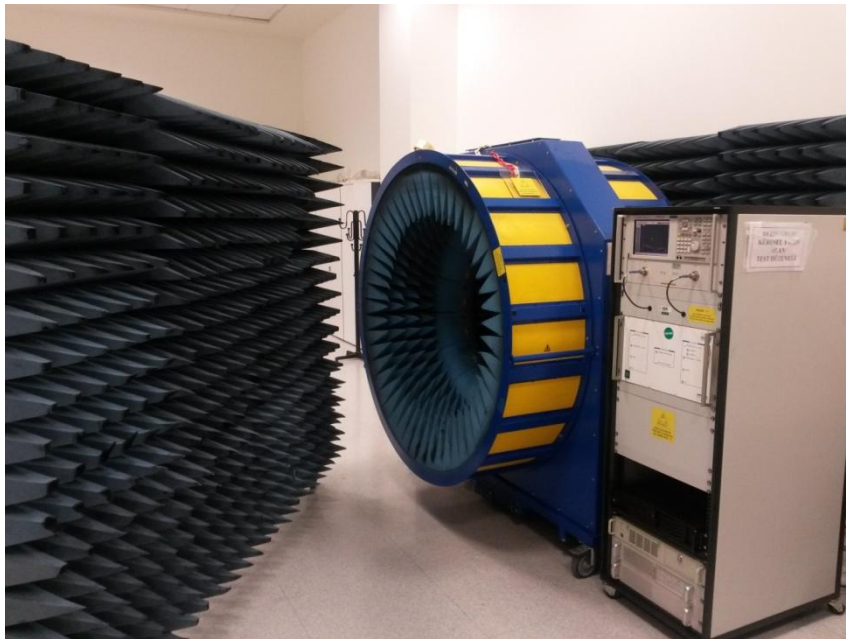


Figure 5.7 Near field measurement system

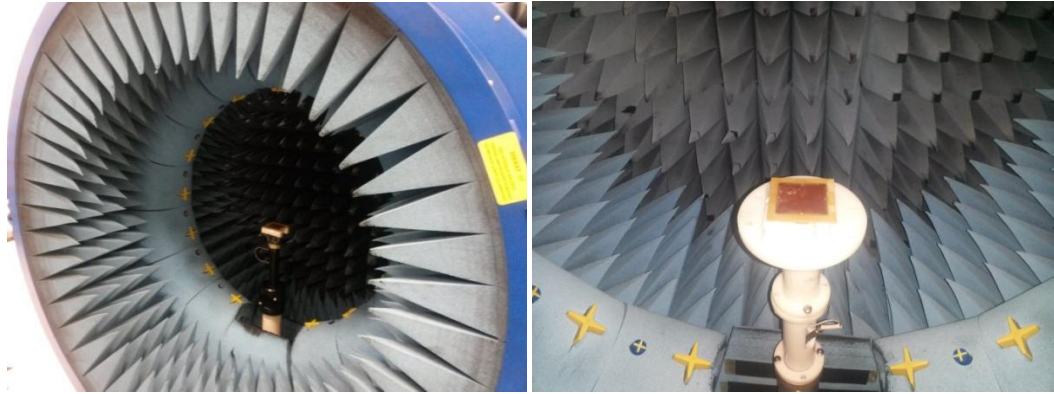


Figure 5.8 Placement of the antenna on the measurement system

Figure 5.9 and Figure 5.10 show the comparison of axial ratio values between the simulation and measurement. Similar to the frequency shift in the return loss, 5-6 MHz shift is observed in the center of the 3dB axial ratio bandwidth. If the same capacitors are used, this little frequency shift can be tuned by changing slot lengths as explained in Chapter 4.8.

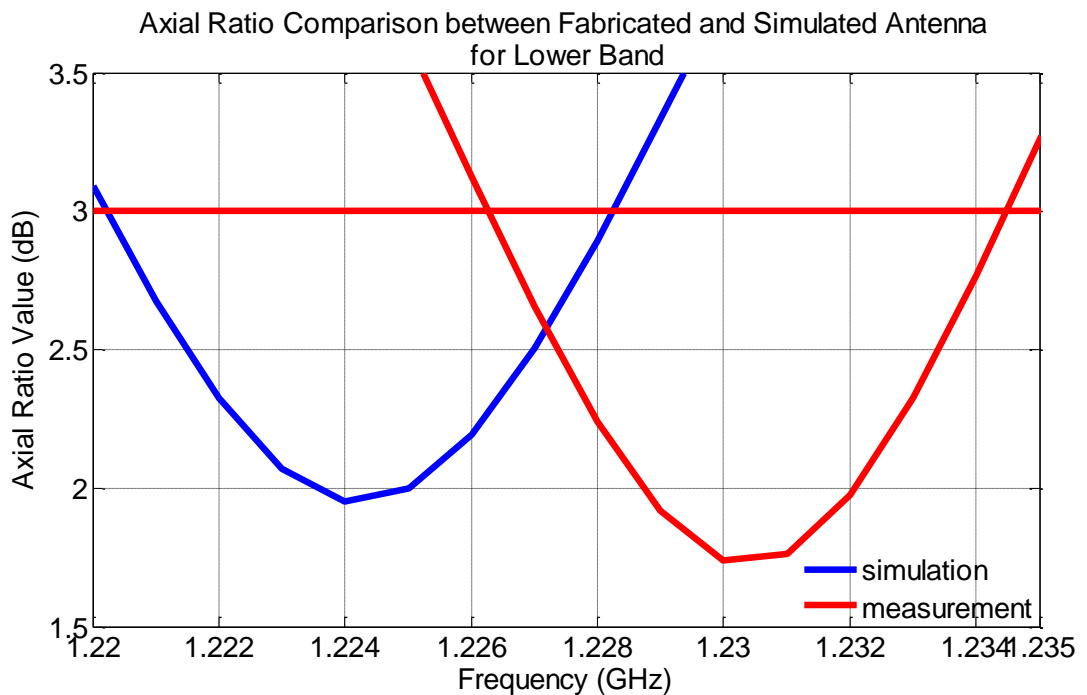


Figure 5.9 Axial ratio comparison between fabricated and simulated antenna for resonance lower band

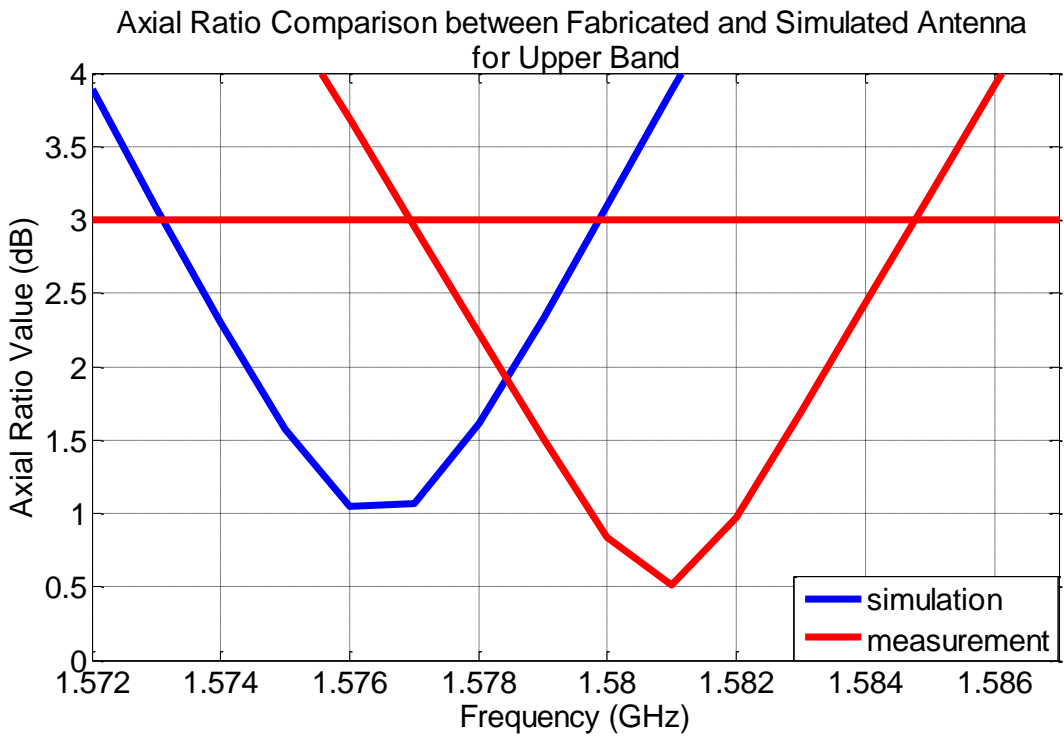
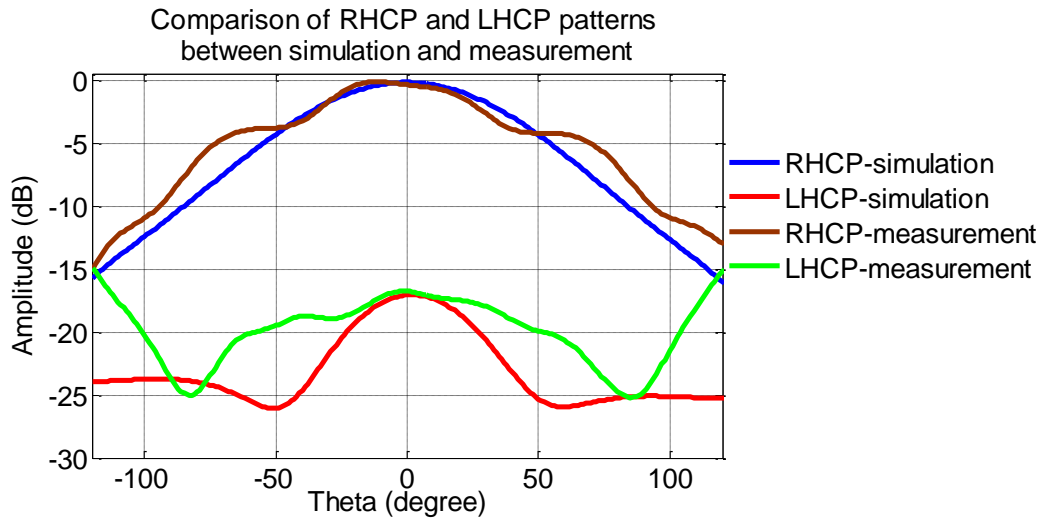
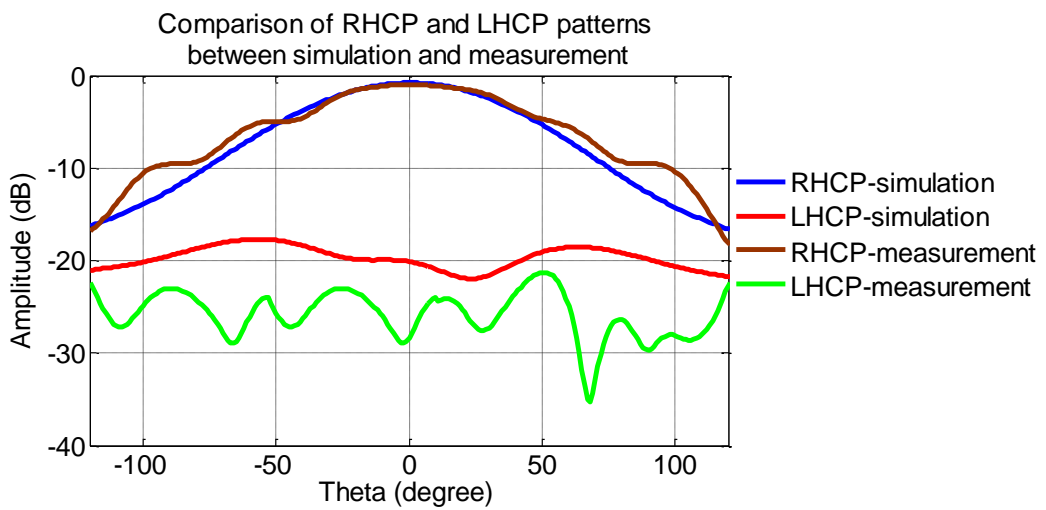


Figure 5.10 Axial ratio comparison between fabricated and simulated antenna for resonance upper band

Figure 5.11 shows the radiation patterns for RHCP (co-pol) and LHCP (cross-pol) at 1227MHz (a) and 1575 MHz (b) for the simulated and measured values. The fabricated antenna provides good circular polarization radiation at the given frequencies.



(a) 1227 MHz



(b) 1575 MHz

Figure 5.11 Comparison of RHCP and LHCP patterns between simulation and measurement

CHAPTER 6

CONCLUSIONS

In this thesis, the design and analysis of a circularly polarized dual band patch antenna is investigated. The main motivation is to use this antenna in L1 and L2 frequency band of GPS. Step by step improvement is done. First dual band operation is studied on a rectangular patch, later circular polarization techniques are tried on a square patch. Dual band operation is succeeded with four narrow slots etched close to radiating edges of the patch. This is an example of a reactive loading technique for multi band operation. The use of narrow slots is not enough to achieve the desired frequency ratio between two operating frequencies of L1 and L2. Chip capacitors are used to provide this frequency ratio. The use of chip capacitors extends the reactive loading and makes the frequency ratio smaller. Circular polarization operation is obtained by reactive loading for the upper resonance frequency band. However the lower resonance frequency band requires applying other techniques for circular polarization operation. Different solutions are considered and the slot loaded nearly square patch is found to be the best among them. In this design the dielectric substrate of FR4 is used. In terms of the return loss, lower resonance frequency band is 50 MHz, while the upper resonance frequency band is 30 MHz. Both of these resonance bands have 8 MHz circular polarization bandwidth for which the axial ratio is less than 3 dB. Parametric analysis of this design is performed to observe the effect of design parameters on return loss and axial ratio value of the antenna. Simulation results are presented and a conclusion is given in Chapter 4.9 about the relationship between design

parameters and antenna performance. The antenna is manufactured and measured. A good agreement between simulation and measurement is observed.

The main difficulty is that the upper circular polarization bandwidth is not affected by most of the design parameters. For future work, the circular polarization bandwidth of the antenna can be improved. To this end, slots may be designed in different shapes (for example, the ends of the rectangular slots may be tapered) to investigate its effect on TM_{300} mode. Another method that may improve the bandwidth is to use aperture coupling in the feed. A parametric analysis of the aperture coupled patch and its feed mechanism can be carried out.

The substrate material affects the resonant frequency, and therefore, for a given frequency the antenna dimensions must be changed. The substrate also affects the size of required ground plane. This effect is observed in the design of an antenna that uses 6002 Duroid Laminated substrate. Antenna dimensions can be reduced by using a substrate with higher relative permittivity. An analysis can be done on various types of substrates.

A relation between circular polarization bandwidth and quality factor is given in [43]. Also, an empirical formula for the quality factor is given in [44] where substrate thickness and dielectric constant are used. A future study is planned to increase the circular polarization bandwidth of the antenna referencing these studies. Substrate thickness will be increased significantly and other parameters will be tuned according to [43] and [44] to improve circular polarization bandwidth.

REFERENCES

- [1] Bernhard Hofmann-Wellenhof, Herbert Lichtenegger, Elmar Wasle, “GNSS – Global Navigation Satellite Systems”, Springer-Verlag Wien, 2008.
- [2] R. Garg, P. Bhartia, I. Bahl and A. Ittipiboon, “Microstrip Antenna Design Handbook” , Artech House, Boston, London, 2001.
- [3] C.A. Balanis, “Antenna Theory Analysis and Design, Third Edition”, Johan Wiley & Sons, United States of America, 2005.
- [4] J.R James and P.S. Hall, “Handbook of Microstrip Antennas”, Peter Peregrinus Ltd., London, 1989.
- [5] Jibendu Sekhar Roy and Milind Thomas Themalil, “Investigations on a New Proximity Coupled Dual-Frequency Microstrip Antenna for Wireless Communication”, Microwave Review, Vol.13, No.1, June 2007, pp12-15.
- [6] <http://hyperphysics.phy-astr.gsu.edu/hbase/phyopt/polclas.html> (2011-10-05)
- [7] S.Maci, G. Biffi Gentili, P.Piazzesi and C.Salvador, “Dual-Band Slot-Loaded Patch Antenna”, IEE Proc.-Microw. Antennas Propag., Vol. 142, No. 3, June 1995.
- [8] C.-Y. Huang, C.-W. Ling and J.-S. Kuo, “Dual-Band Microstrip Antenna Using Capacitive Loading”, IEE Proc.-Microw. Antennas Propag., Vol. 150, No. 6, December 2003.
- [9] J-S. Chen and K-L. Wong, “A Single-Layer Dual-Frequency Rectangular Microstrip Patch Antenna Using a Single Probe Feed”, Microwave and Optical Technology Letters, Vol. 11, No.2, 1996.

- [10] Y. M. M. Antar, A. I. Ittipiboon and A. K. Bhattacharyya, "A Dual-Frequency Antenna Using a Single Patch and An Inclined Slot", *Microwave and Optical Technology Letters*, Vol.8, No.6, 1995.
- [11] Y. Murakami, W. Chujo, I. Chiba, and M. Fujise, "Dual Slot Coupled Microstrip Antenna for Dual Frequency Operation" *Electronics Letters*, Vol.29, No.22, 28 October 1993, pp. 1906-1907.
- [12] M. Deepukumar, J. George, C. K. Aanandan, P. Mohanan and K. G. Nair, "Broadband Dual Frequency Microstrip Antenna", *Electronics Letters*, Vol.32, No.17, 15 August 1996, pp. 1531-1532.
- [13] S. A. Long, M. D. Walton, "A Dual-Frequency Stacked Circular-Disc Antenna", *IEEE Transactions on Antennas and Propagation*, Vol.AP-27, No.2, March 1979, pp. 1281-1285.
- [14] J. S. Dahele, K. F. Lee and D. P. Wong, "Dual Frequency Stacked Annular-Ring Microstrip Antenna", *IEEE Transactions on Antennas and Propagation*, Vol. AP-35, No.11, November 1987.
- [15] J. Wang, R. Fralich, C. Wu and J. Litva, "Multifunctional Aperture Coupled Stack Patch Antenna", *Electronics Letters*, Vol.26, No.25, December 1990, pp. 2067-2068.
- [16] F. Croq and D. Pozar, "Multifrequency Operation of Microstrip Antennas Using Aperture Coupled Parallel Resonators", *IEEE Transactions on Antennas and Propagation*, Vol.40, No.11, November 1992, pp. 1367-1374.
- [17] C. Salvador, L. Borselli, A. Falciani and S. Maci, "A Dual Frequency Planar Antenna at S and X Bands", *Electronics Letters*, Vol.31, No.20, October 1995, pp. 1706-1707.

- [18] Alexandre Moleiro, Jose Rosa, Rui Nunes and Custodio Peixeiro, "Dual Band Microstrip Patch Antenna Element with Parasitic for GSM", IEEE Antennas and Propagation Society International Symposium, Vol.4, July 2000, pp. 2188-2191.
- [19] Jose Rosa, Rui Nunes, Alexandre Moleiro and C. Peixeiro, "Dual-Band Microstrip Patch Antenna Element with Double U Slots for GSM", IEEE Antennas and Propagation Society International Symposium, Vol.3, July 2000, pp. 1596-1599.
- [20] W. F. Richards, S. E. Davidson and S. A. Long, "Dual-Band Reactively Loaded Microstrip Antenna", IEEE Transactions on Antennas and Propagation, Vol.33, No.5, May 1985, pp. 556-560.
- [21] H. Nakano and K. Vichien, "Dual-Frequency Square Patch Antenna with Rectangular Notch", Electronics Letters, Vol.25, No.16, 1989, pp. 1067- 1068.
- [22] D. Sanchez-Hernandez, G. Passiopoulos, M. Ferrando, E. de los Reyes and I. D. Robertson, "Dual-Band Circularly Polarized Microstrip Antennas with a Single Feed", Electronics Letters, Vol.32, No.25, December 1996.
- [23] D. Sanchez-Hernandez and I. D. Robertson, "Analysis and Design of a Dual-Band Circularly Polarized Microstrip Patch Antenna", IEEE Transactions on Antennas and Propagation, AP- 43, No.2, February 1995, pp. 201-205.
- [24] S. S. Zhong and Y. T. Lo, "Single Element Rectangular Microstrip Antenna for Dual-Frequency Operation", Electronics Letters, Vol.19, No.8, 1983, pp. 298-300.
- [25] D. H. Schaubert, F. G. Farrar, A. Sindoris and S. T. Hayes, "Microstrip Antennas with Frequency Agility and Polarization Diversity", IEEE Transactions on Antennas and Propagation, Vol.29, No.1, January 1981, pp. 118-123.

- [26] Rui Nunes, Alexandre Moleiro, Jose Rosa and Custodio Peixeiro, "Dual-Band Microstrip Patch Antenna Element with Shorting Pins for GSM", IEEE Antennas and Propagation Society International Symposium, Vol.4, July 2000, pp. 2208-2211.
- [27] R. B. Waterhouse and N. V. Shuley, "Dual Frequency Microstrip Rectangular Patches", Electronics Letters, Vol.28, No.7, 1992, pp. 606- 607.
- [28] B. F. Wang and Y. T. Lo, "Microstrip Antennas for Dual-Frequency Operation", IEEE Transactions on Antennas and Propagation, Vol.32, No.9, September 1984, pp. 938-943.
- [29] S.Maci, G. Biffi Gentili and G. Avitabile, "Single-Layer Dual Frequency Patch Antenna", Electronic Letters Vol.29, No.16, 1993.
- [30] M. L. Yazidi, M. Himdi and J. P. Daniel, "Aperture Coupled Microstrip Antenna for Dual Frequency Operation", Electronics Letters, Vol.29, No.17, August 1993.
- [31] G. Avitabile, S. Maci, F. Bonifacio, C. Salvador, "Dual Band Circularly Polarized Patch Antenna", IEEE Antennas and Propagation Society International Symposium, Vol.1, 1994, pp. 290-293.
- [32] Pramendra Tilanthe and P. C. Sharma, "A New Dual Band Frequency Reconfigurable Antenna", 2009 International Conference on Emerging Trends in Electronic and Photonic Devices & Systems (Electro-2009).
- [33] Bhumi Desai and Sanjeev Gupta, "Dual-Band Microstrip Patch Antenna", IEEE International Symposium on Microwave, Antenna, Propagation and EMC Technologies for Wireless Communications Proceedings, Vol.1, August 2005, pp.180-184 .

- [34] Kai-Ping Yang and Kin-Lu Wong, “Dual-Band Circularly-Polarized Square Microstrip Antenna”, IEEE Transactions on Antennas and Propagation, Vol. 49, No. 3, March 2001.
- [35] Hamidreza Memarzadeh and M. N. Azarmanesh, “Theoretical and Experimental Analysis of Dual-Band Circularly Polarized Microstrip Patch Antenna”, IEEE Antennas and Propagation Society International Symposium, Vol.1, June 2004, pp. 253-256.
- [36] A. M. El-Tager, M. A. Eleiwa, and M. I. Salama, “A Circularly Polarized Dual-frequency Square Patch Antenna for TT&C Satellite Applications”, Progress In Electromagnetics Research Symposium, Beijing, China, March, 2009.
- [37] A. A. Heidari, M. Heyrani, and M. Nakhkash, “A Dual-Band Circularly Polarized Stub Loaded Microstrip Patch Antenna for GPS Applications”, Progress In Electromagnetics Research, PIER 92, 2009, pp.195–208.
- [38] G. B. Hsieh, M. H. Chen and K. L. Wong, “Single feed dual-band circularly polarized microstrip antenna”, Electronic Letters, Vol. 34, No.12, June 1998, pp. 1170–1171.
- [39] Xiaoye Sun, Zhijun Zhang and Zhenghe Feng, “Dual-Band Circularly Polarized Stacked Annular-Ring Patch Antenna for GPS Application”, IEEE Antennas and Wireless Propagation Letters, Vol. 10, 2011.
- [40] W. Liao and Q.-X. Chu, “Dual-Band Circularly Polarized Microstrip Antenna with Small Frequency Ratio”, Progress In Electromagnetics Research Letters, Vol. 15, 2010, pp. 145-152.

[41] C.Sharma and Kuldip C.Gupta, “Analysis and Optimized Design of Single Feed Circularly Polarized Microstrip Antennas”, IEEE Transactions on Antennas and Propagation, Vol. AP-31,No.6,November 1983.

[42] S. Maci and G. Biffi Gentili, “Dual-Frequency Patch Antennas”, IEEE Antennas and Propagation Magazine, Vol. 39, No. 6, December 1997.

[43] William L. Langston and David R. Jackson, “Impedance, Axial-Ratio and Receive-Power Bandwidths of Microstrip Antennas”, IEEE Transactions on Antennas and Propagation, Vol.52, No.10, October 2004.

[44] Y.T. Lo, B. Engst and R.Q. Lee, “Simple Design Formulas for Circularly Polarised Microstrip Antennas”, IEE Proceedings, Vol. 135, No.3, June 1988.